Lappeenranta – Lahti University of Technology LUT

LUT School of Engineering Science

Master's Programme in Chemical Engineering

Annina Nikula

IMPROVING COST EFFICIENCY USING MICROFIBRILLATED CELLULOSE IN THE INDUSTRIAL PRODUCTION OF THREE-PLY BOARD

Examiners: Prof. Tuomas Koiranen

M.Sc. Heli Viik

Instructors: Prof. Tuomas Koiranen

M.Sc. Heli Viik

TIIVISTELMÄ

Lappeenrannan - Lahden teknillinen yliopisto LUT

LUT School of Engineering Science

Kemiantekniikka

Annina Nikula

Kustannustehokkuuden parantaminen käyttäen mikrofibrilloitua selluloosaa kolmikerroskartongin teollisessa valmistuksessa

Diplomityö
2020

143 sivua, 85 kuvaa, 12 taulukkoa, 5 liitettä
Tarkastajat: Prof. Tuomas Koiranen
M.Sc. Heli Viik

Avainsanat: mikrofibrilloitu selluloosa, MFC, kolmikerroskartonki, kartonki, CTMP, sellu

Mikrofibrilloitua selluloosaa (MFC) ja sen sovelluksia on tutkittu 1980- luvulta lähtien. MFC:aa voidaan käyttää monissa sovelluksissa, kuten paperin ja kartongin valmistuksessa. Paperiteollisuudessa sitä voidaan käyttää paperin ja kartongin lujuusominaisuuksien parantamiseen. Tutkimuksien mukaan 1-3 m-% lisäyksellä on havaittu parannuksia lujuusominaisuuksissa. Tämän diplomityön tarkoituksena oli selvittää MFC:n hyödyt kolmikerroskartongin teollisessa valmistuksessa.

Työn kirjallinen osa käsittelee MFC:n ominaisuuksia, valmistusmenetelmiä sekä paperiteollisuuden sovelluksia sekä patentteja. Kirjallisuusosassa käydään läpi myös koeajoa kartonkikoneella sekä MFC:n kuljettamista. Työn kokeellinen osa koostuu MFC:n jauhatuksesta, laboratorioarkkien valmistamisesta ja testaamisesta sekä tehdaskoeajon suunnittelusta. Koeajon suunnittelu pohjautuu kirjallisuuteen sekä reologiatuloksiin. Tulosten perusteella koivusellun jauhaminen oli energiatehokkaampaa kuin mäntysellun. Mäntysellun fibrillaatio eteni nopeammin kuin koivusellun. Mäntysellua jauhamalla saatiin enemmän fibrillimäisiä kuituja. MFC:n laatuun voidaan vaikuttaa jauhimen terävalinnalla. Tulosten perusteella, MFC, joka on valmistettu mäntysellusta, paransi paperin lujuusominaisuuksia paremmin kuin koivusellusta valmistettu MFC. Reologiamittausten perusteella on mahdollista kuljettaa 3 m-% MFC:aa, sillä sen käsittelemiseen voidaan käyttää epäkeskoruuvipumppua, jonka maksimi viskositeetti on 1000-3000 Pas.

ABSTRACT

Lappeenrannan-lahden teknillinen yliopisto LUT

LUT School of Engineering Science

Chemical Engineering

Annina Nikula

Improving cost efficiency using microfibrillated cellulose in the industrial production of three-ply board

Master's Thesis
2020

143 pages, 85 figures, 12 tables, 5 appendices
Examiners: Prof. Tuomas Koiranen
M.Sc. Heli Viik

Keywords: microfibrillated cellulose, MFC, three-ply board, paperboard, CTMP, kraft pulp

Microfibrillated cellulose (MFC) and its applications have been studied since the 1980s. The growing interest of MFC has created many applications. In papermaking, MFC can be used as a strength additive. According to the studies, 1-3 wt% addition of MFC increases strength properties. The purpose of this thesis was to verify and quantify the benefits of using MFC in a three-ply board product.

The literature part of the work focuses on the properties and production methods of MFC. The main focus is on industrial applications, patents and articles that address MFC usage in papermaking. The literature part also focuses on a full-scale trial planning; transportation and dosing of MFC. The experimental part of the work consists of three main topics; refining of MFC, making and testing of laboratory sheets and a full-scale board machine trial planning. The full-scale trial is planned based on literature and the laboratory results. Based on the results, the refining of the hardwood pulp was more energy-efficient than softwood pulp. The fibrillation proceeded faster in softwood refining and higher number of fibril-like fines was achieved. The quality of MFC can be affected by the choice of the refiner fillings. Based on the results, MFC made from softwood kraft pulp increased the strength properties more than MFC made from hardwood. Based on the rheological measurements, transportation of 3 wt% MFC would be possible since a progressive cavity pump could be used to handle the viscous MFC. The maximum viscosity for these pumps is between 1000-3000 Pas.

ACKNOWLEDGEMENTS

This Master's Thesis was conducted for AFRY Finland Oy. I would like to thank AFRY for this great and interesting opportunity. This work has expanded my knowledge and inspired me. I am truly grateful for the guidance and feedback of my instructors Heli Viik and Tuomas Koiranen.

I would also thank my steering group: Jarkko Kutvonen, Juha-Pekka Huhtanen and Håkan Sjöström for their knowledge and experience. I am truly grateful to Mikael Ankerfors for sharing his valuable knowledge about MFC. I would also thank all the personnel at the Valmet Fiber Technology Center at Inkeroinen, Lappeenranta-Lahti University at Lappeenranta and Aalto University of Bioproducts and Biosystems at Espoo for helping me with my experimental part.

These years of studying at the Lappeenranta-Lahti University of Technology have taught me a lot. I would like to thank all my friends for the support during my studies. Especially Julia, I am grateful for all those coffee moments together. I would also express my gratitude to my family. Thank you, mum and dad, for all the love, support, and encouragement throughout my life. I am grateful to my sister for always being there for me. Finally, my loving thanks to Henri for his love and support. I would not be where I am now without you. I am so grateful to have you in my life.

This is the beginning of a whole new adventure.

Annina Nikula

Kouvola, 30.6.2020

ABBREVIATIONS

APAM	Anionic polyacrylamide
BC	Bacterial cellulose
BCN	Bacterial nanocellulose
CMC	Cellulose microcrystals or Carboxymethyl cellulose
CMF	Cellulose microfibril
CNC	Cellulose nanocrystals
CNF	Cellulose nanofibril
CPAM	Cationic polyacrylamide
CS	Cationic starch
CSF	Canadian standard freeness
CTMP	Chemi-thermomechanical pulp
DOE	Design of Experiments
FBB	Folding boxboard
HW	Hardwood
LPB	Liquid packaging board
MFC	Microfibrillated cellulose, Microfibrillar cellulose
NC	Nanocellulose
NCC	Nanocrystalline cellulose
NFC	Nanofibrillated cellulose, Nanofibrillar cellulose
NSSC	Neutral sulfite semi chemical

PAE	Polyamideamine epichlorohydrin
PLS	Partial least squares
SBS	Solid bleached (sulfate) board
SEC	Specific energy consumption, kWh/t
SEL	Specific edge load, J/m
SEM	Scanning electron microscopy
SR	Schopper-Riegler number, °
SSA	Specific surface area, m^2/g
SUS	Solid unbleached (sulfate) board
SW	Softwood
TEA	Tensile energy absorption, J/m^2
TEM	Transmission electron microscopy
TMP	Thermo-mechanical pulp
WLC	White lined chipboard

SYMBOLS

Roman symbols

$\bar{A}$	Average area of the sample, mm
A	Shear area, m^2
F	Shear force, N
G	Shear modulus, Pa
g	Grammage of the sheet, g/m^2
h	Distance, m
k	Consistency (thickness) factor, -
L	Cutting edge length, km
m	Dry mass flow through refiner, t/h
$\bar{m}$	Average mass of the sample, g
m_p	Production, t/h
n	Rotation speed, 1/s
n	Shear-thickening or-thinning index, -
P_t	Total power consumption, kW
P_w	Idle power, kW
v	Velocity, m/s

Greek symbols

$\dot{\gamma}$	Shear rate, s^{-1}
γ	Strain, -
δ	Average thickness of the sheet, μm
η	Dynamic viscosity, Pas
η_p	Plastic viscosity, Pas
ρ	Sheet density, kg/m^3
τ	Shear stress, Pa
τ_y	Yield stress, Pa

TABLE OF CONTENTS

1 INTRODUCTION

The consumption of paperboards and packaging materials is increasing year by year since sustainability, biodegradability, and eco-friendliness are becoming megatrends. The need for sustainable materials is a demand in a world made of plastic. For being as good as other packaging materials, paperboards need to be competitive. One of the main properties of paperboards is strength. Usually, these strength properties are improved with two primary techniques; refining of pulp fibers and by strength additives. The refining of pulp is known to enhance flexibility and strength. The only downside is that excess refining can have a negative impact on bending stiffness by increasing the density. In papermaking, starch is used as a wet end additive to enhance strength properties.

Microfibrillated cellulose (MFC) has been studied since the 1980s. Turbak et al. (1983) and Herrick et al. (1983) were the first ones to produce a gel-like suspension called MFC. Unfortunately, the energy consumption of the production was too excessive. Nowadays, more energy-efficient methods for MFC production have been discovered. The growing interest of MFC has created many applications and ideas. In papermaking, MFC can be used to enhance barrier properties, improve paper gloss, reduce grammage, and best of all as a strength additive. Taipale et al. (2010) studied the effect of MFC on the drainage of pulp suspension and paper strength. According to the study MFC increases strength properties and decreases the pulp suspension drainage rate. However, drainability can be controlled by the optimum selection of MFC material and process conditions.

The purpose of this thesis is to verify and quantify the benefits of using microfibrillated cellulose in a three-ply board product. By the means of other studies, it could be possible to utilize MFC in paperboard making as strength additive. Some of the kraft pulp could be replaced with chemi-thermomechanical pulp (CTMP) using MFC in a three-ply board product. This would improve the cost efficiency and enhance the strength properties. Effect of other additives such as cationic starch (CS), cationic polyacrylamide (CPAM), and silica on paper properties with MFC is studied also. MFC is produced with low consistency refining using bleached hard- and softwood kraft pulps. The difference between these two raw materials is compared. The effect of screening

in MFC production is also studied. Rheological measurements of hardwood MFC are done to determine the apparent viscosity on pipes when being unloaded and handled.

1.1 Target of the work

The target of the work is to verify and quantify the benefits of using microfibrillated cellulose in the production of a three-ply board product. It is hypothesized that a part of kraft pulp can be replaced with chemi-thermomechanical pulp (CTMP) using MFC in the middle ply of the paperboard product. Using MFC can lower economic costs and improve some mechanical properties.

The literature part of the work focuses on the properties and production methods of MFC. The main focus is on the industrial applications, patents, and articles that address MFC usage in papermaking. The literature part also focuses on full-scale board machine trial planning; transportation and dosing of MFC. The experimental part of the work consists of two main topics; laboratory sheet trials and a full-scale board machine trial planning. The full-scale trial is planned based on literature and the laboratory results. In experimental part following topics are studied:

- Effect of MFCs raw material choice on refining results and paper properties
- Effect of MFC addition and reduction of kraft pulp on paper properties
- Effect of cationic starch, CPAM and silica together with MFC on paper properties
- Effect of screening on the production of MFC and paper properties
- Rheological behavior of MFC made from hardwood

Laboratory sheets are made using CTMP, bleached kraft pulp and two different MFCs, one made with bleached hardwood kraft pulp and the other with softwood kraft pulp. Retention chemicals CPAM and silica together with cationic starch as a strength additive are also used. Sheets are made consisting of 0-3 wt% of MFC. Laboratory sheet testing is done including the following measurements: grammage, thickness, Scott bond, tear, tensile, and compressive

strength (SCT). Umetrics MODDE Pro 12.1 data analysis software is used to analyze the data gained from the laboratory sheet testing. The effect of variables on paper properties is studied with partial least square (PLS) regression using MODDE Pro. Evaluation of data, model fit, parameter importance, and effectiveness are presented in the results.

LITERATURE PART

2 CELLULOSE

Cellulose consists of glucan chains with a repeating β-(1–4)-D-glucopyranose units. This natural biopolymer is the main component in the plant cell wall and the most important polymer in the world. (Lindström et al., 2014) Cellulose can be extracted from multiple different sources such as wood, seed fibers, algae, fungi, and bacteria. Of all these, wood is the most common source of industrial cellulose. Wood consists of cellulose, hemicellulose, lignin and extractives. (Nechyporchuk et al., 2016) Approximately 45% of the woods dry weight is cellulose and hemicellulose makes a total of 25 to 30% of woods dry weight (Pèrez et al., 2002). Woods can be divided into two categories; softwood (SW) and hardwood (HW). Hardwoods such as birches and eucalypti have shorter and narrower fibers than softwoods like spruces and pines. (Alèn, 2000) Pine fibers average length is 1.95 mm and the length of birch fiber is 0.91 mm (Sirviö, 2008). Birch has higher hemicellulose content than softwood, whereas the amount of lignin in softwood is higher. Hemicellulose in hardwood consists mainly of glucuronoxylan (birch 28% and eucalyptus 14%). Hemicellulose on softwood on the other hand consists mainly of glucomannan (pine, spruce 16%). (Sjöström, 1993)

Plant cell consists of cell wall layers such as middle lamella, primary wall, secondary wall layers, and the warty wall. Primary and secondary walls consist of three components: cellulose, hemicellulose and matrix, which is composed of lignin and pectin. (Nechyporchuk et al., 2016; Pèrez et al., 2002) The structure of wood is shown in Figure 1.

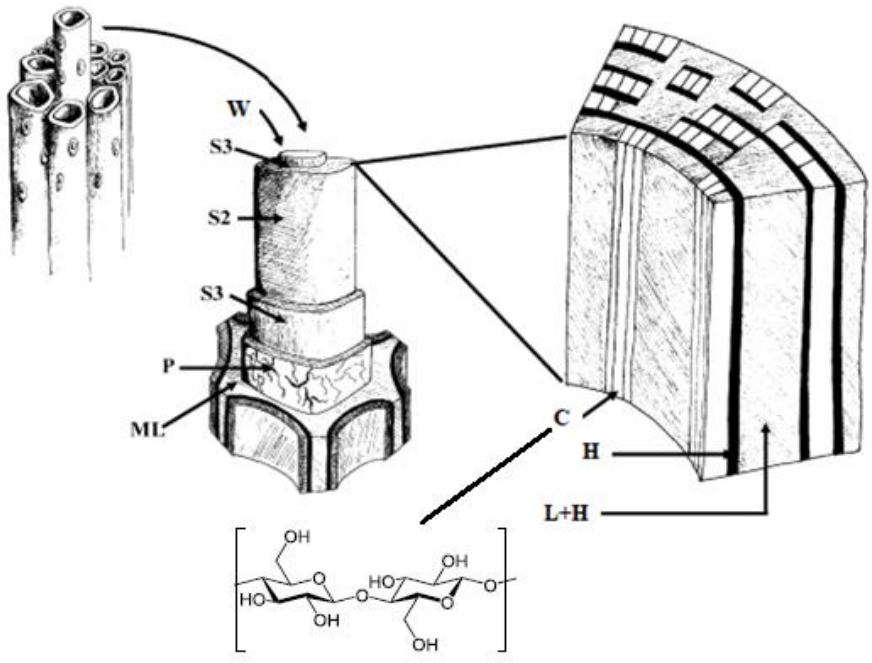

Figure 1 Structure of wood showing middle lamella (ML), primary wall (P), layers of the secondary wall (S1-S3), the warty wall (W), cellulose (C), hemicellulose (H) and lignin (L). (Adapted from Nechyporchuk et al., 2016; Pèrez et al., 2002)

2.1 Nanocellulose

Nanocellulose (NC) or cellulose nanomaterial (CNM) is a material consisting of cellulose with an external or internal dimension between 1-100 nm (ISO/TS 20477:2017). Nanocellulose is produced via mechanical, chemical, and enzymatical methods from cellulosic material such as wood and plants. Although woods and plants are more used, nanocellulose can also be produced from animals, algae, bacteria, and agricultural waste streams. (ISO/TS 20477:2017; Kangas, 2014) Nanocellulose can be categorized into three groups: Cellulose nanofibrils (CNF), cellulose nanocrystals (CNC) and bacterial cellulose (BC) (Lavoine et al., 2012; Kangas, 2014). Cellulose nanofibrils or nanofibrillated cellulose is a type of nanocellulose with dimensions of 5 to 30 nm in width. Cellulose microfibrils also known as microfibrillated cellulose are slightly bigger, with width varying from 10 to 60 nm. (TAPPI Standard WI-3021) In literature, both of these terms are used to describe cellulose nanofibrils and in some cases the difference is not clear. Table I shows nanocellulose types, related terms, and abbreviations.

Table I Nanocellulose types, related terms, and abbreviations used in literature. (Adapted from Klemm et al., 2011)

Type of nanocellulose	Related terms/synonyms	Abbreviations
Cellulose nanofibrils	microfibrillated cellulose, nanofibrillated cellulose, nanofibrillar cellulose, cellulose microfibrils,	CNF, MFC, NFC, CMF
Cellulose nanocrystals	nanocrystalline cellulose, cellulose microcrystals, whiskers	CNC, NCC, CMC
Bacterial nanocellulose	bacterial cellulose	BNC, BC

Cellulose nanocrystals are produced by acid hydrolysis where amorphous sections of cellulose are removed. Usually, sulfuric acid is used for the hydrolysis. After the hydrolysis, cellulose is often treated with mechanical or ultrasonic treatment. The length of CNCs varies between 100-1000 nm and width between 2-20 nm. Plants and algae are typical sources of cellulose used for CNC production. (Kangas, 2014; Klemm et al., 2011)

Bacterial cellulose is produced via biosynthesis by bacteria e.g. Acetobacter xylinum, which produces cellulose from low-molecular-weight sugars and alcohols (Kangas, 2014; Klemm et al., 2011). These BC nanofibrils are usually 2-4 nm wide and length is between 20-100 nm. Produced cellulose does not contain any other substances such as hemicellulose, lignin or extractives. BC is used in pharmaceuticals and food applications. (Kangas, 2014) In Figure 2, is shown the SEM image of BC as well as TEM images of MFC and CNC.

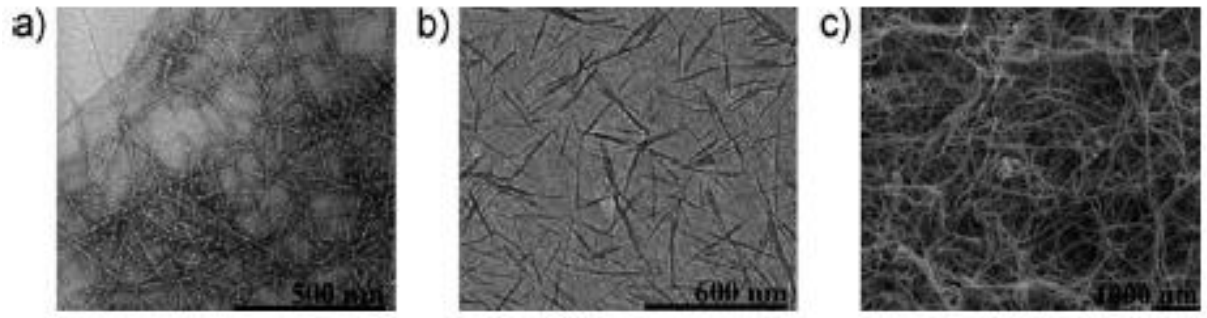

Figure 2 TEM images of a) MFC & b) CNC. SEM image of c) BCN. (Klemm et al., 2011)

3 MICROFIBRILLATED CELLULOSE

Microfibrillated cellulose (MFC) is one of the groups in which nanocellulose is divided (Klemm et al., 2011). MFC and its first production method were discovered in the early 1980 by Turbak et al. (1983) and Herrick et al. (1983) Turbak et al. (1983) found out that homogenization of wood-based cellulose produced a stable gel-like suspension called MFC. However, the energy consumption was too excessive for the production process. The research and number of publications have grown since the mid-2000s. Even though the homogenization method in early the 80s had excessive energy consumption, other methods for MFC production have been discovered over the years. (Sirò & Plackett, 2009) Production methods are discussed later in this chapter. In Figure 3, is shown the number of publications and patents found in years 1981-2019 with the keyword "microfibrillated cellulose".

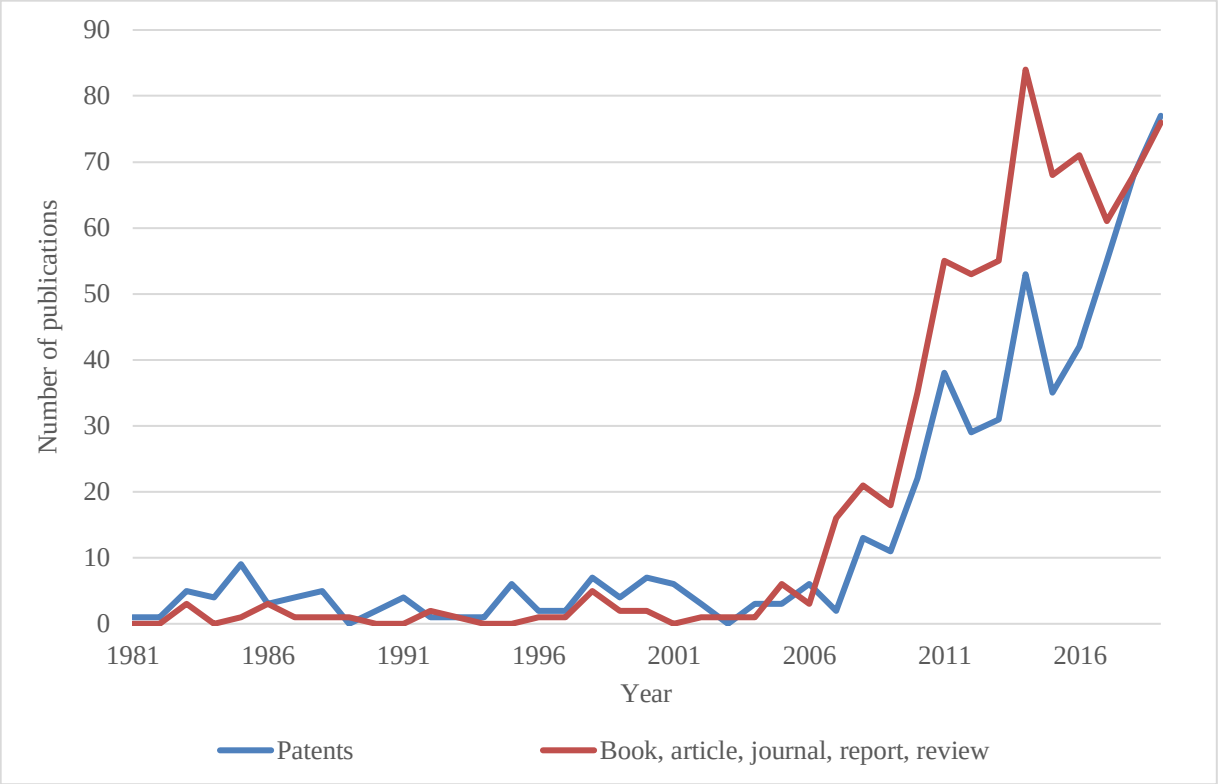

Figure 3 The number of publications (book, article, journal, report, review) and patents found in years 1981-2019 with the keyword "microfibrillated cellulose" using SciFinder (CAS) on 14.1.2020.

In literature, various terms for cellulose nanomaterials and microfibrillated cellulose are used. Technical Association of the Pulp & Paper Industry, TAPPI, has proposed standard for terms and their definition for cellulose nanomaterials. ISO/TS 20477:2017 has standardized the terminology and definitions concerning cellulose nanomaterial. In this work, the term microfibrillated cellulose is used to describe all the synonyms for clarity. In Table II are presented some synonyms and abbreviations for microfibrillated cellulose.

Table II Synonyms and abbreviations for microfibrillated cellulose in literature. (ISO/TS 20477:2017; TAPPI Standard WI-3021)

Term	Synonyms	Abbreviations
Microfibrillated cellulose	microfibrillar cellulose, nanofibrillated cellulose, nanofibrillar cellulose, cellulose nanofibril, cellulose microfibril	MFC, NFC, CNF, CMF

Microfibrillated cellulose can be produced from different cellulosic sources such as wood, potato tubers, hemp, sugar beets, and other agricultural sources. (Lindström et al., 2014) The interest in MFC and its usage in several different applications was understood early. The use of MFC was first explored in cosmetics, pharmaceuticals and food applications. After this, the research has grown and new applications e.g. papermaking additives, barriers, and dispersants in paints have been explored. (Ankerfors, 2015; Kangas, 2014) Papermaking applications are discussed more in chapter 5.

3.1 Structure of microfibrillated cellulose

Microfibrillated cellulose consists of elementary fibrils, microfibrils, which has a length of several micrometers and diameter varies from 20-60 nm (Sirò & Plackett, 2009). Cellulose microfibrils consist of amorphous regions and crystalline parts shown in Figure 4 (Lavoine et al., 2012). Both microfibrillated cellulose and cellulose nanocrystals (CNC) consist of cellulose and its glucan chains. This is the only common thing between these materials. CNCs are often more narrow and shorter than MFC. The structure of MFC is furcate and bendy and CNCs are bacilliform and stiff. (Kangas, 2014) The structures of cellulosic fiber and microfibrillated cellulose are presented in Figure 4.

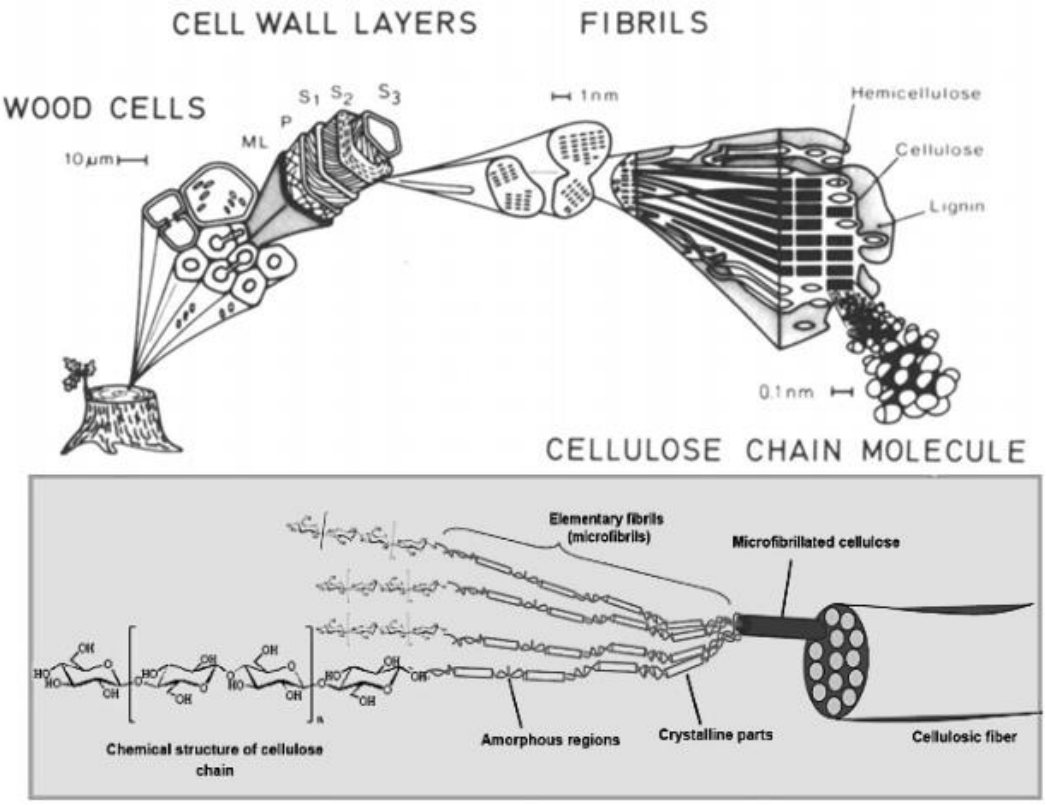

Figure 4 Structure of cellulosic fiber and microfibrillated cellulose. (Adapted from Hoffman et al.,1989; Lavoine et al., 2012)

In an aqueous solution, MFC is a transparent or white gel depending on the production method and raw material used (Lindström et al., 2014). Due to its rheological properties, MFC forms a gel-like suspension in very small consistencies (<0.125 wt%) (Kangas, 2014). In Figure 5, is shown an example of an aqueous suspension of 4 wt% MFC gel produced by refining from bleached birch kraft pulp.

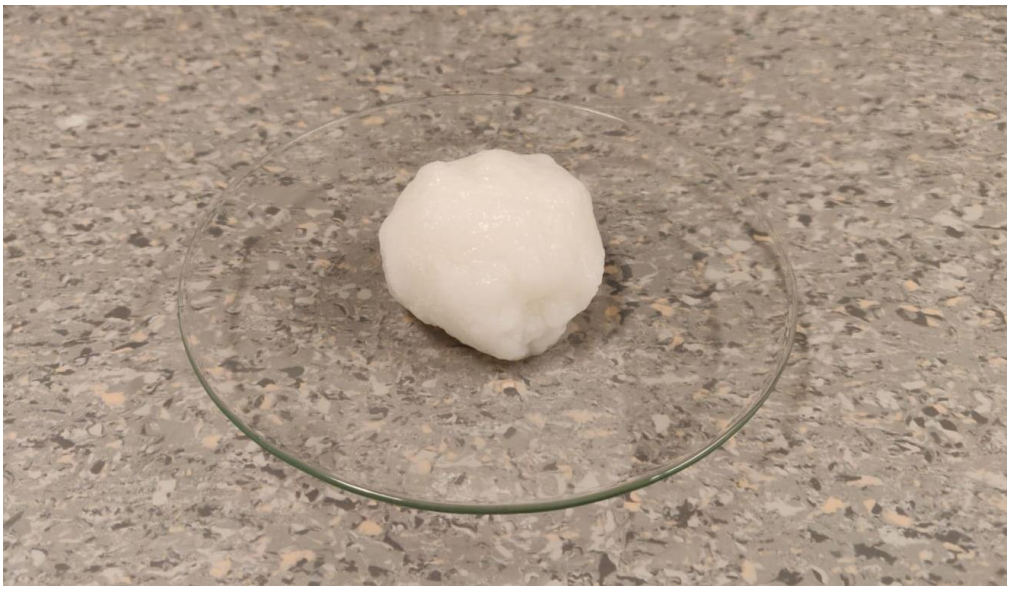

Figure 5 Example of an aqueous suspension of 4 wt% MFC gel produced by refining from bleached birch kraft pulp.

3.2 Properties of MFC

For being biodegradable, sustainable, and light-weighted, microfibrillated cellulose has great properties such as high specific surface area, high aspect ratio, high inherent strength and stiffness (Osong et al., 2017). A high specific surface area (SSA) is one of the most important properties of MFC. MFC made of softwood pulp has the most increased SSA compared to the others. When comparing the original pulp to the homogenized MFC, the original pulp has always lower SSA. (Lavoine et al., 2012) Typically the value of SSA for microfibrillated cellulose is around 100-200 m^2/g depending on the raw material and production method. (Kangas, 2014) The specific surface area is connected to fiber bonding. It is known that the high SSA enhances the bonding between cellulosic fibers. (Retulainen et al., 1993)

What comes to the environmental concerns, it has been shown that microfibrillated cellulose has similar behavior with cellulose. No cyto- or genotoxic properties are found either in a dry or hydrated state. (Vartiainen et al., 2011) It is also shown that MFC based products are considered to be biodegradable and suitable for composting. During the biodegradation process, no toxic products are formed. (Vikman et al., 2014)

3.2.1 Rheology of MFC

Rheology studies the physical properties of solids and liquids; how the stress that is applied affects the material. Deformation can be divided into two categories: reversible or elastic deformation and irreversible or flow deformation. In reversible deformation the internal structure remains intact and in irreversible the structure is destroyed. For liquid materials flow properties are most important whereas elastic properties for solid materials. Ideal elastic behavior, where stress is directly proportional, is called Hookean. A fluid that has an ideal viscous behavior is called Newtonian. For most materials, viscoelastic behavior can be detected. When stress is removed, these viscoelastic materials recover partially. Gels and glues are a typical example of viscoelastic materials. The most used parameters in rheology and flow behavior are shear stress, shear rate, and dynamic viscosity also called shear viscosity. Definitions of rheological parameters are illustrated in Figure 6. (Mezger, 2011: Roper III, 2009: Steffe, 1996)

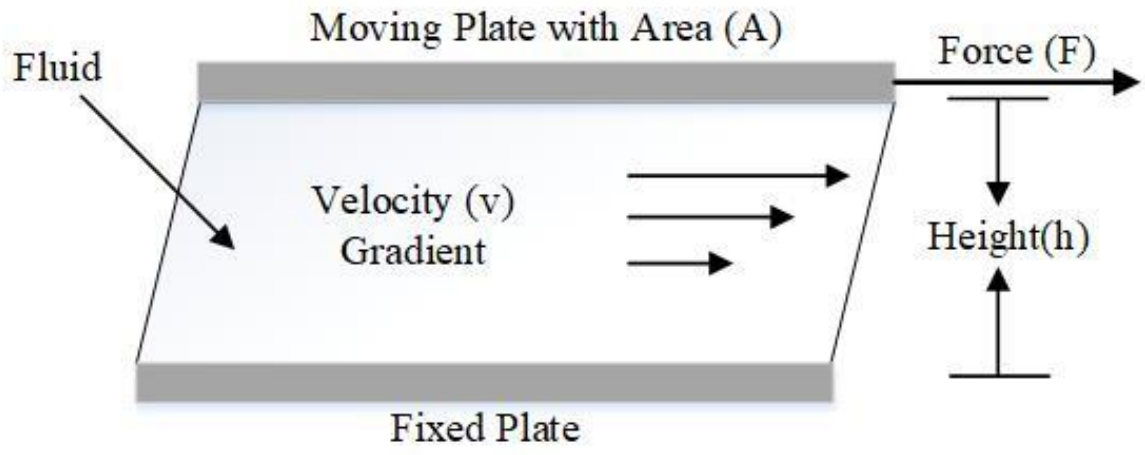

Figure 6 Illustration of rheological parameters. (Adapted from Roper III, 2009)

Shear stress can be calculated from Equation 1. (Mezger, 2011)

$$\tau = \frac{F}{A} \quad (1)$$

Where,

A = shear area, m^2

F = shear force, N

τ = Shear stress, Pa

Shear rate is the ratio of velocity and distance shown in Equation 2.

$$\dot{\gamma} = \frac{dv}{dh} \quad (2)$$

Where,

h = distance, m

v = velocity, m/s

$\dot{\gamma}$ = Shear rate, s^{-1}

Dynamic viscosity is shown in the Equation 3.

$$\eta = \frac{\tau}{\dot{\gamma}} \quad (3)$$

Where,

η = dynamic viscosity, Pas

Type of flow behavior can be detected from curves which illustrates shear stress versus shear rate and viscosity versus shear rate. Flow behavior is divided into Newtonian fluids and non-Newtonian fluids. Newtonian fluids have constant viscosity whereas with non-Newtonian fluids the viscosity is dependent in shear rate. (Roper III, 2009) These curves and flow types are presented in Figure 7.

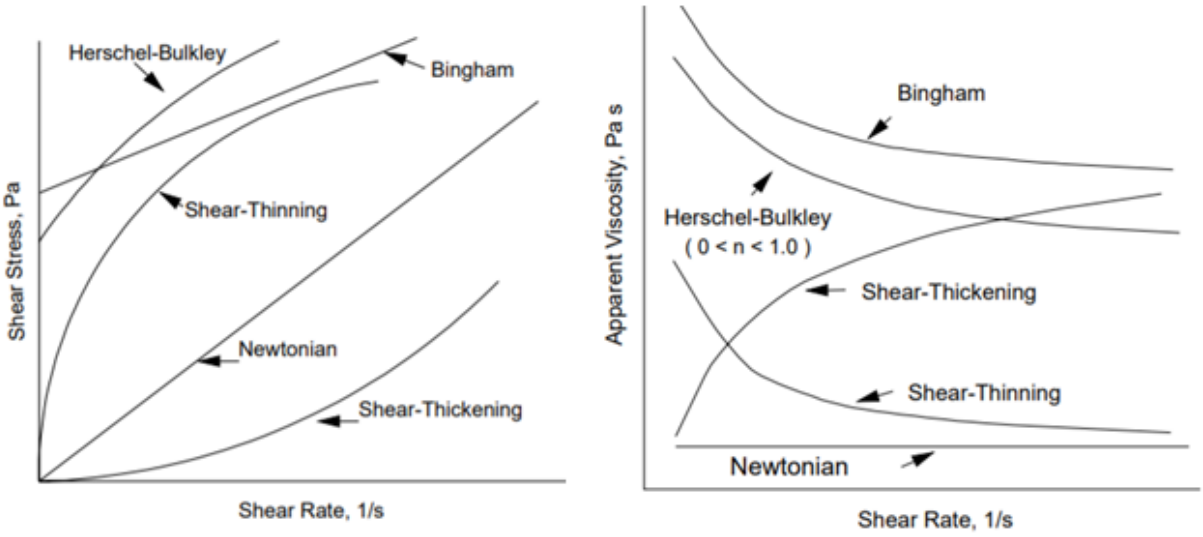

Figure 7 Flow types show in shear stress versus shear rate (left) and viscosity versus shear rate (right) (Adapted from Steffe, 1996).

Usually, the curve plotted on viscosity versus shear rate is straight. This is called a Power Law fluid which Equation 4 is shown below.

$$\tau = k\dot{\gamma}^n \tag{4}$$

Where,

k = consistency (thickness) factor, -

n = shear-thickening or-thinning index, -

As seen from Figure 7, the curve for Newtonian fluid is straight in shear stress plot and a constant flat line in the viscosity curve. Non-Newtonian fluids shown in the illustration are dilatant or shear thickening and pseudoplastic or shear-thinning. For shear-thinning fluids, the shear-thinning factor is less than 1 and for shear-thickening fluids, the shear-thickening factor is greater than 1. For Bingham plastic materials the flow behavior includes yield stress. Above the yield stress, the irreversible deformation can occur, below that the fluid stays put. A combination of yield stress with the pseudoplastic flow can be modeled with the Hershley Buckley model. The equation for Bingham plastic is shown in Equation 5. (Roper III, 2009)

$$\tau = \tau_y + \eta_p \dot{\gamma} \quad (5)$$

Where,

η_p = Plastic viscosity, Pas

τ_y = Yield stress, Pa

The equation for Hershley Buckley model is shown in Equation 6.

$$\tau = \tau_y + k\dot{\gamma}^{(1-n)} \quad (6)$$

Viscoelastic behavior can be measured with an oscillatory test where stress is applied to the material and shear modulus is determined. Equation (7) for shear modulus is presented below.

$$G = \frac{\tau}{\gamma} \quad (7)$$

Where,

G= Shear modulus, Pa

γ = Strain, -

Storage modulus (G') and loss modulus (G'') can be used to characterize the viscoelastic behavior. Storage modulus shows the material's ability to store energy and elastic response whereas loss modulus measures the viscous component and its ability to dissipate energy. The loss factor, tanδ, is the ratio between the viscous and elastic portion. With the loss factor, viscoelastic behavior can be determined. Amplitude sweep is a common oscillatory experiment where the frequency is kept constant and the amplitude of oscillation is varied. (Roper III, 2009) In Table III, is shown the correlation between viscoelastic behavior and the parameters.

Table III Correlation between viscoelastic behavior and the parameters. (Mezger, 2011)

Ideally viscous	**Viscoelastic liquid**	**The gel point, viscoelastic behavior 50/50 ratio**	**Viscoelastic gel or solid**	**Ideally elastic**
$\delta = 90°$	$90° > \delta > 45°$	$\delta = 45°$	$45° > \delta > 0°$	$\delta = 0°$
$\tan\delta \rightarrow \infty$	$\tan\delta > 1$	$\tan\delta = 1$	$\tan\delta < 1$	$\tan\delta \rightarrow 0$
$(G' \rightarrow 0)$	$G'' > G'$	$G' = G''$	$G' > G''$	$(G' \rightarrow 0)$

Microfibrillated cellulose forms a gel-like suspension at low concentrations in water due to the hydrophilic fibrils (Lindström et al., 2014). This three-dimensional network restrains a great amount of water. The critical concentration of fibril suspension is usually reached above 0.125 wt%. (Kangas, 2014) This is a consequence of the interaction between fibrils. MFC suspension has shear-thinning behavior, when the shear rate increases the viscosity decreases. Also shear-thickening behavior has been reported at high shear rates (>105 s^{-1}). The viscosity of MFC suspension is connected to the concentration. (Karppinen, 2014; Moberg & Rigdahl, 2012) According to Pääkkö et al. (2007), the viscosity of 1 wt% MFC suspension produced with homogenization decreased linearly from 100 to 0.1 Pas when the shear rate was 0.1-1000 s^{-1}. Effect of concentration, temperature, ion concentration and pH on flow properties have been studied by Agoda-Tandjawa et al. (2010), Iotti et al. (2011), Pääkkö et al. (2007), and Saarikoski et al. (2012).

Pääkkö et al. (2007) observed that viscosity of 0.25 wt% MFC suspension was dependent on the pH between 2 and 10. The viscosity of MFC decreased when the pH was increased. On the other hand, Agoda-Tandjawa et al. (2010) showed pH variation did not affect the viscoelastic properties of 1 wt% MFC suspension. The effect of temperature on viscosity of the MFC suspension was studied by Iotti et al. (2011). It was shown that the viscosity is dependent on the

temperature in the range of 25-60 °C. Results showed that viscosity decreased when the temperature was increased. This can be due to the reduction of water and the deswelling of the fibers. Raised temperature reduces the ability to take up water on fiber. (Iotti et al., 2011).

Pulp and MFC fibers have some similarities such as the chemical structure of the fibers and the tendency to create flocs. The difference between pulp suspension and MFC suspension is that MFC has smaller dimensions and higher aspect ratio. MFC fibers can create flocs under flow due to the relative motion of the fibers. Especially in high concentrations rotated fibers can collide with other fibers forming flocs. (Karppinen, 2014) In Figure 8, is shown the simulation of floc forming in simple shear flow.

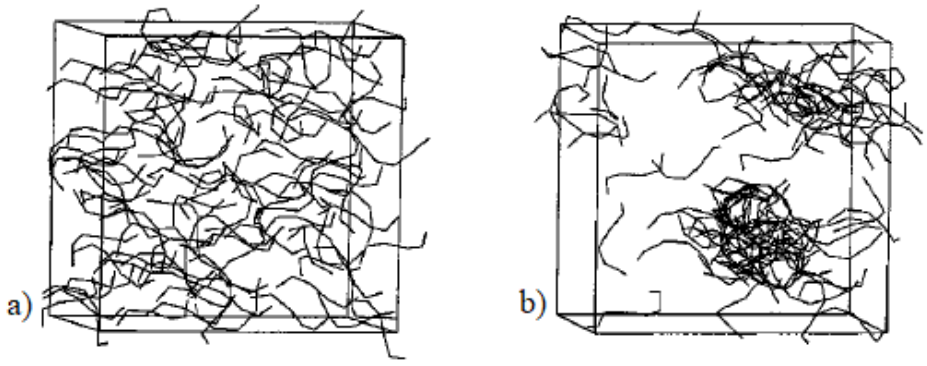

Figure 8 Floc forming simulation in shear flow. a) Fiber network at rest b) under simple shear flow. (Adapted from Schmid & Klingenberg, 2000)

Rheological properties are affected by the floc structure that is dependent on the flow type and shear rate. Flocs can be broken under flow by hydrodynamic forces. For pulp flocs, erosion of the surface fibers and splitting the flocs are suggested. Rheological properties and flocculation of MFC can cause several problems in industrial applications when pumping the material. Due to this lower concentrated MFCs (<1%) are used in most applications. (Karppinen, 2014; Lavoine et al., 2012; Lindström et al., 2014) It has been shown that long storage time can cause deterioration in viscosity of MFC. This must be taken into consideration in the industrial applications. (FIBIC, 2013)

3.2.2 Hornification

Irreversible agglomeration and loss of swelling abilities are called hornification. Hornification is a result of pulp drying. Cellulose fibrils form hydrogen bonds between amorphous parts during drying. These hydrogen bonds cannot be broken by the crystalline parts of cellulose when the hornified cellulose is rewetted. (Sirviö 2008; Eyholzer et al., 2010) Dried pulps have some reduction in strength properties and bonding potential compared to the never-dried pulp due to the hornification (Desmaisons et al., 2017; Hult et al., 2000).

Desmaisons et al. (2017) proved that MFC produced from the never-dried pulp had better quality than from dried pulp. In their study, they used several mechanical, optical and physical properties to verify the difference between different pulps. Kekäläinen et al. (2014) studied the effect of hornification on TEMPO-oxidized MFC. They showed that energy consumption in MFC production from hornified fibers was higher and more chemicals were needed. In their work Spence et al. (2010) found out that hornification did not significantly affect the quality of produced MFC films. Even though hornification does not affect films made of MFC it does not mean that there is no significant impact on MFC used in papermaking. Spence et al. (2010) discovered that the refining of hornified pulp was more difficult compared to a never-dried pulp. This is due to the hydrogen bonding and change in the surface structure.

3.3 Production of MFC

In this chapter, several production methods for microfibrillated cellulose are discussed. The focus is mainly on mechanical methods such as refining without any pre-treatment methods. Microfibrillated cellulose is usually produced mechanically from kraft pulp. To lower the energy consumption, chemical and enzymatical pre-treatment methods are used before mechanical methods such as refining. Several mechanical methods such as homogenization, microfluidization, refining, grinding, cryo-crushing, and ultrasonication have been tested for MFC production. Nowadays homogenization, microfluidization and refining are the most

commonly used methods for the production. (Kangas, 2014) In Table IV, are shown pre-treatment and mechanical treatment methods for MFC.

Table IV Production and pre-treatment methods for MFC production. (Blanco et al., 2018; Lavoine et al., 2012; Osong et al., 2016)

Mechanical treatments	Chemical and enzymatic pre-treatment
Homogenization	TEMPO-mediated oxidation
Grinding	Carboxymethylation
Refining	Acetylation
Cryo-crushing	Enzymatic pre-treatment
Electrospinning	
Ultra-sonication	
Steam explosion	

Chemical and enzymatical treatments are usually used as pre-treatment methods in MFC production. Enzymatical treatments use enzymes to promote cell wall delamination. Enzymatic hydrolysis has been used together with high-pressure homogenization to produce MFC. Carboxymethylation and acetylation are examples of chemical pre-treatment methods. In carboxymethylation, anionic charges are increased in the formation of carboxyl groups. It has been studied that carboxymethylated MFC requires less energy in fluidization. Acetylation on the other hand prevents the hornification of the MFC when dried. This makes it possible to store MFC in a dry form. (Lavoine et al., 2012; Taipale et al., 2010) TEMPO-mediated oxidation is a commonly known method in the production of MFC. Cellulose fibers are oxidized with the addition of NaClO in aqueous suspension. The TEMPO stands for the catalyst used in the process: 2,2,6,6 tetramethyl-1-piperidinyloxy. Also, NaBr can be used as a catalyst. This pre-treatment method decreases the energy consumption used in post-treatment significantly. (Lavoine et al., 2010)

Homogenization of MFC was introduced in the 80s by Turbak et al., (1983) and Herrick et al. (1983). In homogenization, low consistency fiber suspension is fed to a narrow passage using

high pressure. Fibrillation is accomplished with great pressure difference. Since homogenization is not the most energy-efficient way to produce MFC pre-treatment is used to lower the energy consumption. Homogenization can be done with microfluidizer. The suspension is fed into the fluidizer several times to increase the fibrillation rate. (Ankerfors, 2015; Kangas, 2014) The grinding process is based on the breakage of the cell wall structure. The pulp is fed between the grinding stones that generate shearing forces which breaks down the cell structure of the pulp. The revolving speed of the grinding stones is about 1500 rpm. The grinding process takes fewer passes to make MFC than the homogenizer process. (Lavoine et al., 2012) In Figure 9, are shown homogenizer, microfluidizer, and grinding processes.

Figure 9 MFC production methods; homogenizer, microfluidizer, and grinder (Masuko Supermasscolloider). (Adapted from Lavoine et al., 2012)

Other mechanical production methods are cryo-crushing, electrospinning, ultra-sonication and steam explosion. In cryo-crushing the frozen pulp is crushed with liquid nitrogen. This rarely used method is usually used to manufacture MFC from agricultural crops and by-products. (Lavoine et al., 2012) In ultrasonication, cellulose fibrils are isolated by using oscillation power. Hydrodynamic forces of ultrasound create waves that create and collapse small vacuum bubbles. In the steam explosion, the pulp suspension is pressurized with steam for short periods. This causes the fiber cell wall to rupture. In electrospinning, MFC is produced through electrostatic forces. The solution goes through the needle to form Taylor cone at the tip. Electrostatic forces throw liquid jet out of the needle and nanofibers can be collected from the collector afterward. (Blanco et al., 2018)

3.3.1 Mechanical refining

Refining is a mechanical treatment for cellulosic pulp in which fibers are exposed to pressure, shear, and cutting forces. In the refining process, the fiber cell wall is swelled and peeled in aqueous solution. Fiber surface area and volume are increased in the process. (Nechyporchuk et al., 2016) Mechanical refining modifies the pulp fibers to strengthen the paper and making the surface smoother. The formation of the paper can also be improved by shortening the long pulp fibers. The purpose of refining is to get the strength out of fibers not to specifically increase the freeness of the pulp. (Häggblom-Ahnger & Komulainen, 2006; Koskenhely, 2007)

In papermaking, chemical pulp properties are improved by refining. Flexibility, bonding ability of the fibers, formation, absorbency, and optical properties improve after the refining process. However, some properties such as bulk, air permeability, drainage resistance, and tear strength deteriorate after a prolonged refining period. (Taipale et al., 2010) Process conditions such as temperature, pH, and pressure have an effect on the refining results (Koskenhely, 2007).

Refining has several impacts on a fiber: internal fibrillation, external fibrillation, fiber straightening, fiber shortening, and formation of fines (Häggblom-Ahnger & Komulainen, 2006). Delamination of outer fiber layers P and S1 is carried out in internal fibrillation. The second step is external fibrillation where cell layer S2 is exposed. External fibrillation increases the specific surface area of fibrils. (Koskenhely, 2007) Primary and secondary fines can be found in the pulp. Secondary fines are produced during the refining process in external fibrillation and fiber shortening. Primary fines on the other hand can be found in the unbeaten pulp. (Gharehkhani et al., 2014) One of the undesirable impacts of refining is fiber shortening. Longer fibers are desired as they tend to have an increasing impact on paper properties such as tear strength. The last of the effects of refining is fiber straightening. This has an increasing effect on the tensile strength of the paper and elastic modulus. (Koskenhely, 2007) In Figure 10, is shown the effects of refining in fiber.

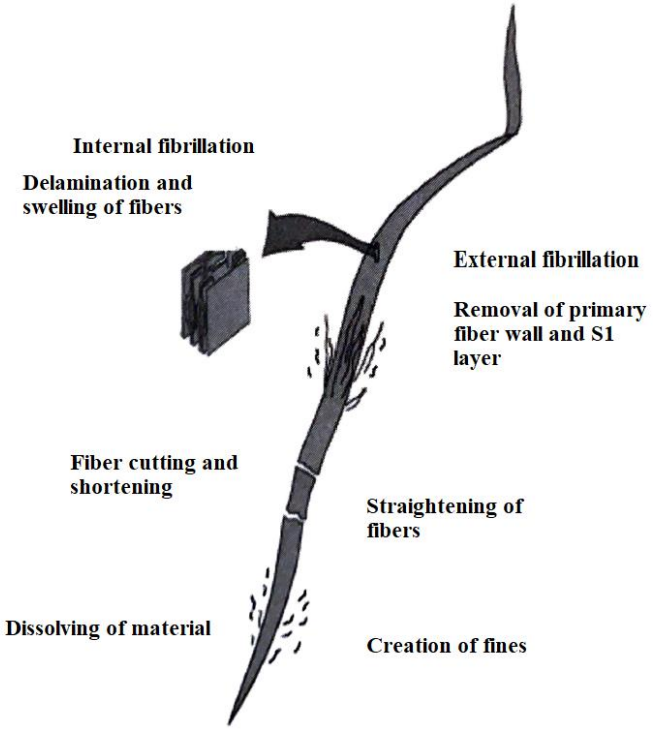

Figure 10 Effects of refining on fiber. (Adapted from Häggblom-Ahnger & Komulainen, 2006)

Hollander beaters were the first machines to produce pulp. Nowadays batch operating Hollander beaters are replaced by continuous refiners with increased capacity. Refiners can be classified into two groups; disc and conical refiners. (Koskenhely, 2007) In conical refiners the pulp is fed into the refiner axially and in disk refiners into the eye of the refiner. Conical refiners have some advantages comparing to disc refiners such as longer residence time, refining sector, and bigger refining area (Häggblom-Ahnger & Komulainen, 2006). In Figure 11, are presented a conical and a disk refiner.

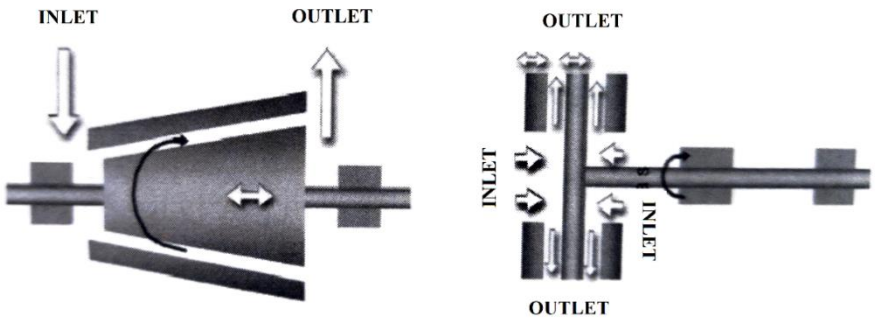

Figure 11 Conical refiner (left) and disk refiner (right). (Adapted from Häggblom-Ahnger & Komulainen, 2006)

Usually, the refining of the pulp is done in low consistency (LC) where pulp consistency is 3.5-6 wt% and the flocculation is strong. (Smook & Kocurek, 1982; Koskenhely, 2007) Increased consistency and length of fibers can cause the formation of larger flocs (Koskenhely, 2007). Compared to high consistency (HC) refining, LC refining reduces specific energy demand significantly (Jahangir & Olson, 2020). In Figure 12, is presented the Valmet OptiFiner Pro refiner used in LC refining.

Figure 12 Valmet. OptiFiner Pro refiner (Valmet, 2020a)

In OptiFiner Pro the pulp is fed from two inlet feeds to inside the rotor and to the bars. Compared to the traditional refiners, OptiFiner Pro treats the stock evenly by spreading it across the bars and directly to the refining zone. This way, all the stock can be treated equally, providing higher refiner capacity and homogeneous material. With OptiFiner Pro, two traditional refines can be replaced with 20 to 40% energy savings. It can be used to all LC-refining applications such as hard- and softwood fibers and recycled fibers. (Huhtanen, 2019; Huhtanen & Partanen, 2013)

According to Suzuki & Hattori (2003) multiple passes through refiner is needed for MFC production. According to the patent of Heiskanen et al. (2017a) refiner must be a certain kind; the height of the blades should be in the range of 6-10 mm. Consistency of MFC in the patent of Suzuki & Hattori (2003) varies from 1 to 6% and patent of Björkqvist et al. (2011) from 1.5 to 4.5%.

In refining, Schopper-Riegler (SR) number, Canadian standard freeness (CSF), and fiber properties, such as fiber length, can be measured on-line. With these, the drainability of a pulp suspension in water can be specified. Refining results can be estimated in different ways. The most common theory is the specific edge load theory where specific energy consumption (SEC), specific edge load (SEL), and specific refining energy (SRE) are calculated. SEC can be calculated with Equation 8, SEL with Equation 9 and SRE with Equation 10. (Häggblom-Ahnger & Komulainen, 2006; Knowpap, 2020)

$$SEC = \frac{P_t - P_w}{m} \quad (8)$$

Where,

m = Dry mass flow through refiner, t/h

P_t= Total power consumption, kW

P_w = Idle power, kW

SEC = Specific energy consumption, kWh/t

$$SEL = \frac{P_t - P_w}{L * n} \quad (9)$$

Where,

L = Cutting edge length, km

n = Rotor speed, 1/s

SEL = Specific edge load, J/m

$$SRE = \frac{P_t - P_w}{m_p} \quad (10)$$

Where,

m_p = Production, t/h

SRE = Specific refining energy, kWh/t

3.4 Raw material in MFC production

Wood is the most important material of cellulosic fibers and is usually used as a raw material of microfibrillated cellulose. The most used materials for MFC production are bleached kraft pulp and bleached sulfite pulp, respectively. (Lavoine et al., 2012) The raw material composition has a major role in the grindability and size distribution of microfibrillated cellulose (Kangas, 2014). Chaker et al. (2013) studied the effect of hemicellulose content on cellulose pulps. They found a correlation between cell delamination and hemicellulose content. The higher hemicellulose content, the easier fibrillation is. Fibrillation between unbleached and bleached pulp has been studied also. Lignin and some hemicellulose content are removed in the bleaching process which leads to lower fibrillation in bleached than unbleached pulp. (Solala et al., 2012) MFC made of unbleached pulp has more homogeneous content than one made from bleached pulp. On the other hand, more heterogeneous material was produced using mechanical pulp with high lignin content. (Kangas, 2014) Fall et al. (2014) showed that the charge density of fibers is correlated to the degree of fibrillation. The highest degree of fibrillation was achieved with the highest

charged sample in this case eucalyptus pulp. It has been suggested that the high hemicellulose content is result of the high charge density. (Fall et al., 2014)

In their study Stelte & Sanadi (2009) studied the difference of cellulose nanofibers between hard- and softwood pulp. Cellulose nanofibers were produced via refining followed by high-pressure homogenization. Stelte & Sanadi (2009) showed that fibrillation proceeded much faster in softwood and due to that required less energy. The strength of films produced with hardwood was slightly lower, but the elastic modulus was higher compared to softwood films. The most significant difference was failure strain which in softwood films was much higher than in hardwood films. (Stelte & Sanadi 2009) Spence et al. (2010) studied the effect of different wood pulps on MFC films. It was shown that MFC films produced from bleached never-dried softwood had higher elastic modulus and tensile strength compared to bleached never-dried hardwood.

Ankerfors et al. (2016) and Osong et al. (2017) used softwood pulp as raw material for MFC in their studies. Both of them studied the effect of MFC in CTMP-based sheets/paperboard. In their study, Ankerfors et al., (2016) used a never-dried softwood dissolving pulp for MFC production. Anionic MFC was produced via carboxymethylation and cationic MFC via cationization both followed by high-pressure homogenization. Never-dried bleached CTMP was used in the study. Osong et al., (2017) used TEMPO-mediated oxidation MFC, softwood spruce CTMP and a flash-dried sulfate pulp for preparing the laboratory sheets.

Lehmonen et al. (2016) studied the effect of cellulose microfibril in strength properties on the middle ply of the board. CTMP and gently refined softwood as well as MFC were used to prepare laboratory sheets. Two different production methods for MFC production were used; high-consistency enzymatic fibrillation and refining with Masuko Supermasscolloider. Bleached softwood pulp was used for high-consistency enzymatic fibrillation and bleached hardwood (birch) pulp was used in refining. According to the study tensile strength, Scott bond, and Z-directional strength increased when hardwood pulp based MFC was used. When the softwood pulp based MFC was used, bulk and bending stiffness was increased. This was due to the fibril morphology. Fibrils in hardwood-based pulp were more flexible and longer compared to the softwood. (Lehmonen et al., 2016)

4 PAPERBOARDS

Paperboards are usually heavier than papers. The usual weight of paperboards is higher than 150 g/m^2, however there are some exceptions. Paperboards are most commonly used as packaging materials. Paperboards can be divided into three groups: carton-, container-, and special boards. Apart from some special boards, paperboards are mostly multi-ply products. (Kiviranta, 2000) The classification of these three paperboard categories is shown in Figure 13.

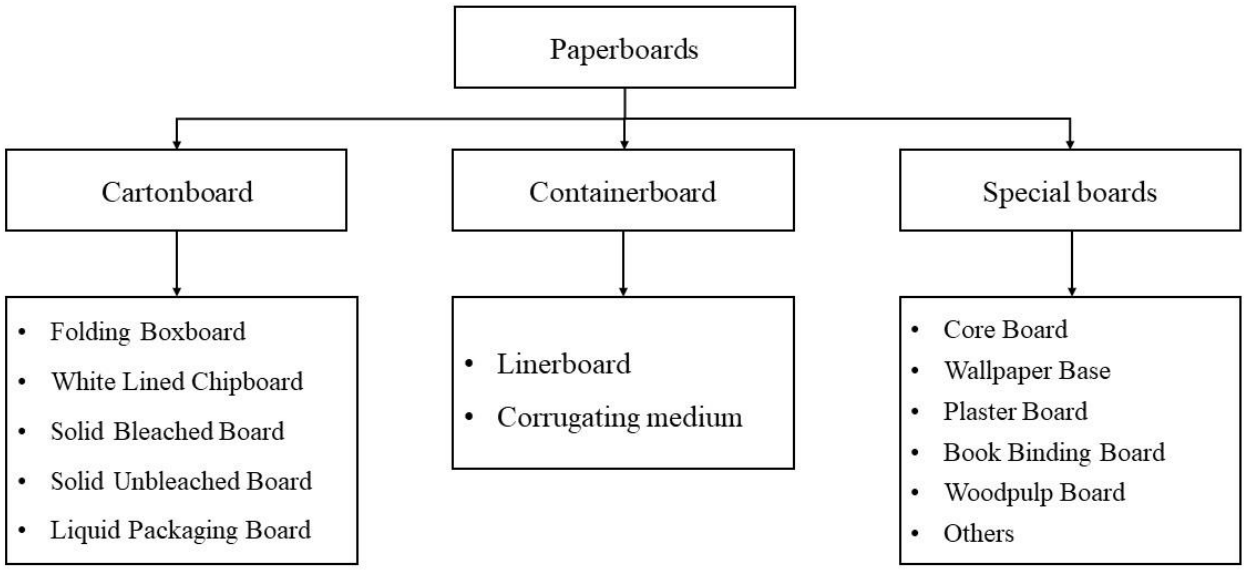

Figure 13 Paperboard categories. Adapted from Kiviranta (2000)

4.1 Cartonboard

Cartonboards are classified into subgroups, as seen from Figure 13 based on the raw material used. Since cartonboards are used to make folding cartons, mechanical strength and bending

stiffness are important properties. Usually, cartonboards are coated to ensure good printing properties. Sheet-fed offset is the most commonly used printing method for cartonboards. Therefore smoothness, good z-directional strength, Scott bond and IGT surface strength are important. (Kiviranta, 2000)

Raw materials used in cartonboards affect the thickness and elasticity which are important factors when it comes to bending stiffness. The most optimal structure for cartonboads is that the middle ply is most bulky, and the top and bottom plies have high elasticity. The top ply should have the biggest possible stretch at break for minimizing the cracking tendency. Top ply's z-directional strength needs to be optimal to avoid a negative impact on the cracking. (Kiviranta, 2000)

For food packages purity, especially microbiological purity, is an important factor. Usually, microbes in paperboards do not cause any health problems but can lead to other problems. Chocolate and cigarettes are products that can be harmed by microbes that cause odor and taint problems. Recycled fiber-based products are more likely to have microbiological purity issues than virgin fiber-based paperboards. Due to this, recycled fiber-based products cannot be used in some food packaging applications. (Kiviranta, 2000)

Folding boxboard (FBB) and liquid packaging board (LPB) are subgroups of cartonboards used for packaging purposes. FBB can be used for packaging of e.g. cosmetics, cigarettes, food and pharmaceuticals. LPB on the other hand is used in liquid packaging applications such as milk and juice packaging. The weight of FBB varies around 160-450 g/m^2. Both of these cartonboards are multi-ply products. Usually, FBBs consist of 3-4 plies and LPBs of 2-3 plies. (Kiviranta, 2000) The structure of FBB and LPB is presented in Figure 14.

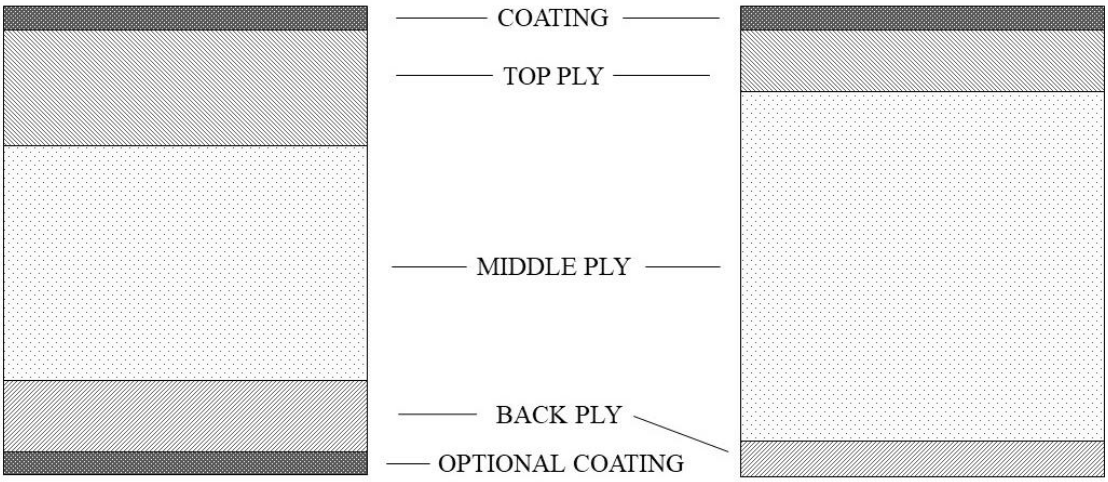

Figure 14 Structure of three-ply folding boxboard (left) and three-ply liquid packaging board (right). Adapted from Kiviranta (2000)

Usually, bleached hard- or softwood pulp is used in the top and back ply of FBB. Middle ply consists of CTMP, TMP, broke, groundwood, or pressure groundwood. In LPB back ply consists of unbleached hard- or softwood pulp and the top ply of bleached or unbleached hard- or softwood pulp. The middle ply of LPB consists of CTMP, broke and unbleached hard- or softwood pulp. The pulp in the top and back ply gives the paperboard high modulus of elasticity and the CTPM or TMP gives maximum bulk for the middle ply. Only virgin fiber can be used in LPB due to purity demands. In the Table V, are presented raw materials used in different cartonboards (Kiviranta, 2000)

Table V Raw materials used in different cartonboards. FBB=folding boxboard, WLC= white lined chipboard, SBS=Solid bleached (sulfate) board, SUS=solid unbleached (sulfate) board & LPB=liquid packaging board. (Kiviranta, 2000)

Raw material	**FBB**	**WLC**	**SBS**	**SUS**	**LPB**
Unbleached hardwood pulp				x	x
Unbleached softwood pulp				x	x
Bleached hardwood pulp	x	x	x		x
Bleached softwood pulp	x	x	x		x
CTMP	x	x	x	x	x
TMP	x				
Groundwood (GW)	x	x			
Pressure groundwood (PGW)	x	x			
Broke	x	x	x	x	x
Deinked pulp		x			
White ledger		x			
Old newsprint		x			
Recycled fiber		x			
Mixed waste		x			
Old corrugated containers (OCC)		x		x	

4.2 Required properties of paperboard

Most mechanical properties of paper and paperboard are correlated to fiber strength, bonding degree of the fiber and strength of those bonds. The network of the paper is formed when cellulosic fibers bond with each other when dried. Paper and paperboard have many mechanical and structural properties which can be roughly classified into seven groups:

- Basic properties
- Optical properties
- Strength properties
- Surface properties
- Stiffness properties
- Structural properties
- Absorption properties

As mentioned earlier most important properties of cartonboards used as packaging are strength and surface properties and some special properties like odor and taste. Some of the most common and important properties are discussed more in this chapter. (Häggblom-Ahnger & Komulainen, 2006; KnowPap, 2020; Levlin, 1999)

4.2.1 Weight, thickness, bulk and density

Paperboard basis weight or grammage is the weight of the paperboard per square meter (g/m^2). Paperboards, which usually are multi-ply products, weigh between 100 to 600 g/m^2. The weight of top ply is typically around 45-60 g/m^2 and back ply 25-30 g/m^2. Weight is added to the middle ply when the grammage of the grade is changed. Normally the price of paperboards is determined based on the weight not the area. Raw material consumption and costs increase as the weight increases. Most properties improve when the basis weight is increased. Although,

these properties can be modified with refining processes, so the weight will remain constant. (Häggblom-Ahnger & Komulainen, 2006; KnowPap, 2020)

The thickness of the paperboard is the distance between the surfaces in a sheet. Thickness can be determined in two ways; sheet thickness and stack thickness. (KnowPap, 2020) Sheet thickness is measured using a single sheet. Stack thickness or bulking thickness is calculated from the thickness of several sheets placed on top of each other. (ISO 534:2011; Häggblom-Ahnger & Komulainen, 2006)

Density and bulk are structural properties that can be calculated with the help of thickness and weight. Density (kg/m^3) is calculated by dividing the weight with thickness. The bulk (cm^3/g) is a multiplicative inverse of density. (KnowPap, 2020) High bulk and low density are desired properties of paperboard. High bulk correlates with different properties that are wanted such as high tear strength and stiffness. (Häggblom-Ahnger & Komulainen, 2006)

4.2.2 Bending stiffness

The ability to resist the effect of the axial or planar forces is called bending stiffness. Good bending stiffness affects many things such as runnability, printing and converting machines. High bending stiffness is desired for strength and good runnability on the packing machine for paperboards. When basis weight is increased the bending stiffness increases. Increasing the basis weight is not the best way to control the bending stiffness because the goal is to decrease or maintain the weight level. (Kajanto, 2008)

For paperboards, especially those meant for packaging purposes, bending stiffness is one of the most important properties. Usually, cartonboards used for packaging consist of more than one layer. Reason for this is that high stiffness can be reached using multilayer structures. The middle layer gives thickness and strength and the surface layers a high elastic modulus. Usually, problems with bending stiffness are encountered when grammage is lowered. (Kajanto, 2008)

4.2.3 Strength properties

Tensile strength (kN/m) tells the highest value that the sample sheet can stand without breaking when being stretched in the surface direction (KnowPap, 2020). Paper and paperboard tensile strength varies between 1-10 kN/m, some of the paperboards over 10 kN/m. Many factors affect the tensile strength such as pulping method, refining, additives, headbox, wire section, wet pressing, and drying. Tensile strength is connected to the basis weight of the product. When the weight increases the tensile strength increases. Other properties like moisture, formation, fiber orientation, and ash content can affect tensile strength also. (Häggblom-Ahnger & Komulainen, 2006; KnowPap, 2020) The tensile tester measures also other tensile properties such as tensile energy absorption (TEA), tensile stiffness and strain at break. From these measurements elongation and modulus of elasticity can be calculated. (Levlin, 1999)

Tear strength (mN) can be measured using Elmendorf-method. This method determines the force that is needed to tear a stack of four samples from an initial cut. Tear strength can be also expressed as a tear index which is calculated by dividing the tear strength by basis weight (mNm^2/g). Tear and tensile strength are some of the most important properties when it comes to the paper machine runnability. Tear strength is connected to fiber length; the longer the fibers are the better the tear strength is. Basis weight and moisture are two most typical properties that can increase tear strength. (Häggblom-Ahnger & Komulainen, 2006; KnowPap, 2020)

Bonding strength (J/m^2 or N/m^2) is the energy per area required to break or delaminate the test sample. Pulp type, starch amount, former type, wet pressing and temperature can all have an impact on bonding strength. Internal and surface sizing can improve the bonding strength. Ply bond, on the other hand, expresses the delamination between different layers of paperboard. (KnowPap, 2020) This can be improved by spraying additives like starch between the plies (Ryu & Lee, 2007). Bonding strength can be determined in many ways. Most used methods are the Scott bond test and z-directional tensile strength. The Scott bond test measures the amount of energy needed to delaminte the sample and the z-directional tensile strength measures the needed force to split the sample. (Fellers et al., 2012; KnowPap, 2020) In Figure 15, is presented the principle of the Scott bond test.

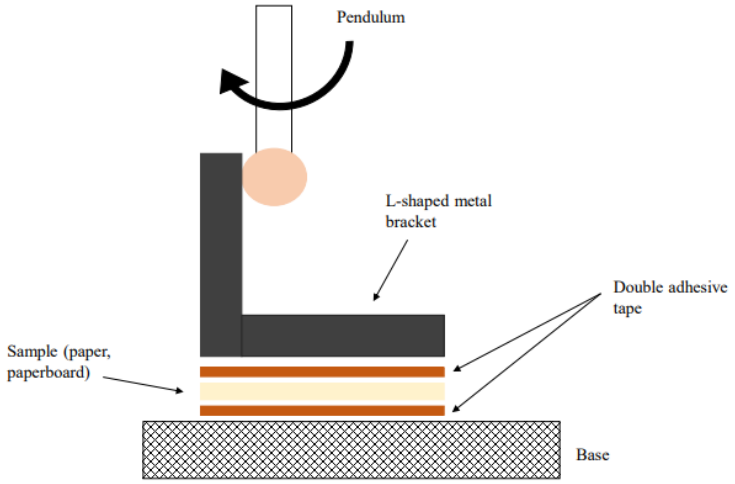

Figure 15 Principle of Scott bond test. The energy required for delamination is determined based on the pendulum. (Adapted from Fellers et al., 2012)

Z-directional strength increases when sheet density is increased. Z-strength is dependent on the pulp type and densification method. In Figure 16, is shown the relationship between z-strength and density with various pulps. As seen from Figure 16, chemical pulps tend to improve the strength properties better than mechanical pulps.

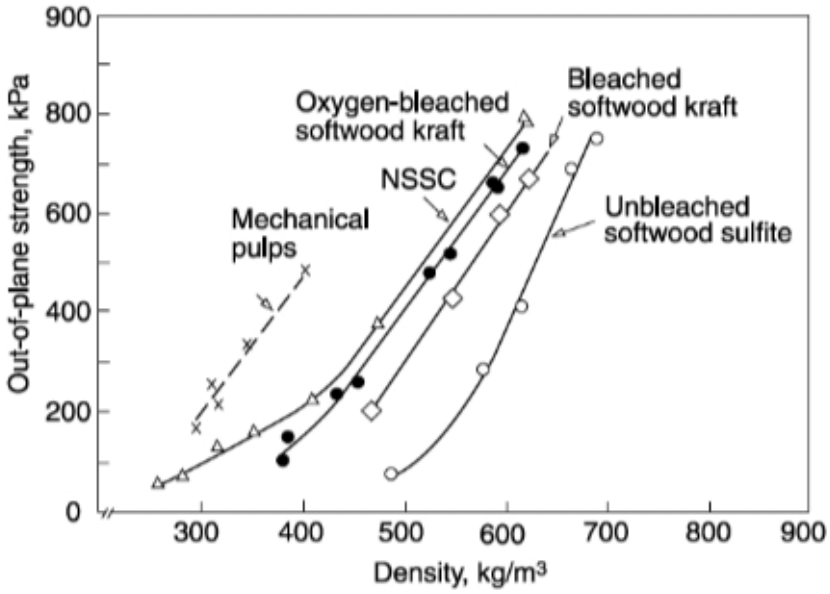

Figure 16 Z-strength as a function of sheet density. NSSC= Neutral sulfite semi chemical (Kajanto, I. 2008)

Compression strength or short span compression strength (SCT) is one of the most important strength properties of packaging boards. For example, boxes must be able to place on top of each other without damage. This concerns mostly on corrugated boards. (KnowPap, 2020) In boxboards, compressive strength comes from bending stiffness and edgewise compressive strength. It is usually defined as force per unit width. Compressive strength is usually one-third of the tensile strength. (Kajanto, 2008)

5 INDUSTRIAL APPLICATIONS OF MICROFIBRILLATED CELLULOSE

Microfibrillated cellulose can be used in a different range of applications due to its properties. MFC can be used for strengthening purposes in papermaking, packaging materials, composite and even textile applications. Due to high the specific surface area and its ability to form porous aerogels and strong transparent films MFC can be used in different applications such as in paints, food applications, pharmaceuticals, cosmetics and paper applications. MFC films can be used in papermaking as a barrier material. This strong and flexible film reduces the number of unwanted substances going inside the package. (Lavoine et al., 2012; Kangas, 2014) In this chapter, the focus is on the paper and board applications. Table VI shows potential applications for MFC.

Table VI Potential applications for MFC. (Adapted from Kangas, 2014)

Field	Applications
Paper and board	coatings and films wet-end and strength additive to improve retention to improve ink adhesion and printing quality
Packaging	packaging composites and fillers transparent films to improve barrier properties
Rheology modifier	foods pharmaceuticals cosmetics hygiene and absorbent products

5.1 MFC in papermaking applications

There are many possible and potential applications for cellulosic nanomaterials like microfibrillated cellulose in papermaking. One of the most researched applications is to use MFC as a strength additive in paper and paperboard products. MFC can also be used to improve some properties like gloss and to reduce the grammage of the product. It can be also used in food packaging to enhance the barrier properties and to enable smart packaging. (Osong et al., 2016) In many studies and patent terms, NFC and MFC are used. Usually, these terms are corresponding and term MFC is used in this chapter.

The most promising field of using MFC in papermaking is a wet end strength additive. Strength properties are affected by many factors such as specific bond strength, fiber-fiber bonded area, fiber length, sheet formation and stress concentrations. Usually, these strength properties are

improved with two primary techniques; refining of pulp fibers and by strength additives. Excess refining can cause problems like paper densification. This usually has a negative effect on bending stiffness. Due to this, chemical additives are used in papermaking. (Ankerfors et al., 2013; Taipale et al., 2010) Starch is one of the used chemical strength additives, which improves mechanical strength properties in papermaking. MFCs properties such as high specific surface area, strength and stiffness have an important role when it comes to papermaking. Due to these MFC improves the bonding between fibers. (Taipale et al., 2010) According to several studies the addition of MFC in CTMP or TMP improves the strength properties (Ankerfors et al., 2014; Ankerfors et al., 2016; González et al., 2012; González et al., 2013; Kajanto & Kosonen, 2012; Lemonen et al., 2017; Osong et al., 2017; Taipale et al., 2010) Using MFC as strength additive, raw material cost can be reduced by using less pulp or increasing the filler content. (Ålander et al., 2017)

In their study, Osong et al. (2017) studied the effect of MFC, cationic starch, and sulfate pulp in addition to CTMP. CTMP blends with 5% TEMPO-based MFC, 10 and 20 kg/t cationic starch, 80% CTMP and 20% sulphate pulp was used in the experiment. The study showed that sheets with MFC and cationic starch (10 kg/t) had an increasing effect on strength properties without compromising the sheet density too much.

Ankerfors et al. (2016) studied the effect of multilayering MFC onto CTMP. They used anionic and cationic MFC in one series and cationic polyamideamine epichlorohydrin (PAE) resin and an anionic MFC in the second series. Results were compared using cationic and anionic starch in multilayering. The study showed that mechanical properties such as tensile and z- strength were improved using MFC multilayers.

Lehmonen et al. (2017) used MFC in the middle ply of the board together with TMP to study the effects on strength properties. In their work, they used MFC (VTT Native grade) produced with Masuko grinding and MFC produced with high consistency enzymatic fibrillation (HefCel). The VTT Native MFC was produced from bleached birch pulp and the HefCel MFC from bleached softwood pulp. It was noticed that the addition of MFC improved the strength properties such as z-strength, Scott bond, and bending stiffness. It was shown that better results

were achieved with VTT Native MFC grade except for bending stiffness which improved better with HefCel MFC.

In their work Kajanto & Kosonen (2012) studied the effect of MFC addition in papermaking with a high-speed pilot paper machine. Two different MFC grades were used at 1 wt% and 2 wt% addition levels with 1 wt% addition of cationic starch. In their trial good runnability was achieved and dewatering levels remained at an acceptable level during the trial. Kajanto & Kosonen (2012) showed that up to 8 g/m^2 grammage reduction was achieved and the tensile strength improved with MFC. They showed that the air permeability and light scattering coefficient were a little lower. Ankerfors et al. (2014) also studied the use of MFC in paper manufacturing with a pilot-scale paper machine. It was shown that the addition of MFC and cationic starch improved the mechanical properties of highly filled paper. Some dewatering issues were encountered but overall there were not any major runnability issues.

5.2 MFC as a coating material

MFC gel shows promising results in printing and food applications as films or nanocomposites. MFC gel has an improving effect on the barrier and mechanical properties of the paper and paperboard. (Lavoine et al., 2012) In this chapter, MFC barrier applications in food packaging and printing applications are discussed.

There are several coating techniques, such as size press, spray coating, roll-to-roll coating and foam coating. In papermaking, the foam coating is usually used for web moisturizing before calendaring. (Kinnunen-Raudaskoski et al., 2014) Valmet Wet End Applicator can be used for applying MFC in coating purposes. A liquid dispersion of MFC, can be applied onto the wet stock to enhance surface properties in papermaking. With Valmet Wet End Applicator, MFC, among other additives can be applied onto the wet stock as a full-width curtain. It has been shown that this coating system improves properties like bond, burst, SCT, smoothness and tensile. With this system, a better functionality for barrier coating applications can be achieved. (Valmet, 2020c)

Many studies focus on the barrier properties of microfibrillated cellulose for packaging. Barrier properties can be divided into four groups based on the material that is wanted to avoid. These groups are oxygen, water vapor, aqueous liquid, and grease/oil barrier. Several studies related to microfibrillated cellulose films and barrier properties in food packaging applications have been made. (Aulin et al., 2010a; Aulin et al., 2010b; Pääkkö et al., 2007; Syverud & Stenius, 2009; Österberg et al., 2013) MFC can also be used in printing applications as a coating to printing papers and a coating agent to improve the printing quality. Ankerfors et al. (2009) have applied a patent for composition for the coating of printing paper.

Syverud & Stenius (2009) were among the first ones to show paper coated with MFC. In their study they showed that air permeability of the sheet decreased when MFC in the coating was increased. Later Aulin et al. (2010a) and Aulin et al. (2010b) confirmed that reduction in surface porosity was a consequence of the improved barrier properties. It was also shown that oil resistance was improved. MFC provides also a good oxygen barrier by forming a dense structure (Paunonen, 2013). Among other properties, Plackett et al. (2010) studied the oxygen permeability of different MFC films. It was shown that oxygen permeability decreased when the addition of MFC was increased.

5.3 Patents

Since the 1980s many patents related to microfibrillated cellulose production and applications have made as seen from Figure 3. In this chapter, some of the patents in MFC usage in papermaking are shown. Focus is mainly on papermaking, instead of MFC films and their applications. The aim of the patent review was to find patents related using MFC as a strength additive in paper/board production. More closely, patents that use MFC as a wet end additive together with cationic starch in multi-ply board production. In Table VII, are shown patents related to MFC in papermaking applications.

Table VII Patents related to MFC in papermaking applications.

Publication number (WO/EU)	Publication year	Applicant	Title	Status	Reference
WO2009123560/ EP3095912	2009	Rise Inneventia AB	Composition for coating of printing paper	Validated (Finland)	Ankerfors et al., 2009
WO2019227186	2019	Klabin S.A.	Paper and process for manufacturing paper using MFC between the layers thereof	Demand for International preliminary examination	Damàsio & Coelho dos Santos Muguet Soares, 2019a
WO2019227187	2019	Klabin S.A.	Paper and process for manufacturing paper using MFC in the cellulose pulp	Demand for International preliminary examination	Damàsio & Coelho dos Santos Muguet Soares, 2019b
WO2011056135/ EP2496766	2011	Stora Enso Oyj	Process for the production of a paper or board product and a paper or board produced according to the process	Oppositions pending (Finland)	Heiskanen et al. 2011
WO2017163176/ EP3433428	2017	Stora Enso Oyj	Board with improved compression strength	Pending (EU)	Heiskanen et al. 2017b
WO2013160553/ EP2841649	2013	Stora Enso Oyj	Fibrous web of paper or board and method of making the same	Non-valid (Finland)	Kinnunen & Hjelt, 2013
WO2020003129	2020	Stora Enso Oyj	A ply of a linerboard and a lightweight linerboard for corrugated board	-	Lampainen et al., 2020

Patent of Ankerfors et al. (2009) is the only one related to papermaking using MFC as a coating material that is validated in Finland. This patent focuses on using MFC for the coating of printing papers. The invention focuses on composition for coating of printing paper, which reduces the linting and/or dusting of paper. The first layer of the coating consists of polysaccharide hydrocolloids such as starch or gums and the second layer of MFC.

In their first patent Damàsio & Coelho dos Santos Muguet Soares (2019a) use 0.5 to 1.5 g/m^2 of MFC to replace starch in multilaminar paper production in a weight range of 60 to 440 g/m^2. MFC is placed between the layers of the multilaminar paper. The multilaminar paper in this invention is characterized to be a cardboard of corrugated board. The diameter of the MFC preferably needs to be less than 250 nm. In the second patent Damàsio & Coelho dos Santos Muguet Soares (2019b) uses MFC as a strength additive in papermaking. The paper in this invention is characterized to be kraft, sack kraft, testliner, corrugated paper or paperboard. The diameter of MFC used has a mean diameter between 1 to 568 nm. The MFC is added to a cellulose pulp together with starch. The starch addition varies from 1-10 kg/t and the amount MFC varies from 1 to 1.5 wt%. The weight of the final product varies from 60 to 440 g/m^2. Both of these patents are in Portuguese and demand for an international preliminary examination.

In their patent Heiskanen et al. (2017b) use MFC for corrugated board or linerboard production. The aim is to increase the compression strength by adding 1 to 5 wt% of MFC to the base pulp which Schopper-Riegler value is between 15 to 28 ml. European Patent Office has published the invention in 2019 and is now pending.

Most relevant patents concerning this work are by Heiskanen et al. (2011) and Lampainen et al. (2020). In their patent Heiskanen et al. (2011) use 0.1 to 5 g/m^2 of MFC in multi-ply board production. The board consists at least of three plies. MFC is placed to the surface of the first ply by spraying to increase the bonding of the plies. The second ply is attached on top of it so the MFC is located between these plies. This will increase the bond of the plies and reduce the delamination. Other additives such as clay, silica, bentonite or starch can be used together with MFC to create an even stronger bond. In Finland the patent is still pending but the European Patent Office (EPO) has granted this patent.

In their invention Lampainen et al. (2020) use MFC for corrugated board or linerboard production as a strength additive. The ply consists of 20 to 80 wt% of CTMP and 80 to 20 wt% of chemical pulp. 1 to 10 wt% of MFC is added together with anionic/cationic polymers such as carboxymethyl cellulose (CMC), anionic polyacrylamide (APAM), or cationic polyacrylamide (CPAM) or starch or combination of these. Additives can be pre-mixed before added to the pulp. World Intellectual Property Organization has published the patent in 2020.

5.4 Challenges

While having unique and remarkable properties, a few challenges with MFC have been encountered in different applications. MFC having a large specific surface area can be a good property in some cases. In very dilute aqueous suspensions MFC forms a gel-like structure with pseudoplastic behavior. (Lehmonen et al., 2017) In papermaking, this high water retention capacity can cause dewatering issues. Due to the swelling and high surface area the drainage is decreased. (Taipale et al., 2010)

Taipale et al. (2010) studied the effect of MFC on the drainage and strength properties. They concluded that usually the drainage rate increases when MFC is added into the pulp suspension. However, the drainage rate can be controlled by optimal process conditions and optimum selection of MFC material without compromising the acquired strength properties. (Taipale et al., 2010) Gonzàles et al. (2013) noticed that the addition of 1.5 wt% MFC gave acceptable drainage rate values for papermaking. In their study Rantanen & Maloney (2013) also noticed the dewatering issue. They noticed that higher grammage had a harmful effect on the press dewatering. However, the effect was insignificant with lower grammage in pressure-controlled dewatering.

Rheology and high specific surface area of MFC can cause problems in transportation and handling. MFC becomes hard to handle and pump when consistencies rise above 5 wt%. Typically, MFC is used in lower consistencies like 1-2 wt%. However, transportation becomes expensive quickly if the MFC is diluted in lower consistencies. (Ålander et al., 2017) When

being a great strength additive, the use of MFC can also cause problems with other paper properties. MFC reduces paper permeability and optical properties such as opacity and brightness. This is a consequence of reduced specific surface area and porosity of the sheet. (Brodin et al., 2014) In paperboard production where MFC is used in middle ply, these problems become meaningless.

Microfibrillated cellulose can easily deteriorate like other biomasses over time. It has been studied that long storage time can affect the quality and usability of MFC. It has been shown that microbes can utilize the MFC as a nutrient. After a few days of storage microbial activity has been detected by pH and redox potential measurements. The redox potential of MFC made from bleached hardwood kraft pulp decreased from 325 mV to around 10 mV in 12 days. Long storage time effects dewatering and bonding which causes deterioration in viscosity and strength properties. MFC should be cooled down after the production and stored at low temperatures. Biocide treatment, proper storing and transportation can help with spoilage of MFC. Biocide treatment on the other hand cannot be used in paperboards grades that are used for food packaging. (FIBIC, 2013; Kangas, 2014) According to Huhtanen (2020), MFC produced by refining does not decompose over time. Decomposition and spoilage of the MFC can be affected by the raw material and production method. (Huhtanen, 2020)

MFC has many rival materials used in papermaking. Cationic polyelectrolytes such as cationic starch, hydrophilic wet-end gums and carboxymethyl cellulose (CMC) are also used as a strength additive in papermaking. (Eriksen et al., 2008; Taipale et al., 2010) The biggest increase in paper strength properties has been achieved with MFC combined with cationic starch (Ankerfors, 2015; Retulainen & Nieminen, 1996). Retulainen & Nieminen (1996) showed that the addition of 1.2 wt% of cationic starch improved the kraft papers strength properties as much as 10 wt% of kraft fines. Economically it is more cost-efficient to use starch as a strength additive. The price of MFC consists of the energy used in production and the raw material. Bleached softwood pulp price in 2020 was around 550 to 600 €/t and the price of corn starch was around 250 to 300 €/t. (Investing, 2020a; Investing, 2020b) However, there is a limit of using starch as a strength additive. After a certain amount of starch (1.5-2 wt%) the tensile strength has reached its limit and stays constant. (Krogerus, 2007) When comparing mechanically produced MFC and CMC, it can be said that the chemically modified CMC a has

better impact on paper strength properties than mechanical MFC. However, the production of CMC is more expensive than the mechanical production of MFC. (Hollertz et al., 2017)

6 INDUSTRIAL SCALE PAPERMAKING TRIAL

Paper and paperboard production are controlled by on-line and off-line measurements. The main idea for process monitoring is to manage the paper quality, product grade changes, solids content, and flow. One of the main tasks is troubleshooting. In paper production web breaks, product defects and undesired variability in quality must be detected. Process conditions and quality can be measured continuously during a run with on-line measurements in papermaking. This helps to maintain good and homogeneous quality. Paper quality can be measured also off-line. Off-line measurements are done in the laboratory and during the process with paper testing machines such as Valmet PaperLab. (KnowPap, 2020; Ritala, 2009) Gained process data can be analyzed with different tools such as statistical analysis programs that are DOE (Design of Experiments) supported. An example of DOE supported analysis software is Umetrics MODDE Pro. (Umetrics, 2020)

6.1 On-line measurements

Paper quality can be measured on-line during a run. The goal of on-line measuring is to maintain homogeneous quality during the papermaking. It is easier to make changes to process conditions when the product is measured during the run. The automation and control system of a paper machine is divided into six subsystems:

- distributed basic automation, machine controls and drive controls
- quality measurements and controls, and higher-level optimizations
- profile controls and their actuators
- optical fault detection of the paper web

- web break monitoring
- paper machine condition monitoring

On-line measurements are categorized into process and quality measurements. Basic process measurements are temperature, pressure, flow level, force, rotation speed, consistency, conductivity and pH. The most common measurement in the process industry is temperature. Temperature is measured through the entire paper production with instrumentation methods like resistance and thermoelements. The pressure is the second common measurement in the process industry. Relative measurement is used to measure the pressure. This method measures the pressure relative to atmospheric pressure. Flow measurements can be targeted to measure volume flow, mass flow, flow rate or flow volume. Level measurements are used to measure the fluid or solid level in containers. Hydraulic and pneumatic cylinders are used as actuators in a paper machine. To control these, force must be measured. Force adjustment correlates with paper quality; web tension and compression of the nip. Rotation speed that is measured with a tachometer is directly or indirectly connected to thickness, speed, or quantity. When cooking and bleaching pulp and coating the paper pH measurements have a great role. pH has an impact on chemical reactions on these processes. Conductivity measurements are used to detect ions in the solution. In paper the industry, conductivity measurements are used to detect the dissolved amount of inorganic matter. Lastly, there are consistency measurements that are used to measure the pulp consistency which tells the percentage of dry matter. Consistency of pulp has an impact on the process in many ways such as water, chemical and energy consumption, dewatering, web structure and properties, pumping and mixing of the pulp, and circulation rate of water. (KnowPap, 2020; Tomberg, 2009)

Paper quality is continuously measured with sensors that are attached to measurement platforms. Scanner beam guides these platforms across the web. Usually, the scanner beam crosses the web in 10-15 seconds and scans the paper. It is also possible to measure specific points on web in the machine direction. As high accuracy is needed the sensors in the beam need to be secured properly. As the process operates in high temperature, air cooling liquid and protections gas flow in the scanner beam. (Häggblom-Ahnger & Komulainen, 2006; KnowPap, 2020) In Figure 17, is shown the structure of a scanner.

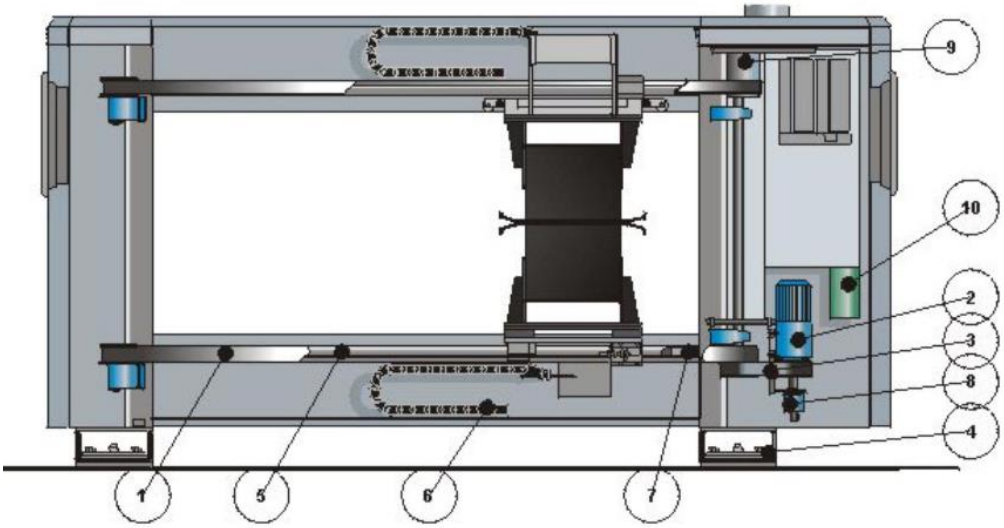

Figure 17 Structure of a scanner where 1) drive belt 2) motor 3) motor drive belt 4) base 5) rail 6) cable chain 7) protection limit switch 8) location sensor 9) disconnector switch 10) lubrication oil tank for the rail. (KnowPap, 2020)

Basic quality measurements can be divided into physical, optical and printability properties. On-line measurements of paper quality usually include grammage, moisture, ash content, formation, fiber orientation, caliper, smoothness, gloss, opacity, color, brightness, porosity and coat weight. Also holes and dirt spots can be detected with cameras. Quality measurements can be done from pulp and end product. Pulp properties like consistency, thick stock ash, retention, fiber length, freeness, and shive content can be measured. Valmet Pulp Expert (Valmet, 2020d) and Valmet Fiber Furnish Analyzer MAP Q are one of the most used pulp quality analyzers. Pulp Expert is an on-line quality control measuring tool that measures consistency, drainage (CSF, SR), brightness, coarseness, curl, light scattering coefficient, tensile strength, fiber length, and fiber length distribution from pulp sample. After measuring data is transferred to mills network and can be presented graphically. With Valmet MAP Q, fiber properties like fibrillation, kink, curl, and size distribution, among other properties can be measured from the pulp on-line. (Tomberg, 2009; Valmet, 2020e)

6.2 Off-line measurements

Off-line measurements are direct measurements done in the laboratory and on the production site from the end product. Samples are taken from the parent reel and cut using sample a cutter before measuring. (KnowPap, 2020) On production site off-line measurements can be done for example with Valmet PaperLab-ASF, -C and -SF. Different measurement modules can be added according to the needs. (Valmet, 2020b) In Figure 18, is shown the Valmet PaperLab testing laboratory.

Figure 18 Valmet PaperLab – automated board and paper testing laboratory. (Valmet, 2020b)

Properties like grammage, thickness, formation, smoothness and strength properties such as tensile, compression, and tear strength as well as some optical properties can be measured. It depends on the paper or paperboard grade which properties are measured to ensure the desired quality. (KnowPap; 2020; Levlin, 1999) Many standards and test methods have been established for the paper industry. Most used methods and standards have been published by ISO (International Organization for Standardization), TAPPI (Technical Association of The Pulp and Paper Industry), and SCAN (Scandinavian Pulp and Paper Association). (Adanur, 1997)

6.3 Statistical data analysis

Process data can be analyzed with different tools e.g. Umetrics MODDE Pro. MODDE is a statistical analysis software that is DOE (Design of Experiments) supported. MODDE Pro uses partial least square (PLS) regression and MLR (multiple linear regression). (Umetrics, 2020) In this work, the main focus is on PLS regression. PLS regression is a multivariate method that can be used to analyze noisy and collinear data. It is a method that finds a linear model using predicted and observed variables. The aim of PLS regression is to find a relation between X and Y matrices. It can be used in various industries such as the pharmacy and food industry in multivariate process control and product modeling. (Kohonen et al., 2009; Olivieri, 2018)

The goodness of the fit (R^2) and goodness of prediction (Q^2) values are used to estimate the model's goodness. R^2 measures the amount of variation and the Q^2 tells the variation of the response predicted by the model according to cross-validation. If the R^2 value is close to 1, it indicates that the model fits the data very close. In a very good model, the R^2 should be above 0.9, and the Q^2 value higher than 0.7. These values can be used when data is collected from laboratory trials where thee experimental plan conducted. For process data the goodness of fit and prediction values can be lower, $R^2 > 0.8$ and $Q^2 > 0.6$. When R^2 is lower than 0.5 the model has rather low significance. In some cases when $Q^2 > 0.5$ the model is considered to be good. The difference between these two values should not be greater than 0.3 for a good model. (Sartorius Stedim Data Analytics, 2017; Wolfgang & Léopold, 2012)

Predicted vs. observed plot is used to determine the dispersity of the data points. It displays the observed versus predicted values. A good model is indicated if the points in the plot are close to the straight line. If the Degrees of Freedom (DF) is under 3 the model is implicitly good. A coefficient plot shows the interaction of parameters used in modeling the data with a 0.95 confidence limit. Usually, weight factors are also used to determine the parameter interaction. The significant the model term is the further away the parameter is from y=0. The model term can be positive or negative. Dependence of variables can also be shown with response contour plots Response contour plot displays the predicted response values for the selected response. These plots are used in DOE supported analysis programs such as MODDE Pro. (Sartorius Stedim Data Analytics, 2017)

6.4 Papermaking trial plan

In this chapter transportation and processability of MFC are discussed. Since MFC can be hard to handle some methods of transportation and unloading are shown. Also, the dosing of MFC to the papermaking process and required process measurements are discussed.

6.4.1 Processability of MFC

Processability, like mixing and pumping, of different MFC grades, has been studied. At low flow rates, MFC has a shear-thinning and laminar flow. Energy loss is higher when compared to water flow. On the other hand, in high flow rates, MFC has a turbulent flow. This fluidized regime is preferred when pumping MFC with a centrifugal pump. The fluidized pipe flow is shown with green in Figure 19. As seen from Figure 19 a screw pump is more efficient with higher consistencies and lower flow rate. (FIBIC, 2013)

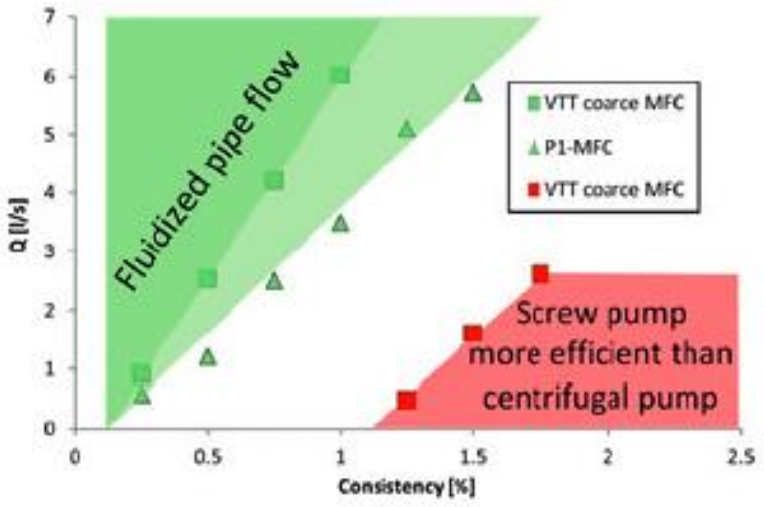

Figure 19 Preferable flow rate (Q) and pump types to certain MFC grade. (VTT coarse; MFC made from bleached HW kraft pulp, dynamic viscosity (10 rpm, 1.5 wt%): 23 176 mPas. P-1 MFC: dynamic viscosity (10 rpm, 1.5 wt%): 2 784 mPas) (FIBIC, 2013)

Centrifugal pumps can be used in lower consistencies (<1 wt%) when the MFC behaves like water (FIBIC, 2013). After all, according to Huhtanen (2020), centrifugal pumps e.g. Sulzer medium-consistency (MC) pumps (Sulzer, 2020) can be used for handling 4 wt% MFC. These pumps are already in use in the refining line of MFC. (Huhtanen, 2020) When MFC is pumped in higher consistencies (>1 wt%) screw pumps are more efficient when the flow rate is kept low (FIBIC, 2013). Mixing MFC with pulps is quite complicated with traditional tank mixers because of the shear-thinning flow behavior. MFC forms a fluidized cavity around the impeller and the MFC near the walls remains stationary. It was shown that at 1 wt% consistency both MFC and SW kraft pulp behaved like water when mixing of MFC and kraft pulp was studied with laboratory mixer. When the consistency was raised the power dissipation with MFC was higher than with kraft pulp. Most clearly this was shown when the consistency was raised to 3 wt%. At this consistency, the energy consumption was 50% higher with MFC than with kraft pulp. (FIBIC, 2013)

MFC forms a gel that is highly viscous in concentrations above 1 wt%. This makes it hard to handle when transported and unloaded. If MFC is transported at lower consistencies such as 1 wt%, it would mean that the average tank truck in which capacity is around 44 tons can transport only 440 kg (dry substance) of MFC. (Tamper et al. 2012) Tamper et al. (2012) have published a patent (granted at EPO) for transporting viscous liquids like nanofibrillar cellulose in higher consistencies of 2 to 5 wt%, in some cases up to 8 wt%. Tamper et al. (2012) consider MFCs which zero-shear viscosity is above 5000 Pas and especially above 10000 Pas hard to handle. Screw pumps especially progressive cavity pumps and twin-screw pumps can be used to discharge viscous materials. (Kajanto et al., 2014; Tamper et al., 2012) These pumps can handle viscous materials up to 1000-3000 Pas (FlowExperts, 2020; SPA, 2020) In their patent they introduce how nanofibrillar cellulose is transported and unloaded along a pipe to a target location. Illustrations of these methods are introduced in Figure 20.

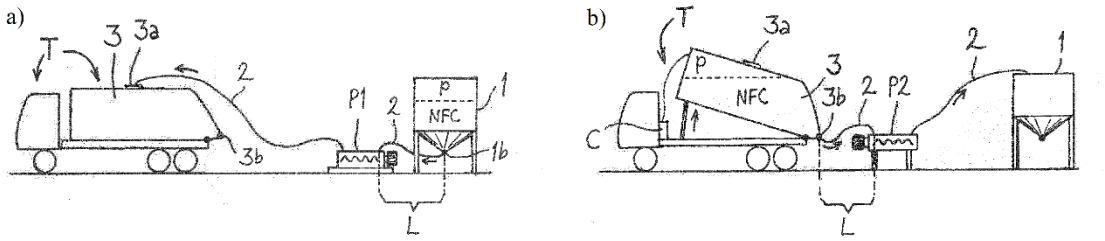

Figure 20 a) Illustration of a loading method used for NFC/MFC b) Illustration of unloading NFC/MFC from container along a pipe to a target location. (Tamper et al. 2012)

In Figure 20, is shown a loading method that can be used for MFC. MFC is loaded to a tippable tank truck container at the top. The tank truck must be tapering downwards as seen from the illustrations. MFC is loaded to the tank container from a storage container that has a discharge outlet at the bottom. The storage container used can have a downward tapering bottom which helps with the discharge. MFC needs to flow through the discharge outlet with the help of gravity. MFC is pumped with a progressive cavity pump which operates on a positive displacement principle. This kind of cavity pump can produce higher pressure than a centrifugal pump. The pump discharges the MFC dispersion to the tank container through a hose. The distance between the discharge outlet and the pump suction side is kept as short as possible, preferably not longer than 2 meters. If a shorter hose cannot be used, a storage container can be pressurized so the overpressure helps the MFC to flow to the discharge outlet. The pressure of a gas is kept preferably at 1.5-2 bar. If the pressure is used the length of the hose can be up to 6 meters. This is dependent on the pressure level and the pipe diameter. The distance between the pressure side of the pump and the discharge to the tank container is kept not longer than 20 meters. (Tamper et al., 2012)

In the unloading stage three things makes it possible to unload the MFC from the tank container:

- gravity: tipping the tank truck container
- pressurization of the tank containers inner volume
- distance between the discharge outlet of the tank and pumps suction side

The tank truck is tipped to help the MFC flow towards the discharge outlet. The tank container is pressurized to 1.5 to 2 bar with a compressor. MFC is then pumped again with a progressive cavity pump to the container. If movable containers are used the unloading pressure can be between 2 to 4 bar. The connection hose diameter between the pump, tank container and storage container must be preferably at least 75 mm. This transporting and unloading method can be applied to all vehicles and container types such as rail tank wagons. If the container is not tippable the unloading takes place through the lowest discharge outlet position of the container. (Tamper et al., 2012)

6.4.2 Dosage and process measurements

Cationic starch is commonly used as a strength additive in papermaking. Usually, starch is added to the thick stock early in the process. This ensures the most effective strengthening effect on the product. Starch retains to the fibers and increases the number of bonds between fibers. This affects the strength of the paper, especially to the z-directional strength. (Krogerus, 2007) According to Ankerfors (2020) MFC needs to be dosed together with starch or as close as possible to the starch dosing since the addition of MFC boosts the effect of starch. It is wanted that the MFC retains to the fiber surface together with starch. (Ankerfors, 2020) In their work Ankerfors et al. (2014) used MFC in fine paper manufacturing. MFC and cationic starch were dosed before the dilution to white water into thick stock. CPAM and silica were dosed to the diluted stock.

In their work Ankerfors et al. (2014) monitored the runnability and retention during the paper machine trial. Dry content on the wire section and after the press section was observed to determine possible dewatering issues. Paper properties such as grammage, density, dry tensile properties, z-strength, and tear index were analyzed. In their trial, Kajanto & Kosonen (2012) used MFC as a reinforcement agent in paper production. They also monitored the retention and dewatering on the former section and press section. Sheet density, tensile strength and air permeability were measured from the product. In both studies major runnability issues were not encountered during the trials. (Ankerfors et al., 2014; Kajanto & Kosonen, 2012)

7 CONCLUSIONS OF LITERATURE PART

Microfibrillated cellulose and its applications are widely studied since more energy-efficient production methods have been invented. Since MFC is not harmful to the environment it is used in many different industrial applications. In papermaking, MFC can be used as a coating material and as a wet end strength additive like cationic starch. MFC can be produced enzymatically, chemically, and mechanically. Usually, enzymatical and chemical methods are used as a pre-treatment before mechanical methods. LC-refining is an energy-efficient way to produce MFC without any pre-treatment methods.

It has been shown that strength properties have been improved with 1-5 wt% addition of MFC. One of the main problems using MFC in papermaking is dewatering. Due to the hydrophilic fibrils, MFC restrains great amounts of water and forms a gel-like suspension in low consistencies. Dewatering problems can be controlled with the optimum selection of MFC material and process conditions. A gel-like MFC is a very viscous material in low shear rates which causes problems with pumping and transportation. It has been studied that with screw pumps can pump MFC in higher consistencies better than centrifugal pumps. However, centrifugal MC pumps are used for handling 4 wt% MFC in the refining of MFC.

Many patents have been published according to the production of MFC and its use in different applications. Patent concerning MFC use in the paper coating is granted in Finland. Tamper et al. (2012) have invented a patent concerning a transportation and unloading viscous materials like MFC. This can be used as a guide for handling MFC when full-scale board machine trial is planned. Screw pumps especially progressive cavity pumps can be used to handle highly viscous materials such as MFC. In papermaking trials, MFC has been dosed together with starch to the thick stock. Paper/board machine runnability and dewatering must be monitored during the trials. Paper properties such as grammage, thickness, tear and tensile strength and z-directional strength can be measured from the end product.

EXPERIMENTAL PART

8 MATERIALS AND METHODS

The experimental part consists of the refining and screening of MFC, laboratory sheet trials, rheological measurements, and full-scale board machine trial planning. MFC was produced by refining from soft- and hardwood kraft pulp. Effect of screening hardwood MFC was studied on refining results and paper properties. Laboratory sheets were prepared using refined/screened MFC, CTMP, and kraft pulp. Cationic starch was used as a strength additive together with MFC. CPAM and silica were used as a retention system. Gained data from the laboratory sheet testing was analyzed using DOE supported analysis software MODDE Pro. Rheological measurements were done using MFC made from hardwood.

Refining and screening of the MFC were done at the Valmet Fiber Technology Center FIB at Inkeroinen using industrial-scale conical OptiFiner Pro refiner and OptiScreen FS-50. Valmet FS5 fiber analyzer was used to analyze the fiber properties of the pulp. Laboratory sheets and rheological measurements were done at the Lappeenranta – Lahti University of Technology in Lappeenranta. The laboratory sheet testing was done at the Valmet Fiber Technology Center FIB at Inkeroinen and Aalto University's Department of Bioproducts and Biosystems in Espoo. The purpose of the laboratory sheet trial was to determine the difference between soft- and hardwood produced MFC and to study the effect of replacing the kraft pulp with CTMP. The effect of screening, starch addition, and storage time of MFC on paper properties was also studied. Rheological flow properties were studied to determine the apparent viscosity in different flow rates, pipe sizes and consistencies of MFC.

8.1 Used materials

MFCs for laboratory sheet trials were produced by refining bleached birch kraft pulp and bleached pine kraft pulp from the case mill. The refining of MFC was done at Valmet Fiber

Technology Center FIB at Inkeroinen. Before the laboratory sheet making MFCs were diluted with deionized water to 0.75 wt% using pulp disintegrator shown in Figure 21.

Figure 21 Pulp disintegrator used to dilute and disintegrate MFC from ~4 wt% to 0.75 wt%.

CTMP, bleached birch kraft pulp, cationic wheat starch (CS; HI-CAT® 3353A), cationic polyacrylamide (CPAM; Fennopol K 3400P) and colloidal silica (FennoSil 5000) for laboratory sheet trials were provided by the case mill. CTMP and kraft pulp were diluted suitable with tap water. Consistencies were measured before making the sheets.

CPAM and silica were provided in liquid suspensions and diluted suitable with deionized water. Starch was provided in a solid form and cooked afterward. 6 grams of cationic wheat starch was added to 400 ml deionized water. After this, the mixture was heated to 90 °C in a water bath and cooked for 15 minutes constantly stirring. The solution was cooled down to room temperature and diluted to the volume of 2 liters.

All materials were stored at a low temperature of 4 to 6 °C except silica, which was stored in a dark place at room temperature according to the safety data sheet. Storage time before the first

laboratory sheet making was 2-3 days. For the second laboratory sheet making, the storage time was around 38-40 days. Sheets made from screened MFC were done 1-2 days after refining and screening.

8.2 Methods

MFC was refined using two different raw materials bleached birch and pine kraft pulp using Valmet OptiFiner Pro conical refiner. Screening trials using bleached birch kraft pulp were done with OptiScreen FS-50. Laboratory sheets were made using MFCs made from these trials. Methods for refining and screening, laboratory sheet making and testing, and rheological measurements are presented in this chapter. Laboratory sheet compositions are presented in Appendix II.

8.2.1 Refining of MFC

MFC was refined from bleached birch kraft pulp and bleached pine kraft pulp with Valmet OptiFiner Pro conical LC-refiner shown in Figure 22. Before refining pulp was diluted to the consistency of 6 wt% and slushed at 50 °C for 10 minutes with Valmet OptiSlush bale pulper equipped with JP rotor and extraction plate (Ø 18 mm). Rotor rotation speed was 220 rpm and pulper power for birch was 30 kW and for pine 35 kW. To avoid bacterial growth preservative biocide BIM MC 4901 was added to the pulp (17.5 L/t).

After slushing the pulp was pumped to the refiner feed chest and diluted to the consistency of 4 wt%. Refining was done using Valmet OptiFiner Pro conical refiner using PRO1F01 fillings shown in Figure 22. The cutting length of the fillings was 18.9 km/rev. Rotor speed was 1500 rpm and refiner feed flow for hardwood refining was 15 L/s and for softwood refining 20 L/s. Production of hardwood refining was 2.2 t/h and softwood 2.8 t/h.

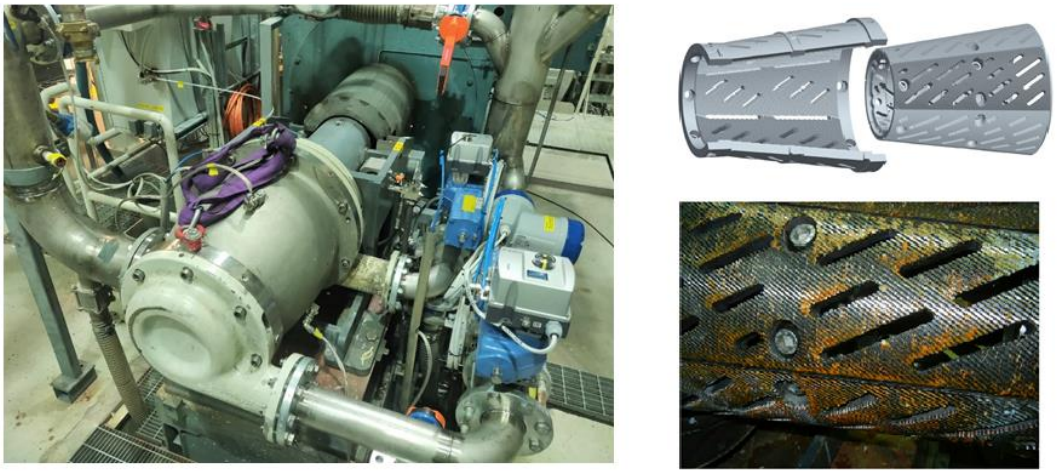

Figure 22 Valmet OptiFiner Pro conical refiner (left) and PRO1F01 fillings used in MFC refining (right).

Pulp was fed into the refiner with two inlet feeds (2&3) from the feed chest. The homogenization round was done first with fillings gap 0.6 mm to homogenize the pulp. MFC made from bleached birch kraft pulp was circulated through the refiner 26 times and the MFC made from bleached pine pulp 42 times. Cumulative specific energy consumption (SRE) for hardwood was 820 kWh/t and for softwood 1540 kWh/t. The process flow sheet of the slushing and refining process is shown in Figure 23.

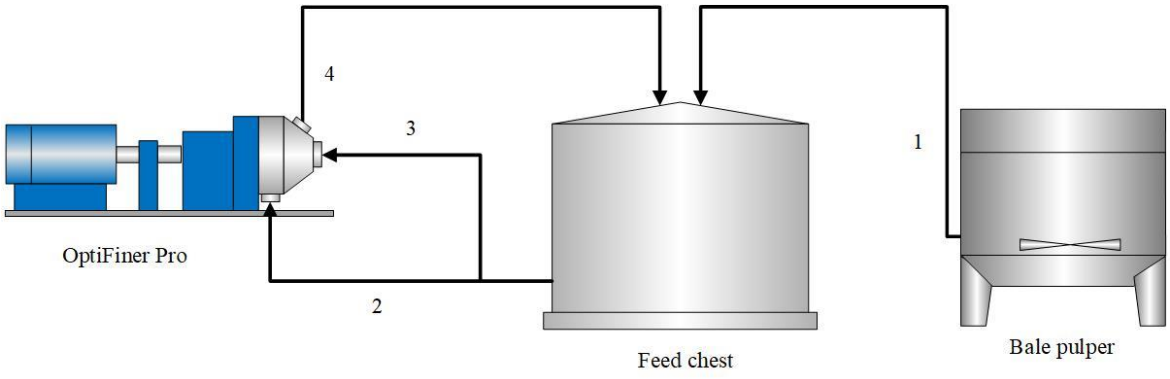

Figure 23 Slushing and refining process flowsheet. Before refining pulp was fed from the bale pulper to the feed tank chest (1). Pulp was fed into the refiner with two inlet feeds (2&3) and circulated back to the feed tank (4).

Sample from the feed was taken during the homogenization round. Samples from the refined product were taken after every pass. Schopper-Riegler number, consistency, and fiber properties were measured from every third sample. Fiber properties were analyzed using the Valmet FS5 fiber analyzer shown in Figure 24. FS5 measures fiber dimensions, fines, kinks, fibrillation, flocs and curl.

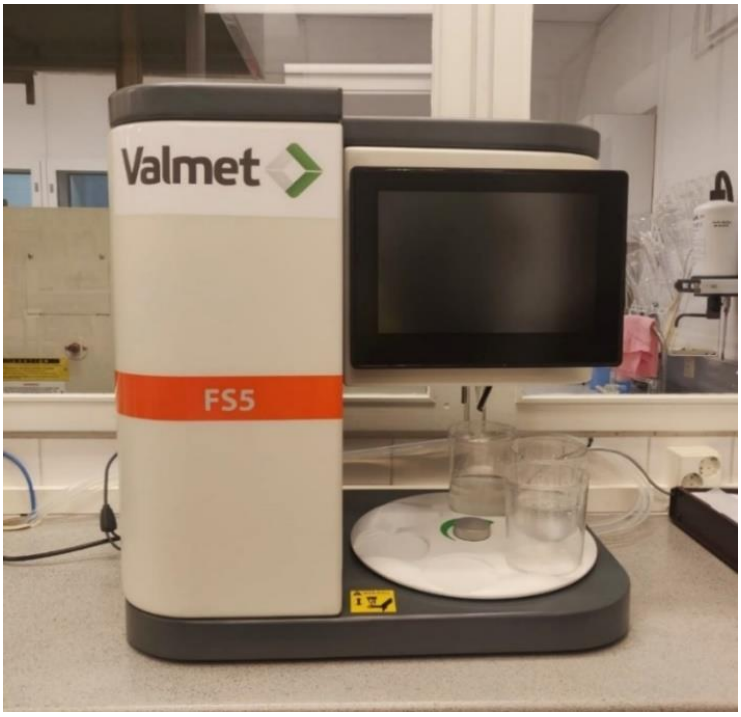

Figure 24 Valmet FS5 fiber analyzer.

The minimum width for hardwood fibers was set to 5 µm (hardwood program) and for softwood fibers to 10 µm (softwood program). Both samples were measured also using minimum width of 0 µm (MFC program). In Table VIII are shown the definitions of FS5 fiber analyzer properties.

Table VIII Valmet FS5 fiber analyzer definitions.

Property	Definition
Fiber length Lc(l) Tappi, mm	Particles whose width is 10-75 µm and length 0.00-7.60 mm
Fiber length Lc(l) ISO, mm	Particles whose width is 10-75 µm and length 0.20-7.00 mm
Fiber width, µm	Calculated from particles whose length is 0.20-7.60 mm and width 10-75 µm.
Fines A, %	Dust-like fines, which is the sum projection area of particles shorter than 0.20 mm and under 75 µm in width compared to the sum projection area of all particles
Fines B, %	Fibril-like fines, which is the sum length of particles 0.20-7.60 mm in length and under 10 µm in width compared to the sum length of particles 0.20-7.60 mm in length and under 75 µm in width
Fines F(n), %	Number of particles 0.00-0.20 mm in length and 10-75 µm in width compared to the number of particles 0.00-7.60 mm in length and 10-75 µm in width
Fibrillation, %	Recorded from particles whose length is 0.50-7.60 mm and width 10-75 µm. Fibrillation index is calculated in ratio to the Tappi fibers and fibrillation
Curl, %	Calculated from particles whose length is 0.05-7.60 mm and width 10-75 µm
Kinks, %	Recorded from particles whose length is 0.20-7.60 mm and width 10-75 µm

8.2.2 Screening of MFC

MFC produced in screening trial was made from the same bleached birch kraft pulp as in refining trials. The same process conditions and parameters for slushing were used as in refining trials for hardwood pulp. After the slushing pulp was diluted to the consistency of 4 wt%. After this the refining was done with OptiFiner Pro conical refiner with fillings shown in Figure 22. Refiner feed flow was 20 L/s and production was 2.9 t/h. Pulp was circulated 13 times through the refiner and the cumulative SRE was 340 kWh/t.

After the refining pulp was diluted to 2.0 wt% and pumped to the fractionation feed chest. Screening trials were done using OptiScreen FS-50 equipped with a C-rotor circulating the accept and reject flows back to the feed chest. Two different types of slotted screen baskets were used: #0,15 mm 100C (0,9) and #0,10 mm 90 (0,0). MFC produced with #0,10 mm 90 (0,0) was used to make laboratory sheets. In Table IX, are shown the process conditions used in the screening of MFC which was used for making the laboratory sheets.

Table IX Process conditions in the screening of MFC used in laboratory sheets.

Screen basket	**Screen rotor [rpm]**	**Reject ratio by volume, RRV [%]**	**Reject ratio by mass, RRM [%]**	**Thickening factor**
#0,10 mm 90 (0,0)	558	30.0	57.8	1.93

As in refining trials, samples were taken after every pass. Schopper-Riegler number, consistency, and fiber properties were measured from every third sample. Fiber properties were analyzed with the Valmet FS5 Fiber analyzer. Hardwood program was used where minimum fiber length was set to be 5 µm. Samples were collected from the feed, accept, and reject. The same measurements were done from the screening samples as from the refining samples.

8.2.3 Laboratory sheet preparation

Laboratory sheets were done according to the ISO 5269-1 standard. Pulp for each laboratory sheet was mixed 1200 rpm with an overhead stirrer shown in Figure 25. CTMP, birch kraft pulp, and water were weighted and stirred for 1 minute. Then MFC was added and stirred for 30 seconds. After this cationic starch was added with an automated pipette and stirred for 2 minutes. Then CPAM was added and stirred for 30 seconds. Lastly, silica was added and stirred 30 seconds. Laboratory sheets were done using 60 wt% of CTMP, 40 wt% of kraft pulp, 0.5 wt% of CS, 0.02 wt% of CPAM, and 0.05 wt% of silica. The amount of CS, CPAM, and silica was increased in some samples.

After the mixing, the pulp mixture was poured into the KCL sheet former (165 x 165 mm) which was filled with tap water. Freshwater was used for sheet making. The air agitator was activated, and the drainage valve was opened 10 seconds after agitation was completed. The sheet was drained on the wire 10% of the draining time. One new blotter and two used blotters were placed on top of the sheet. The couch was placed on top of the sheet and blotters for 20 seconds as seen from Figure 25. Sheets were piled on a straight pile for wet pressing. Each sheet was between new blotters and used blotters. In Figure 25, are shown the overhead stirrer and KCL sheet former.

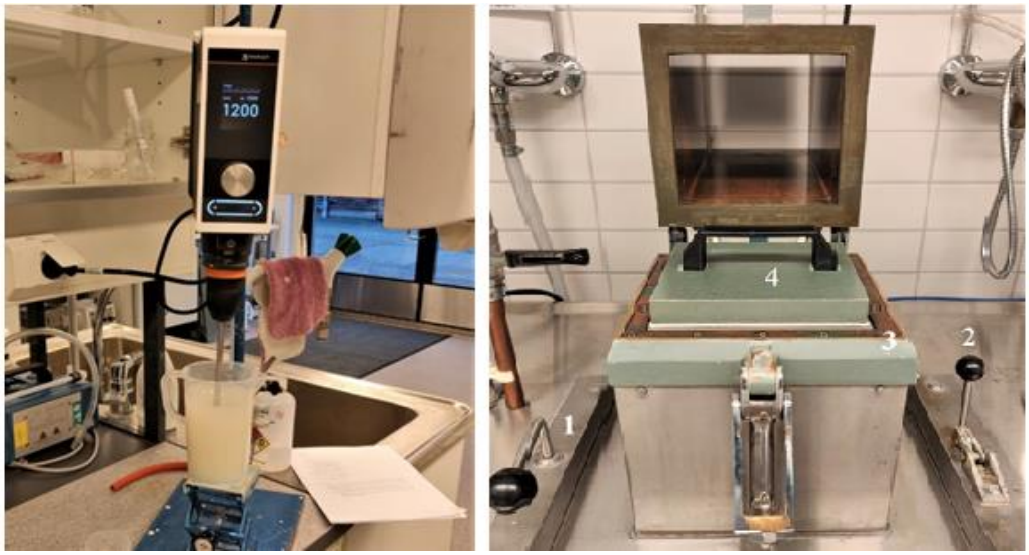

Figure 25 Overhead stirrer (left) and KCL sheet former (right). 1) Water valve 2) Drainage valve 3) Wire 4) Couch

Sheets were pressed between press plates and blotters for 5 minutes under 410 kPa. After the wet pressing sheets were dried in a drum dryer for 2 hours at 60 °C. The drum dryer was heated before sheets were placed to dry. In Figure 26, are shown the wet pressing machine and a drum dryer. Laboratory sheet testing was done after conditioning samples for at least 4 hours in a condition room.

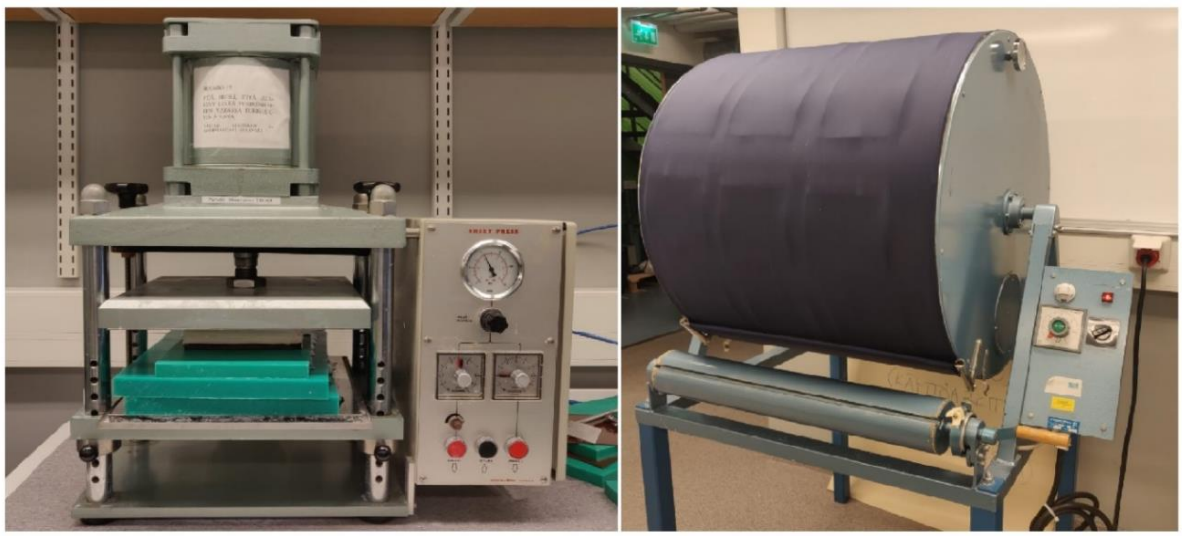

Figure 26 Wet pressing machine (left) and drum dryer (right).

8.2.4 Laboratory sheet testing

Measurements were done in a condition room at 23°C and relative humidity of 50%. Samples were stored in a condition room at least for 4 hours before testing according to ISO 187. Sheets were cut to 155 x 155 mm size before testing. Measurements and standards used are shown in Table X. Other measurements except the SCT compressive strength were measured at Valmet Fiber Technology Center FIB at Inkeroinen. SCT compressive strength was measured at Aalto University's Department of Bioproducts and Biosystems in Espoo.

Table X Measurements and standards of laboratory sheet testing.

Property	Equipment	Measurement method/standard
Grammage	-	ISO 536:2019
Thickness	L&W SE51D2M type 221	ISO 534:2011
Tear strength	L&W Elmendorf SE09ED type 1-1 Type A App. 09ED	ISO 1974:2012
Tensile strength	L&W Tensile Tester 066 (200 N)	ISO 1924-2:2008
Compression strength (SCT)	TMI Compression SCT K455 Buchel	ISO 9895:2008 TAPPI T826
Internal bond strength, Scott bond	Huygen Internal ScottBond	ISO 16260:2016 TAPPI 569 om-14

Grammage was calculated from each sheet that was used for measurements according to the ISO 536:2019 standard from Equation 11.

$$g = \frac{\bar{m}}{\bar{A}} * 10^6 \quad (11)$$

Where,

$\bar{A}$ = Average area of the sample, mm

g = grammage of the sheet, g/m^2

$\bar{m}$ = Average mass of the sample, g

Thickness was measured from two sheets after the grammage measurements according to the ISO 534:2011 standard. 10 parallel measurements were done, five from each sheet. Density was calculated from thickness and grammage with Equation 12. Bulk is the inverse of density, 1/density, expressed as cm^3/g.

$$\rho = \frac{g}{\delta} * 10^6 \quad (12)$$

Where,

δ = Average thickness of the sheet, µm

ρ = Sheet density, kg/m^3

Tear strength was measured according to the ISO 1974:2012 from a pile of four test pieces. 6 parallel measurements were done from three sheets. Test pieces were 62 mm ± 0.5 mm in height and 50 mm ± 2.0 mm in width.

Tensile strength was measured according to the ISO 1924-2:2008 from 8 test pieces that were cut to 155mm length and width of 15 mm. Test pieces were cut from two sheets. The distance between clamps was set to 100mm.

Compression strength was measured according to ISO 9895:2008 and TAPPI T826 from test pieces that were cut to a width of 15 mm. 30 parallel measurements were done from three sheets.

Internal bond strength was measured according to ISO 16260:2016 and Tappi 569 om-14 from two sheets. Test pieces were cut to a length of 155 mm and a width of 25.4 mm. The test piece was placed between the double-sided tape. Aluminum base and angle were placed on top of the tape and test piece. Test pieces were pressurized at 6.9 bar for 10 seconds. After this the samples were cut to 5 pieces (25.4 x 25.4 mm), placed to the sample holder and pendulum was released.

8.2.5 Rheological measurements

Rheological properties of MFC were measured with Anton Paar MCR 302 modular compact rheometer using concentric cylinder geometry CC27 and ST24-2D/2V/2V-30/109 stirrer. Measurements were carried out at shear rates from 1 to 100 s^{-1} in three different concentrations 1, 2, and 3 wt% at 20 °C. The effect of temperature was studied at 10 and 30 °C with 2 wt% concentration. Samples were diluted to target concentrations and dispersed with overhead stirrer overnight shown in Figure 25. Three parallel measurements were done with 21 points in 2 seconds. Samples were stirred 30 minutes before the first measurement, then 5 minutes between the measurements. 1 wt% sample was stirred in 500 s^{-1}, 2 wt% in 1000 s^{-1} and 3 wt% in 1500 s^{-1}. Amplitude sweep was done at 2 wt% concentration with shear strain from 0.1 to 1000 % and angular frequency of 10 rad/s. Before the amplitude sweep measurement, the sample was stirred at 1000 s^{-1} for 5 min.

9 RESULTS AND DISCUSSION

In the following chapters results from laboratory sheet trials, refining and screening trials and results from rheological measurements are presented. Partial least squares (PLS) regression was done with Umetrics MODDE Pro 12.1 (www.umetrics.com/product/modde-pro) to analyze the data from laboratory sheet testing.

9.1 Refining and screening

In every third passes through the refiner samples were analyzed with Valmet FS5 fiber analyzer. Results from refining and screening trials are shown in Appendix I. In Figure 27, is shown Schopper-Riegler number as a function cumulative SRE.

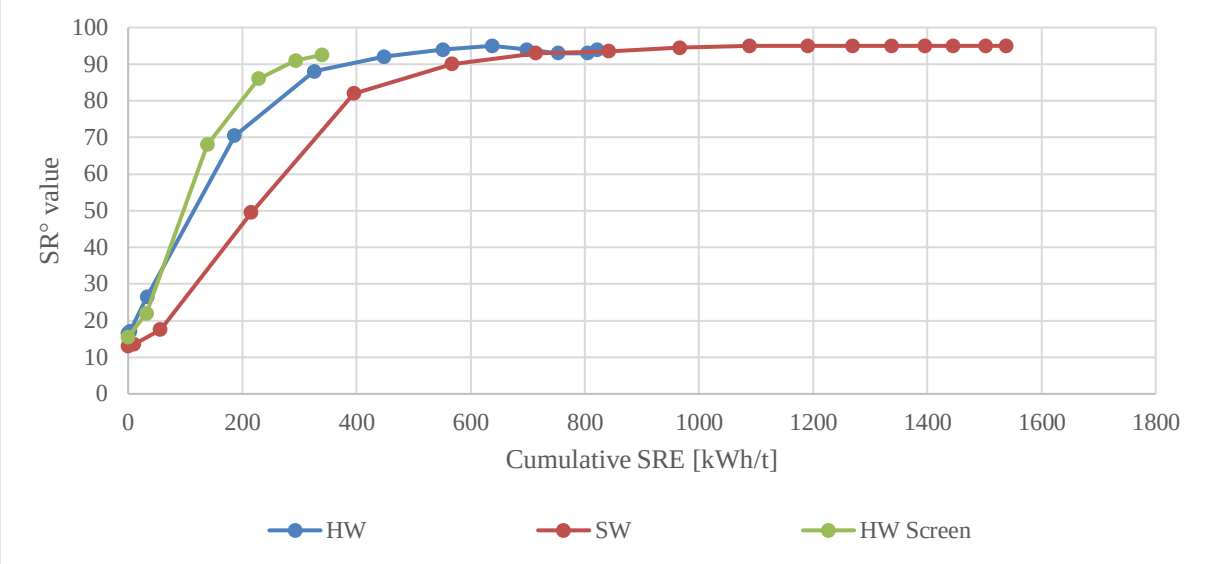

Figure 27 Schopper-Riegler number as a function of cumulative SRE.

As seen from the results Schopper-Riegler number of 93° was achieved in all of the refining trials. In SW refining the number increased from 13 to 94° in 16 passes through the refiner. Cumulative SRE was 840 kWh/t when SR number 94° was achieved. In HW refining the number increased from 17 to 94° after 13 passes at cumulative SRE of 550 kWh/t. Measured SR number of the final SW and HW pulp were 95° and 94°, respectively. In screening trials, the pulp was circulated 13 passes before the screening. SR number increased from 16 to 93° at a cumulative SRE of 340 kWh/t. In soft- and hardwood refining the number stayed constant after 13 to 16 passes through the refiner. This is due to the fact that the Schopper-Riegler measurement loses accuracy when the fibrils and fines pass the wire used in the measurements. For achieving the best understanding from the refining other parameters like fibrillation and the number of fines were measured. In Figure 28, is shown the fines particles F(n) as a function of cumulative SRE.

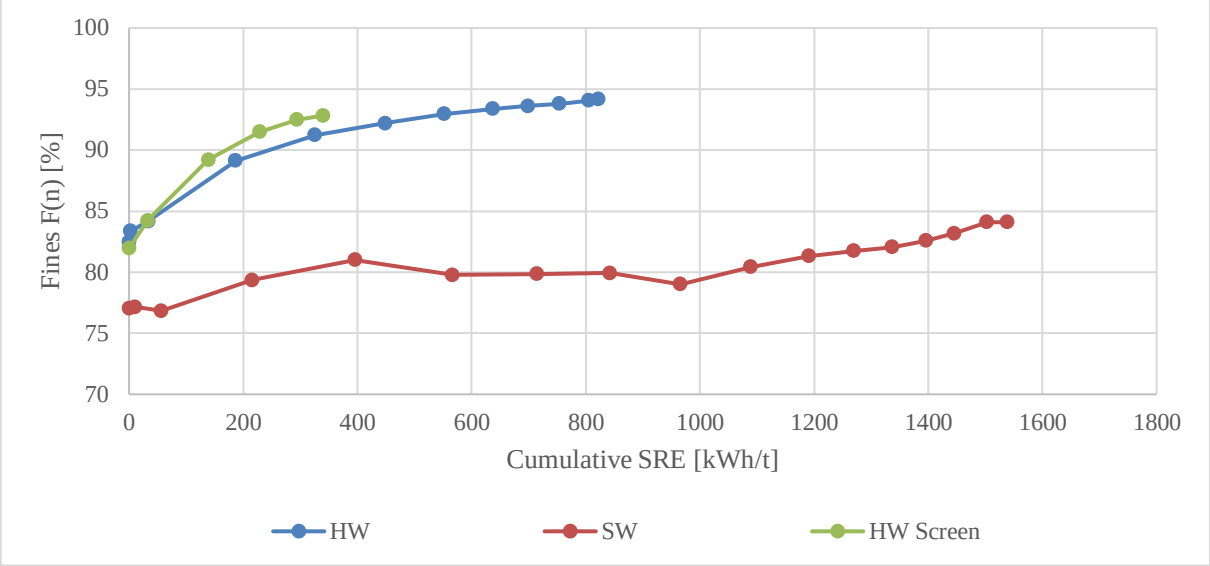

Figure 28 Fines F(n) as a function of cumulative SRE.

The number of fines particles increased from 77 to 84% in SW refining and 83 to 94% in HW refining. In the screening trial, the number of fines particles in unrefined pulp was 82% and after 13 passes 93%. The number of fines particles increased slightly faster in screening trials than with HW MFC refining trials. The number of dust-like fines A are presented as a function of cumulative SRE in Figure 29.

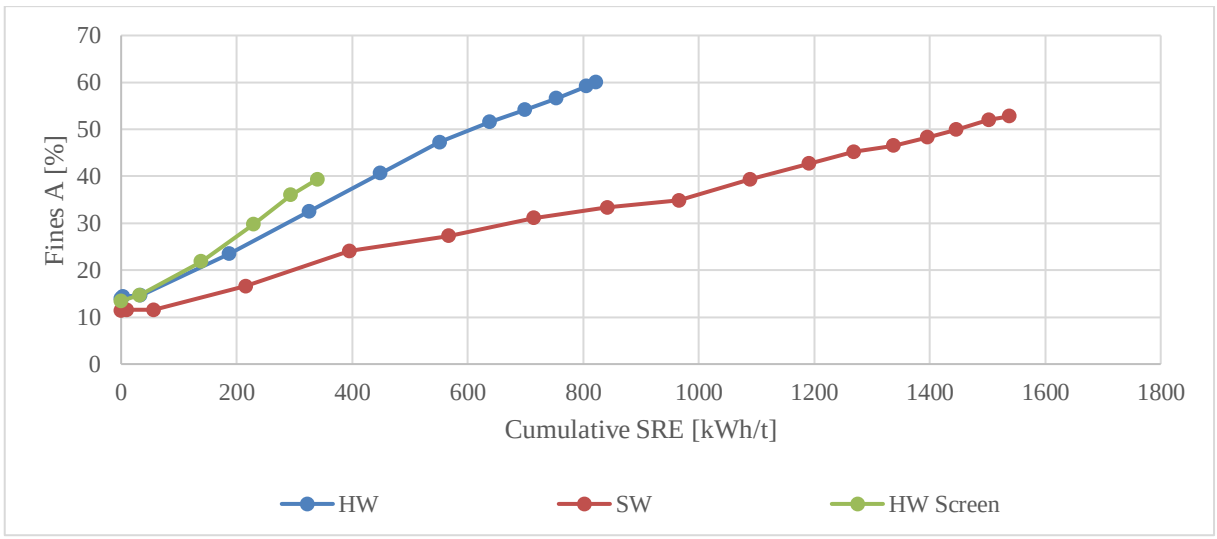

Figure 29 Fines A as a function of cumulative SRE.

According to Figure 29 in SW refining the number of dust-like fines was increased from 11 to 53 %. In HW refining the increase was from 14 to 60 %. In HW refining the number of fines A increased faster than with SW MFC. After 13 passes the number of fines A was increased from 14 to 39% in screening trials and for the HW refining trials from 11 to 47 %. In Figure 30, is shown the development of fibril-like fines B.

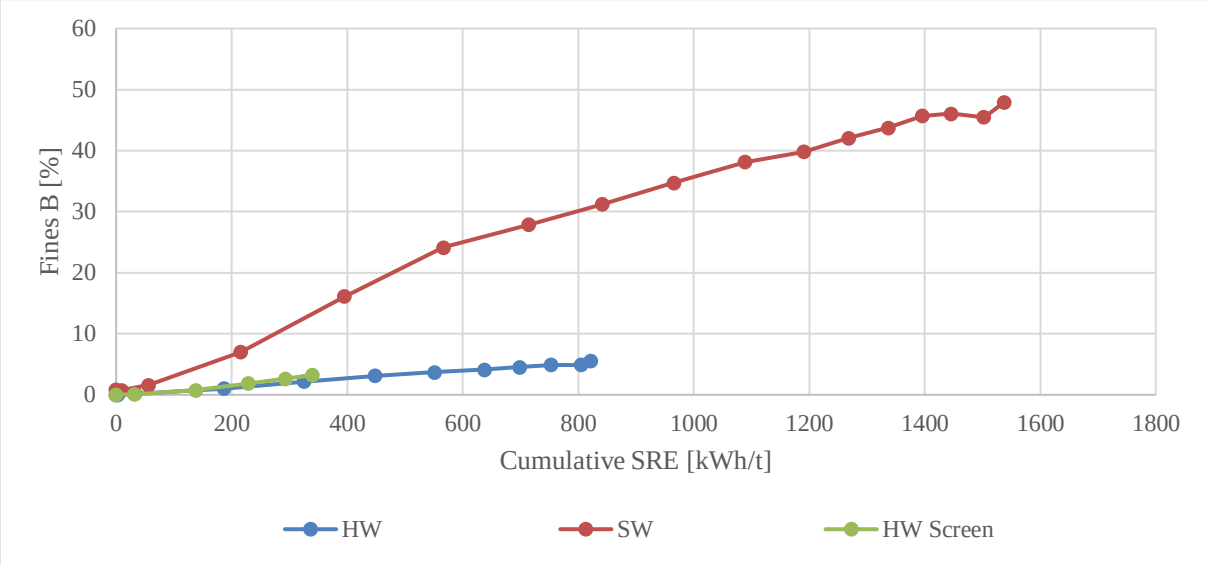

Figure 30 Fines B as a function of cumulative SRE.

In SW refining the number of fibril-like fines was increased from 1 to 38%. In HW refining the development was slighter from 0% to 6%. In screening trials, the increase achieved with cumulative SRE of 340 kWh/t was from 0 to 3%. In HW refining the number of fines B was 2% when cumulative SRE was around 330 kWh/t. In SW refining the development of fines B was faster and the number fines B greater. In Figure 31, is shown the fibrillation as a function of cumulative SRE.

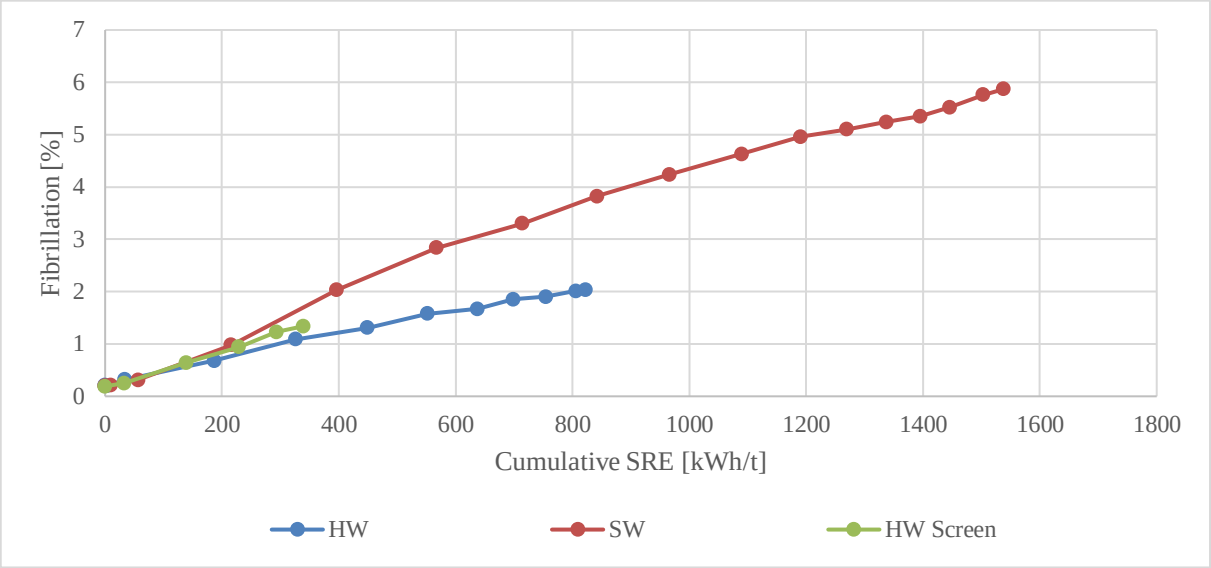

Figure 31 Fibrillation as a function of cumulative SRE.

The fibrillation of SW MFC proceeded faster than the HW MFC requiring less energy to certain fibrillation level. Fibrillation in screening trials proceeded a little faster than in refining trials. The same kind of results were shown in study of Stelte & Sanadi (2009). In their study, they showed that the fibrillation of softwood pulp proceeded faster than with hardwood pulp. It was also shown that the homogenization of softwood pulp was more energy-efficient and needed fewer passes through the homogenizer than hardwood pulp. (Stelte & Sanadi, 2009) However, these results cannot be compared since different production methods were used. Even though the fibrillation proceeded faster with softwood a greater number of smaller fines (Fr(l) 0.00-0.20 mm) were achieved with less energy in HW refining than in SW refining. The number of these fines in HW MFC was 69% and with SW MFC 46%. These results are shown in Appendix I.

In Figure 32, is presented a comparison between refining trials and screening trials. Fiber length Tappi, Fines F(n), Fines A, Fines B and some length weighted fractions Lc(I) Tappi are shown.

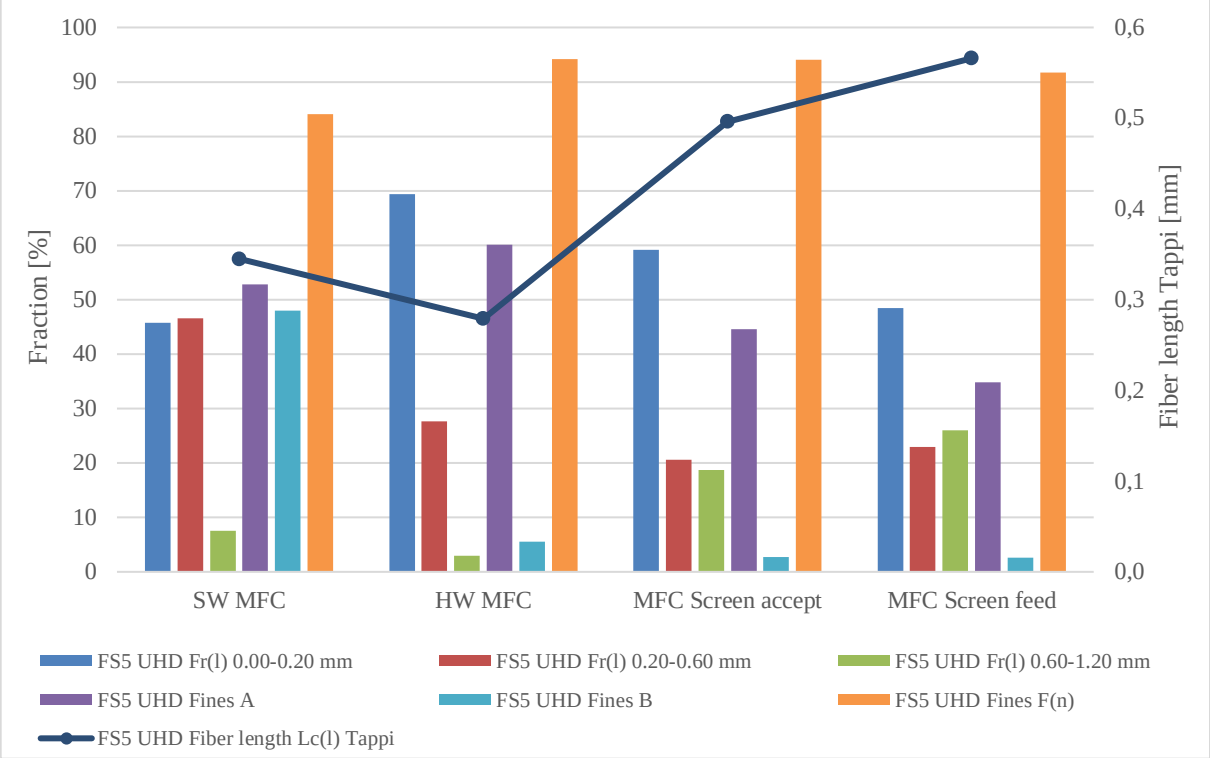

Figure 32 FS5 results. Comparison between refined SW and HW MFC, screened MFC, and feed. UHD=ultra-high definition, Fr(l)= weighted length fractions Lc(I) Tappi.

When comparing the SW and HW refining together the quality of the final MFC was different. The number of fibril-like fines (fines B) in SW refining was 43% and in HW refining only 6%. Energy applied in SW refining was 1540 kWh/t and in HW refining 820 kWh/t. This is due to the length of fibers in softwood. Softwood has longer fibers than hardwood, so the breaking of these fibers requires more energy than shorter hardwood fibers. This can be shown also from the passes through the refiner. In softwood refining, the pulp was circulated 42 times and in hardwood refining 26 times. The major difference between the fines B amounts can also be due to the longer fibers of softwood. Fiber length Tappi with SW MFC was 0.35 and with HW MFC 0.28. Since the refining intensity is inversely proportional to the cutting edge length, greater amount of fines B for HW MFC could have achieved using different fillings. For example, the cutting edge length of FF1 fillings is 2.5 times bigger than with used F01 fillings. In her work, Korelin (2020) used FF1 fillings in the refining of MFC from bleached eucalyptus pulp. The MFC produced in her work, had higher strength potential compared to the HW MFC produced

in this work with F01 fillings. In the work of Korelin (2020), the obtained number of fines B with energy consumption around 820 kWh/t was 13.5%. The difference between these HW MFCs can be due to the different fillings used in the refining. In her work, Korelin (2020) used 2.5 wt% of MFC for making both CTMP and OCC sheets.

When HW refining and screening trials are compared the energy needed in refining at screening trials was slightly lower than with HW refining. In HW refining after 13 passes the cumulative SRE was 550 kWh/t and in screening trial 340 kWh/t. When compared to the refining trials the fiber properties developed slightly faster in screening trials. When the quality of screened MFC was compared to the refined HW MFC it can be seen that the number of fines B was smaller in screened than in refined. In refined MFC the fines B amount was 6% and in screened MFC only 3%. This is due to the fewer passes through the refiner. Fiber length Tappi in accept was longer than with refined HW MFC. In refined MFC the length was 0.28 and with screened MFC 0.50.

When screened MFC accept is compared to the feed sample it can be seen that the amount fines B increased slightly when the sample was screened. Amount fines B in the accept was 2.7% and in feed 2.6%. Fines A increased from feed to accept from 35 to 45%. The number of 0-0.20 mm fines was greater with the accept than in the feed sample. Also, the fiber length Tappi was longer with the feed sample than it was with the accept. For gaining better results, screening trials should be done using different screen baskets, process parameters, and smaller slot widths and hole baskets. Also, the timing of the screening stage could affect the results. In this case, the screening was done from pulp that was in the middle of the refining process.

9.2 Paper properties

The impact of different variables on paper properties was studied. Results are presented in index form which means that the strength property is divided by the average grammage of the sheet. All the results are compared to reference points and the change in percentages is shown. PLS regression was done using the mean results. Outliers (<10% of data points) were removed from the results before the mean results were calculated. In indices plots error bars show the standard deviation of the data points.

In the first laboratory sheet trial, the effect of raw material and the base pulp composition were studied. Also, cationic starch addition from 0.5 to 0.8 wt% was studied. In the second laboratory sheet trial, the effect of cationic starch and storage time of MFC was studied. Refined HW MFC was used and the CTMP/kraft pulp ratio was 60/40. In the third laboratory trial, the effect of screened HW MFC was studied and the results were compared with refined HW MFC.

9.2.1 First laboratory sheet trial - Effect of raw material and base pulp composition

The effect of raw material was studied using bleached birch and pine kraft pulp for the refining of MFC. Base pulp composition was also studied by increasing the CTMP dosage in sheets. The CTMP dosage was 60 wt% and kraft pulp 40 wt%. The effect of kraft pulp on paper properties are shown in MODDE Pro results. All the results are compared to a reference point and presented in index form. Figure 33 shows the internal bond indices.

Figure 33 Internal bond indices of hard- and softwood MFC.

As seen from Figure 33, both MFCs had an increasing impact on internal bond strength. Any great differences using soft- and hardwood MFC were not shown. Figure 34 shows the coefficients of the fitted model for which the factors were centered. In Figure 33, is shown the observed versus predicted plot, when the goodness of the fit, R^2, was 0.89 and the goodness of prediction, Q^2, was 0.83.

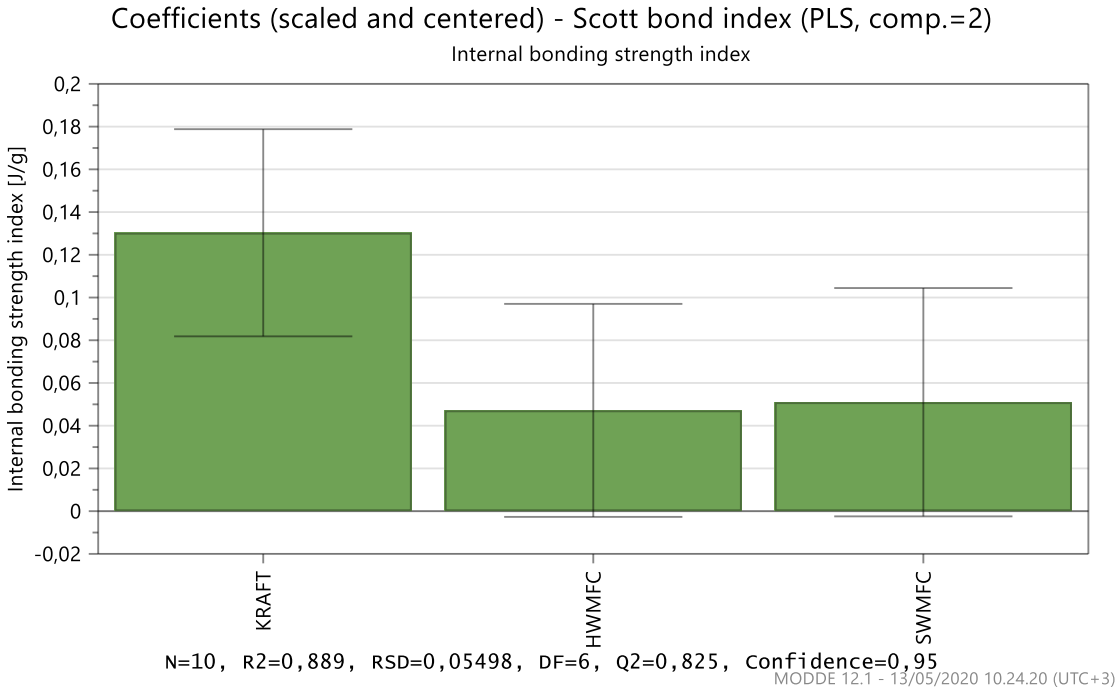

Figure 34 Scaled and centered coefficient plot of kraft pulp, HW MFC, and SW MFC for internal bond index.

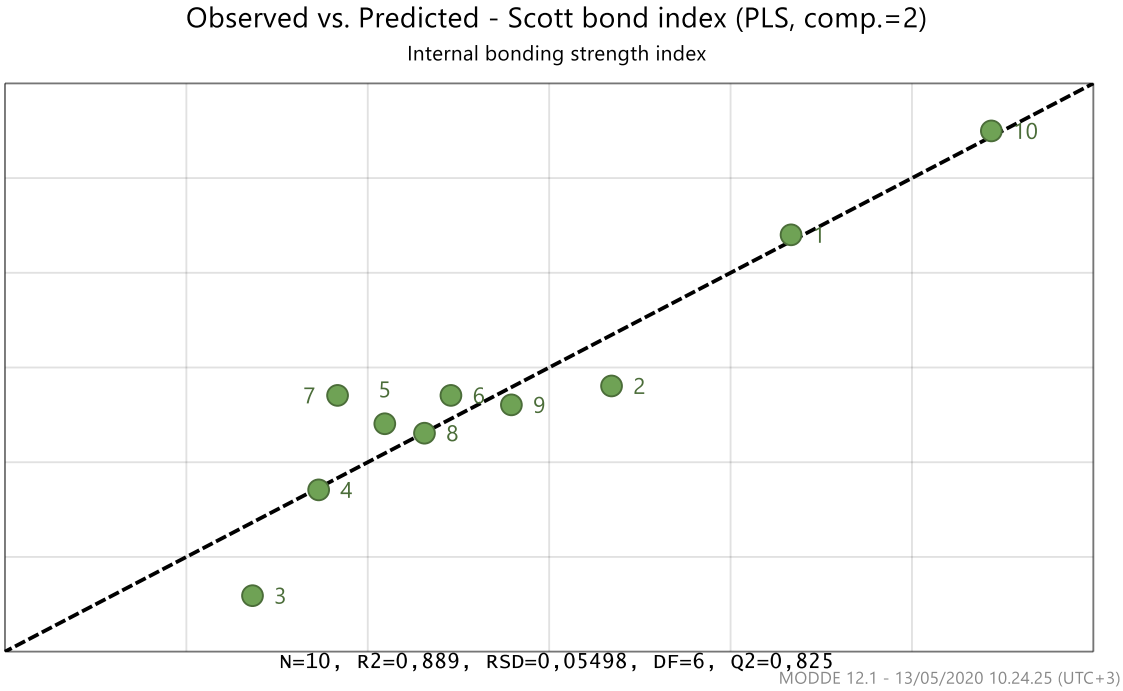

Figure 35 Observed vs. predicted plot of internal bond indices for HW and SW MFC.

Since the R^2 is nearly 0.9 and the Q^2 is higher than 0.7 the model is considered to be reliable. The observed versus predicted plot displays the observed values versus predicted values. A plot, where points are close to the straight line, indicates a good model. As seen from Figure 35, the model is considered good, since most of the points are close to the line. Since the parameters are close to y=0, the effect of these parameters is not that significant. As seen from the coefficient plot, the error bar for kraft pulp is smaller than the parameter effect. The effect of HW MFC and SW MFC are not as clear as the effect of kraft pulp because the parameter effects are smaller than the error bars. However, HW and SW MFC have the same impact on internal bond strength. Figure 36 and Figure 37 shows the response contour plots of kraft pulp as a function of SW and HW MFC.

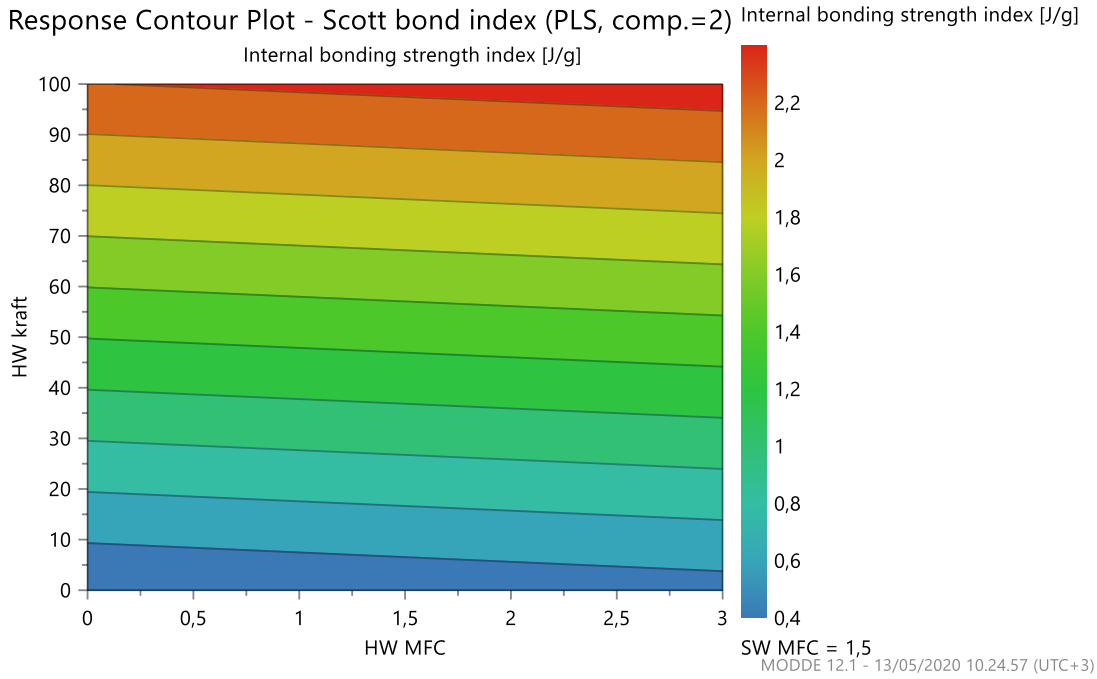

Figure 36 Response contour plot of internal bond index showing kraft pulp as a function of HW MFC.

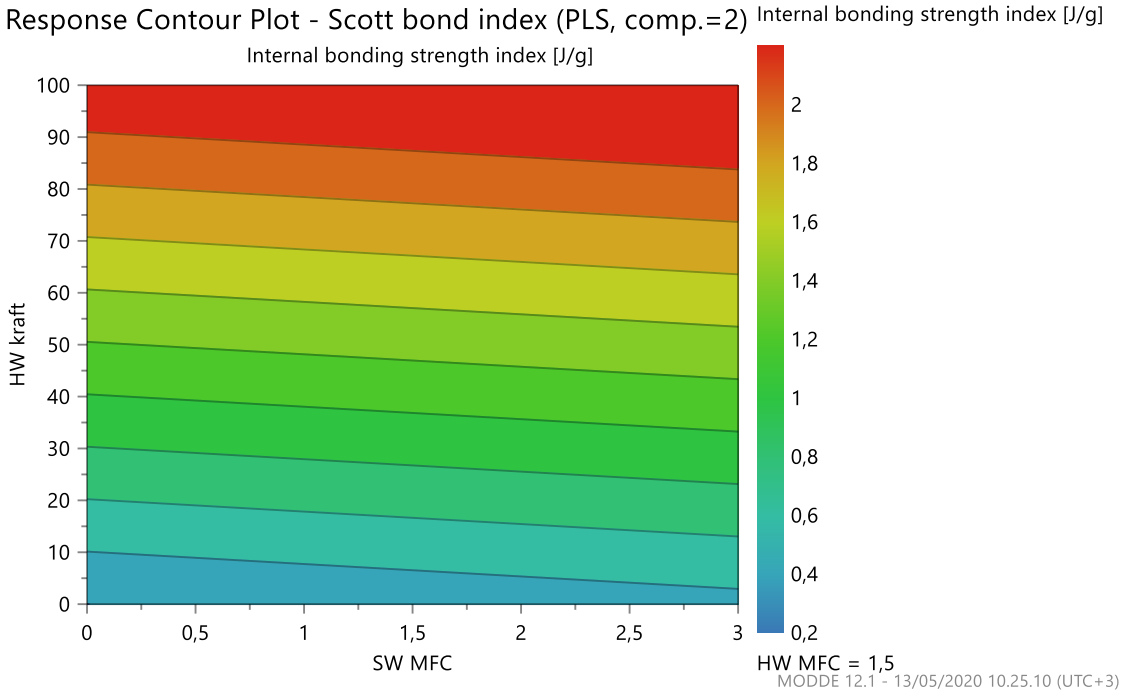

Figure 37 Response contour plot of internal bond index showing kraft pulp as a function of SW MFC.

From the response contour plots, the correlation between the internal bond index and kraft pulp/MFC can be seen. The more kraft pulp and MFC are added to the sheets the higher the internal bond index increases. As seen from Figure 36 and Figure 37, there are no great differences between SW and HW MFC.

In Figure 38, are shown tear indices using HW and SW MFC.

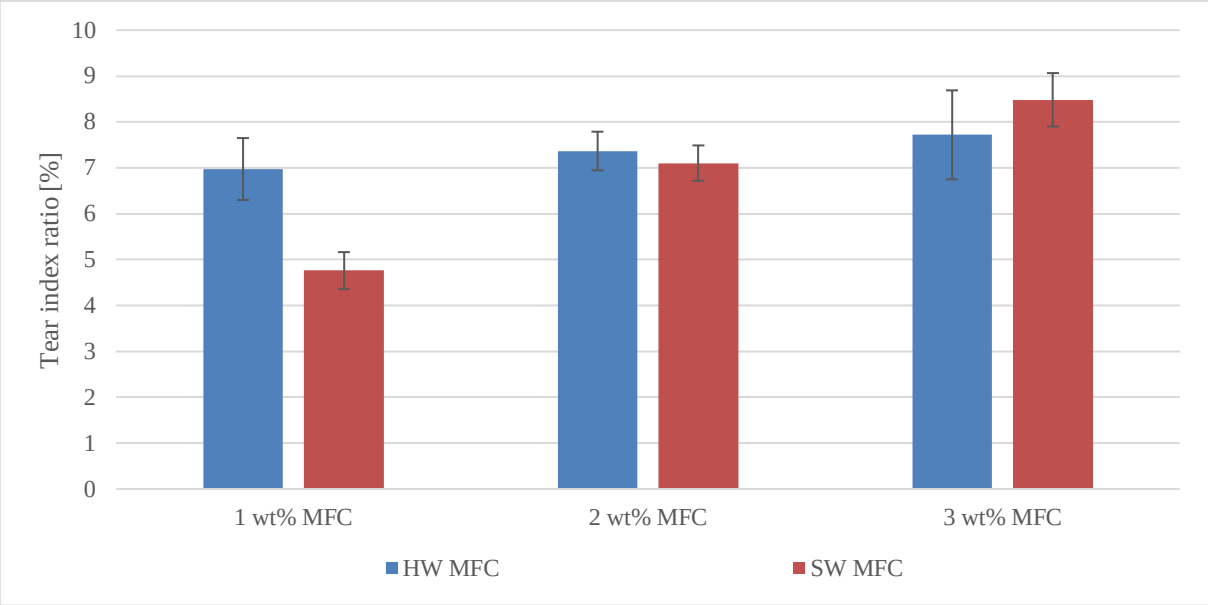

Figure 38 Tear indices of hard- and softwood MFC.

As seen from Figure 38, both HW and SW MFC had a slightly increasing impact on tear indices. Figure 39 shows the coefficients of the fitted model for which the factors were centered. In Figure 40, is shown the observed versus predicted plot when R^2 is 0.83 and Q^2 is 0.67. From these, the effect of the MFC and the model fit can be seen.

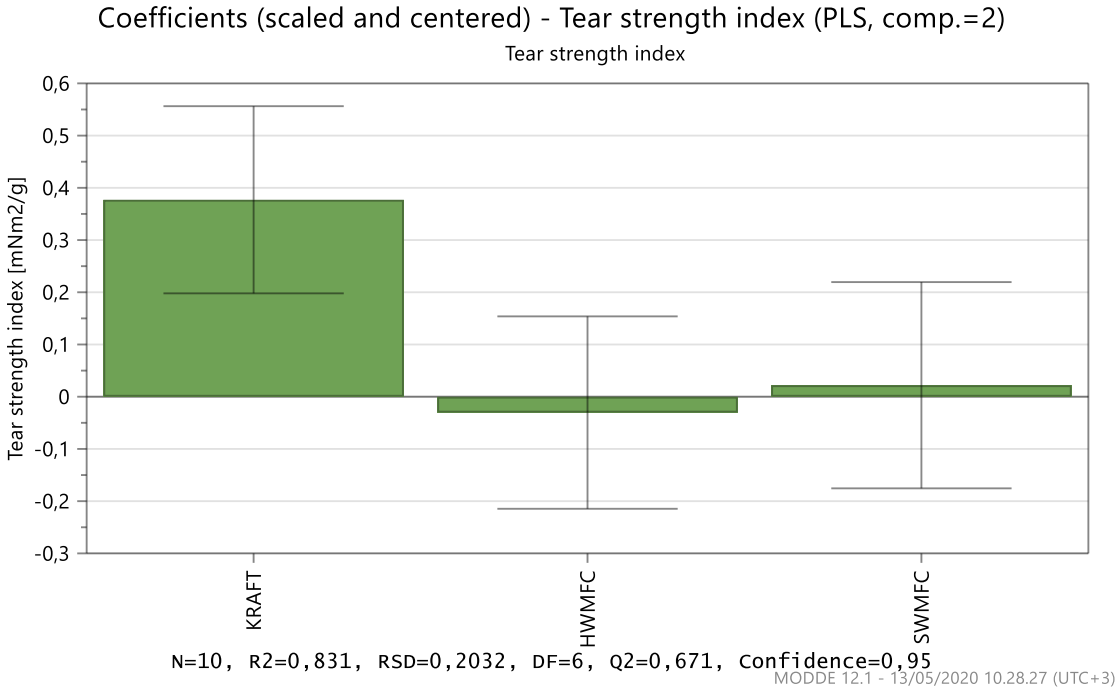

Figure 39 Scaled and centered coefficient plot of kraft pulp, HW MFC, and SW MFC for tear index.

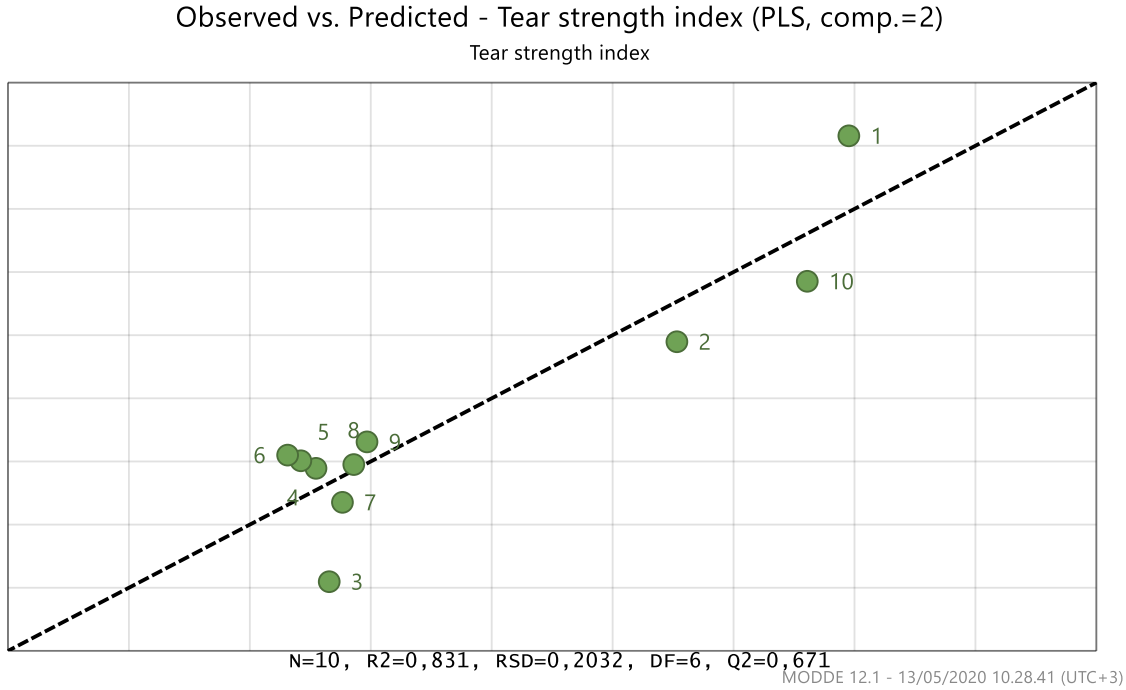

Figure 40 Observed vs predicted plot of tear indices for HW and SW MFC.

Based on the R^2 and Q^2 the model can be considered good. However, the points in observed versus predicted plot are not as close to the line as possible. As seen from the coefficient plot, the error bar for kraft pulp is smaller than the parameter effect. The effect of HW MFC and SW MFC is not as clear because the parameter effects are smaller than the error bars. Since the parameters are close to y=0, the effect of these parameters is not that significant. Figure 41 and Figure 42 shows the response contour plots of tear index.

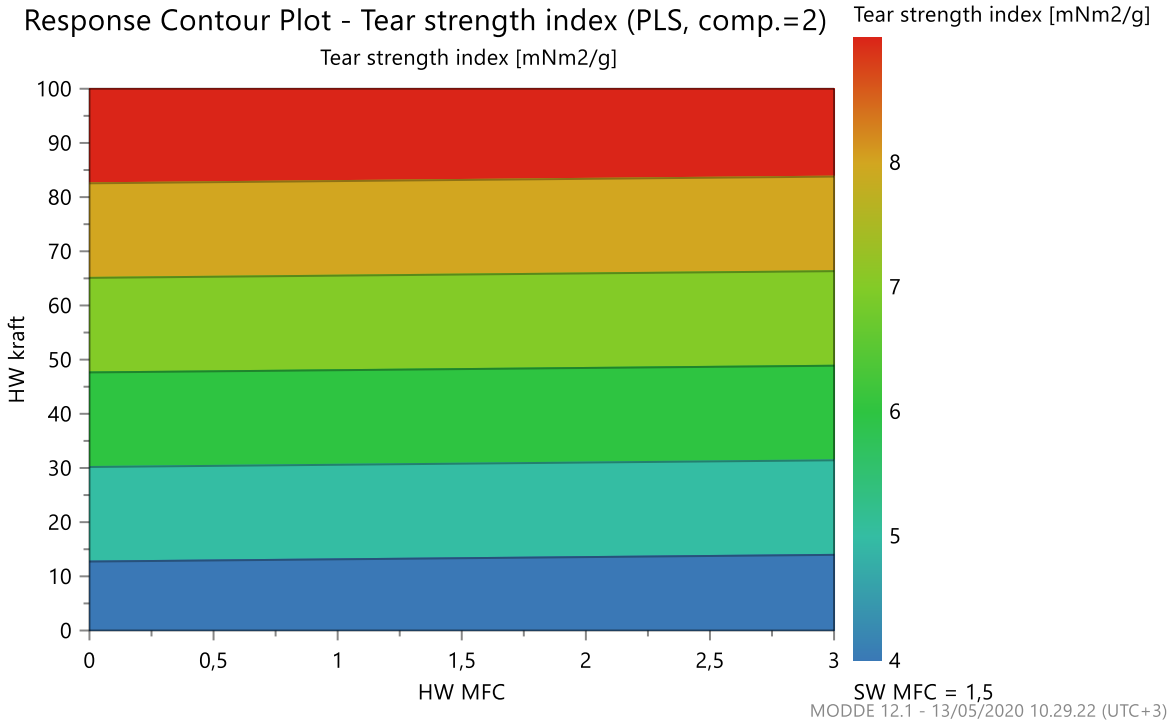

Figure 41 Response contour plot of tear index showing kraft pulp as a function of HW MFC.

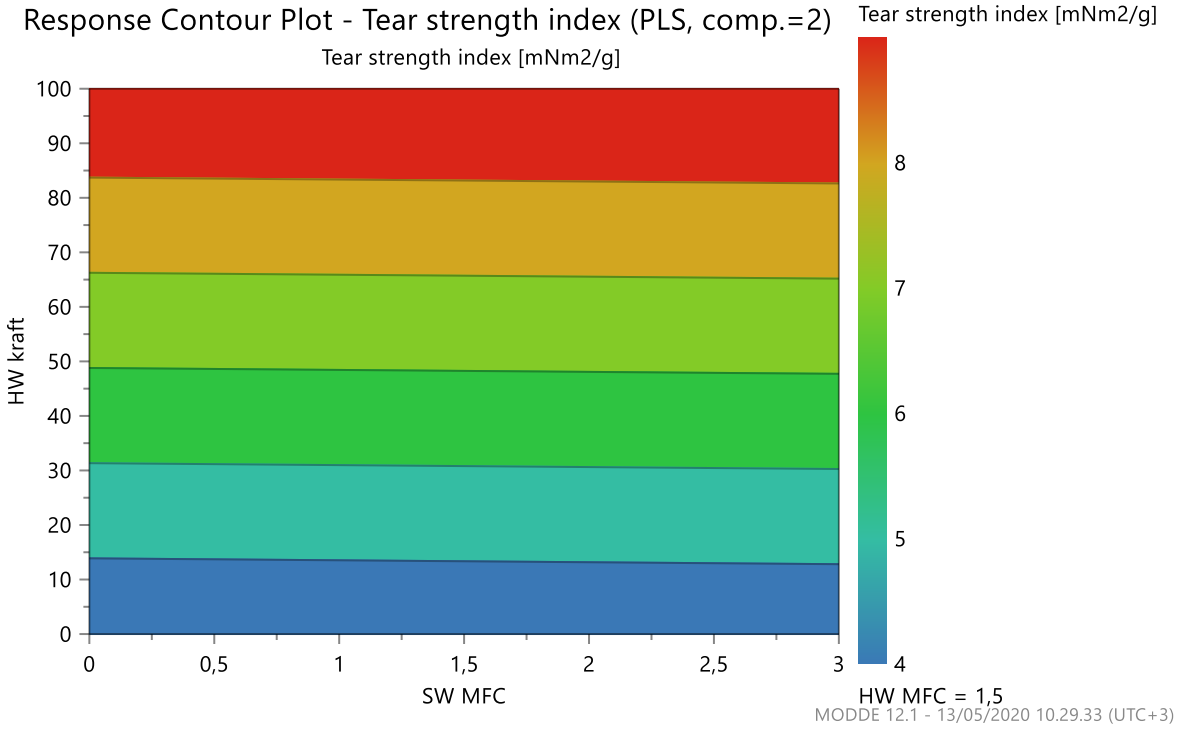

Figure 42 Response contour plot for tear index showing kraft pulp as a function of SW MFC.

From the response contour plots, the correlation between tear index and kraft pulp/MFC can be seen. As seen from the response contour plots MFCs had a very slight impact on tear index. This verifies the effect of MFC seen from the coefficient plot in Figure 39. The more kraft pulp is added to the sheets the better the tear index gets.

In Figure 43, are shown the tensile indices of HW and SW MFC.

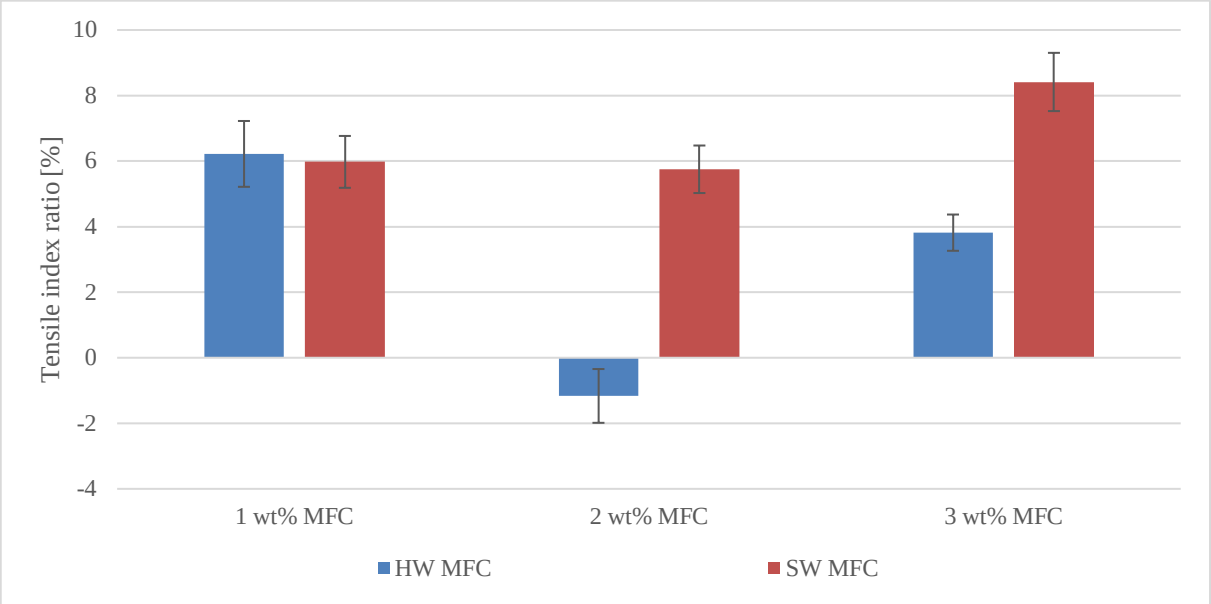

Figure 43 Tensile indices of hard- and softwood MFC.

According to Figure 43, SW MFC had a slightly increasing effect on the tensile index. The effect of HW MFC is not as clear as the effect of SW MFC. Figure 44 shows the coefficients of the fitted model for which the factors were centered. In Figure 45, is shown the observed versus predicted plot when R^2 is 0.86 and Q^2 is 0.59.

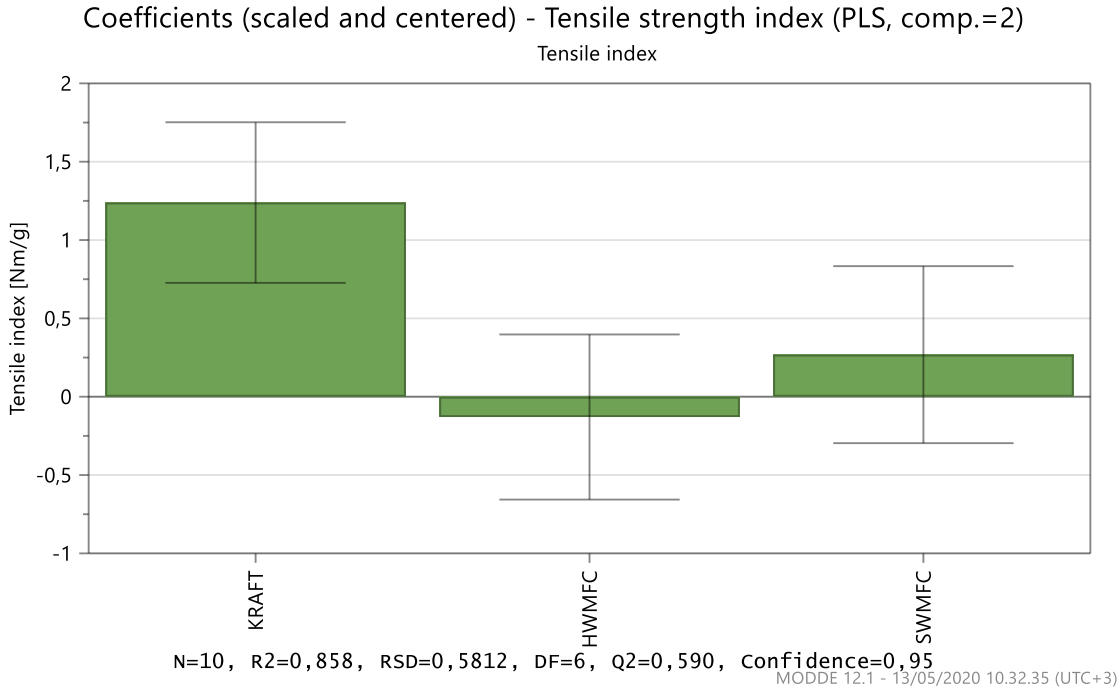

Figure 44 Scaled and centered coefficient plot of kraft pulp, HW MFC, and SW MFC for tensile index.

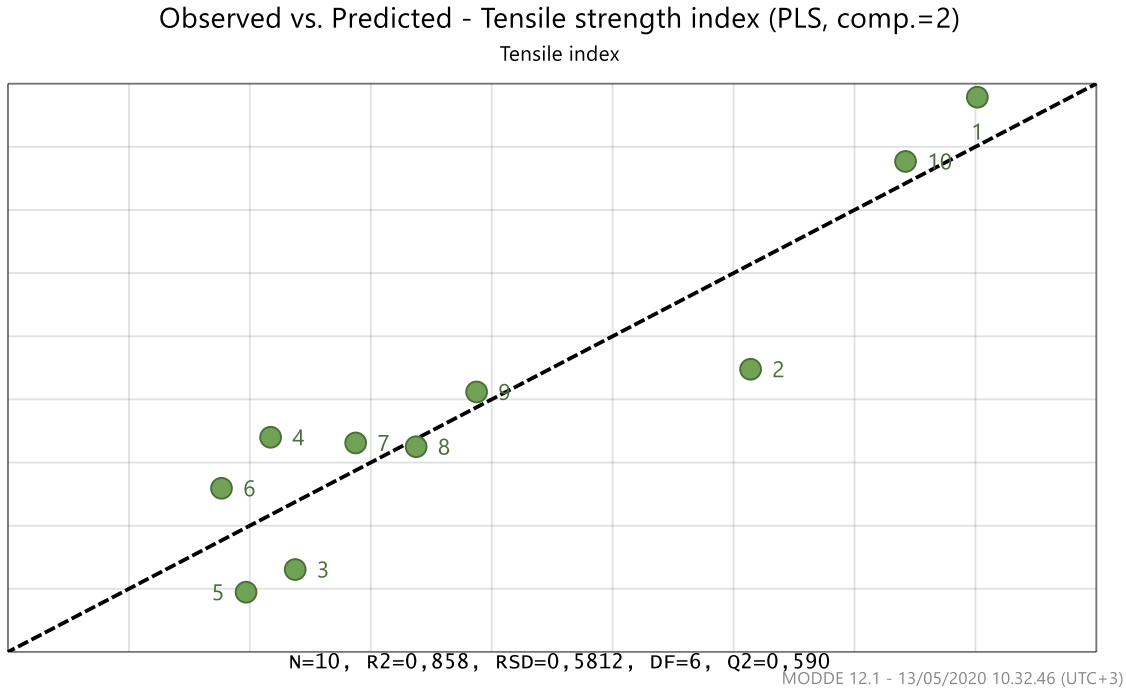

Figure 45 Observed vs predicted plot of tensile indices for HW and SW MFC.

Based on the R^2 and Q^2 the model can be considered acceptable. Points in observed versus predicted plot are relatively close to the line, which indicates a good model. As seen from the coefficient plot, the error bar for kraft pulp is smaller than the parameter effect. The effect of HW MFC is not as clear because the parameter effect is smaller than error bars and the parameter value is relatively close to y=0. The effect of SW MFC is not clear either since the parameter effect is smaller than error bars. However, the effect of SW MFC on tensile strength is bigger than HW MFC. This can be also seen from the response contour plots in Figure 46 and Figure 47.

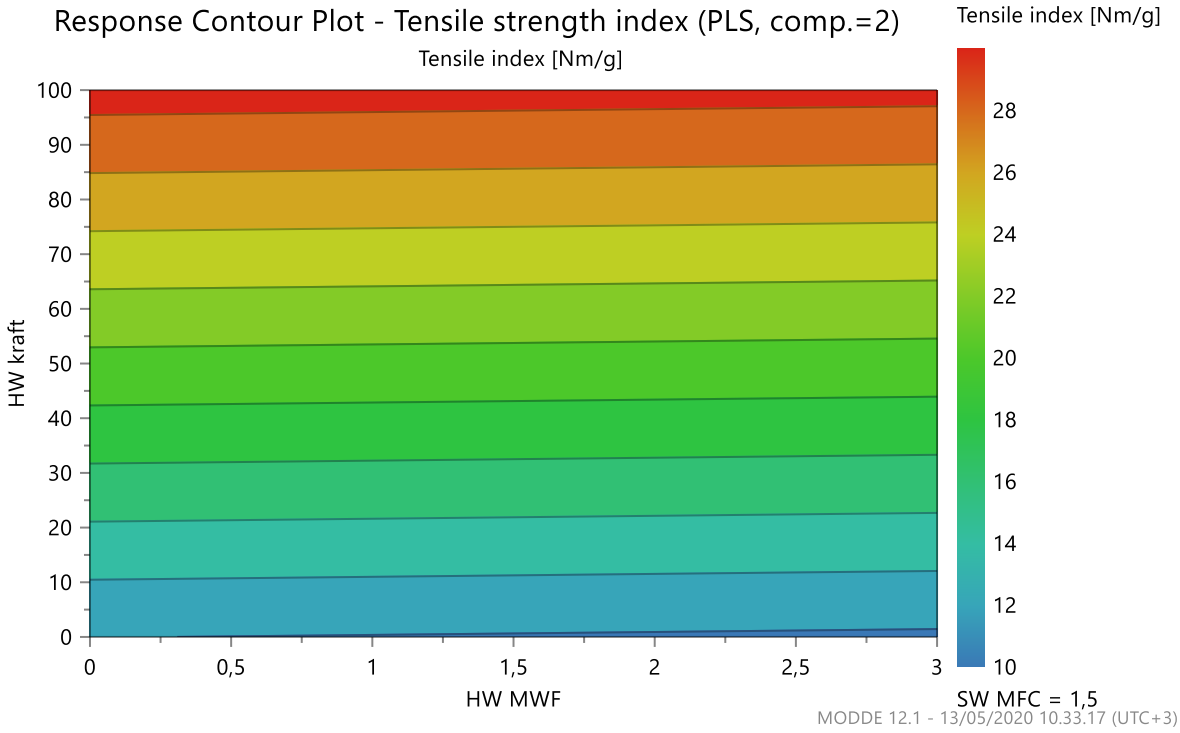

Figure 46 Response contour plot of tensile index showing kraft pulp as a function of HW MFC.

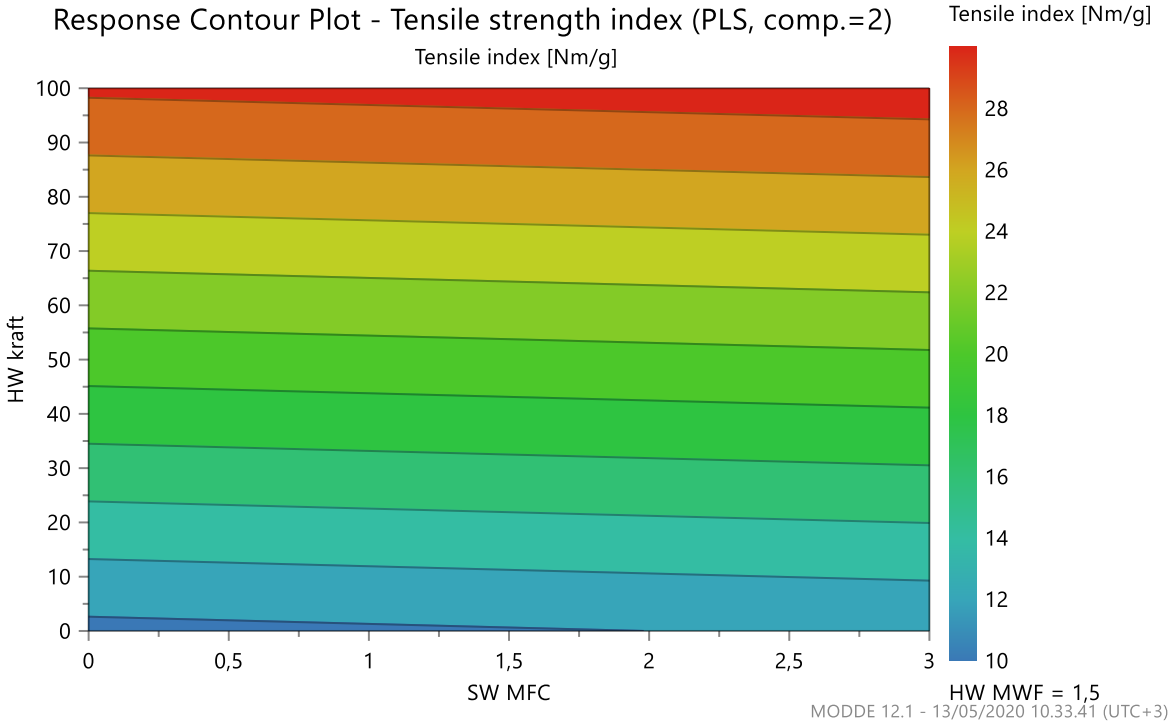

Figure 47 Response contour plot of tensile index showing kraft pulp as a function of SW MFC.

The response contour plots show the correlation between tensile the index and kraft pulp/MFC. SW had a slightly increasing impact on tensile strength. The more SW MFC is added the better the tensile index gets. However, according to the results HW MFC has no impact on tensile strength or it is slightly decreasing.

Tensile energy absorption (TEA) indices are shown in Figure 48.

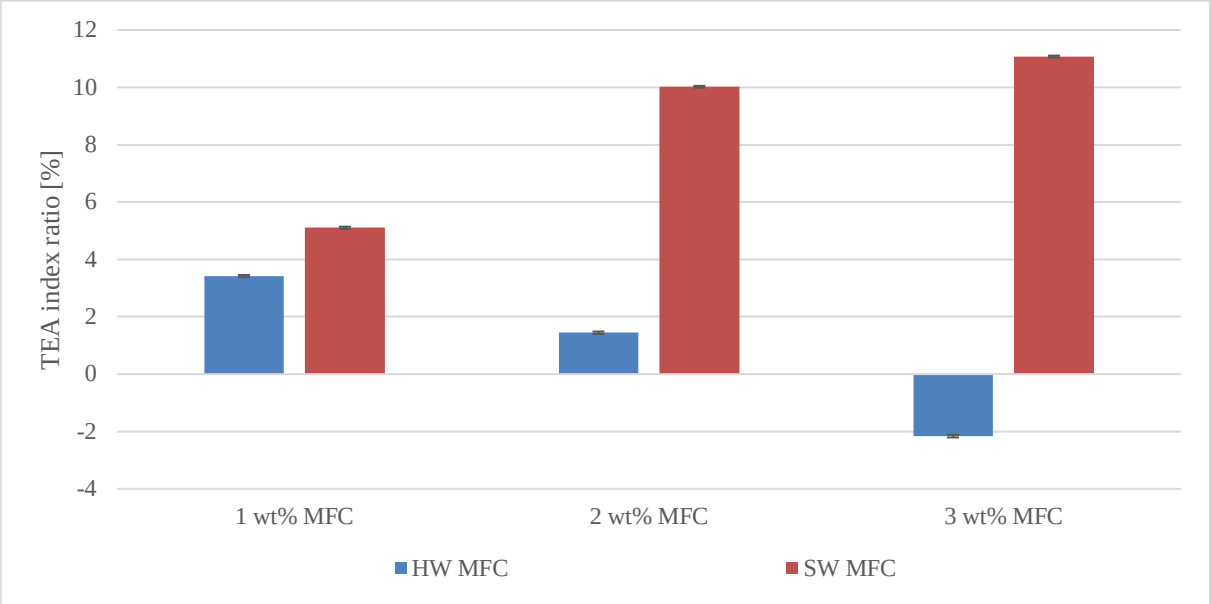

Figure 48 TEA indices of hard- and softwood MFC.

The same kind of effects can be seen on the TEA index than with the tensile index. SW MFC had a slightly increasing impact on TEA. The coefficient plot that shows the coefficients of the fitted model for which the factors were centered is shown in Figure 49. In Figure 50, is shown the observed versus predicted plot when R2 is 0.99 and Q2 0.95.

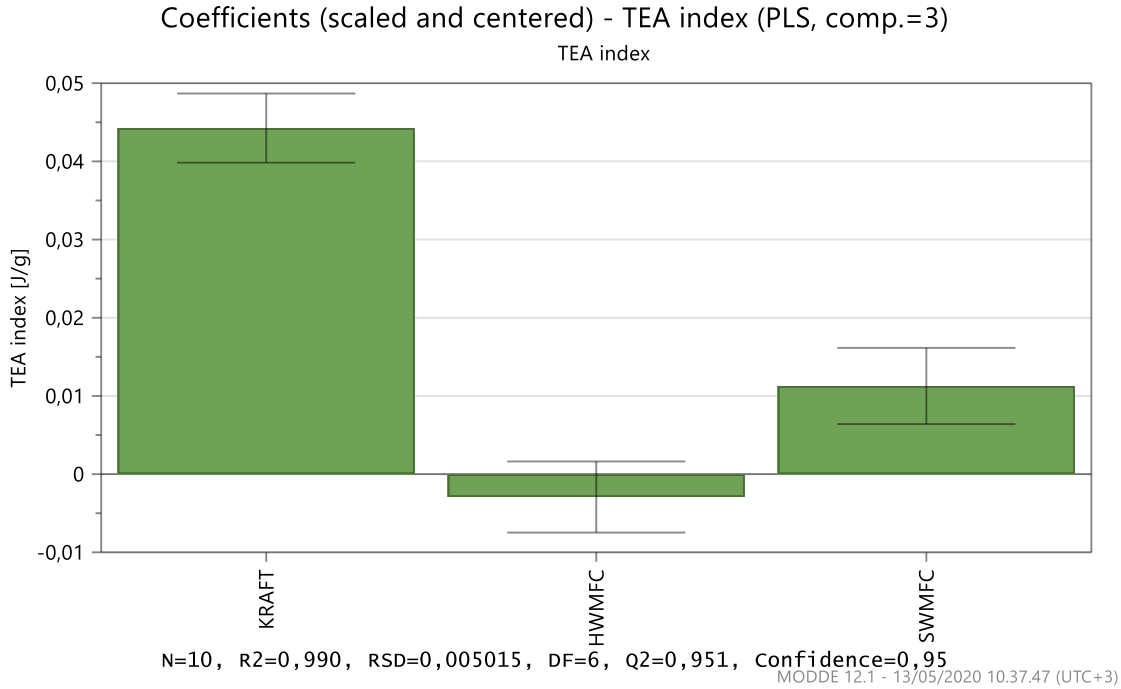

Figure 49 Scaled and centered coefficient plot of kraft pulp, HW MFC, and SW MFC for TEA index

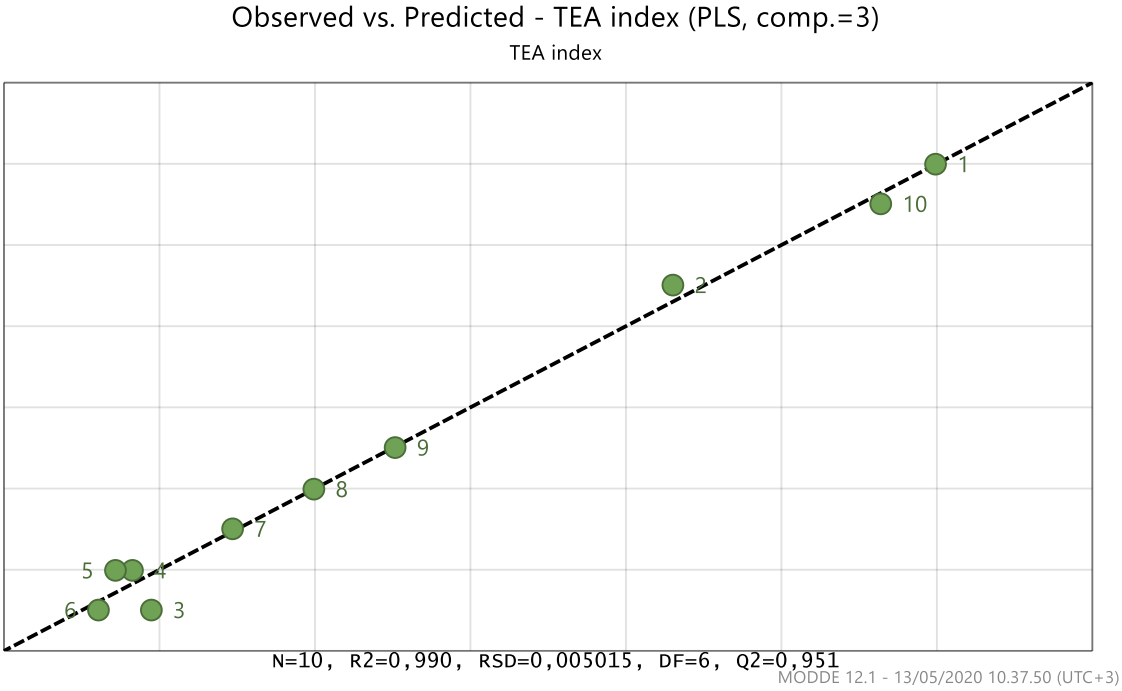

Figure 50 Observed vs. predicted plot of TEA indices for HW and SW MFC.

Based on the R2 and Q2 the model can be considered almost perfect. Almost all points in observed versus predicted plot are close to the line, which indicates a good model. As seen from the coefficient plot, there is no significant impact with HW and SW MFC on the TEA index. The error bar for kraft pulp is smaller than the parameter effect which indicates some sort of effect. However, the parameter value is close to y=0. The effect of HW MFC is not as clear because the parameter effect is smaller than error bars and the parameter value is relatively close to y=0. The effect of SW MFC is slightly more significant than HW MFC since the parameter effect is the same size as the error bar. Figure 51 and Figure 52 shows the response contour plots.

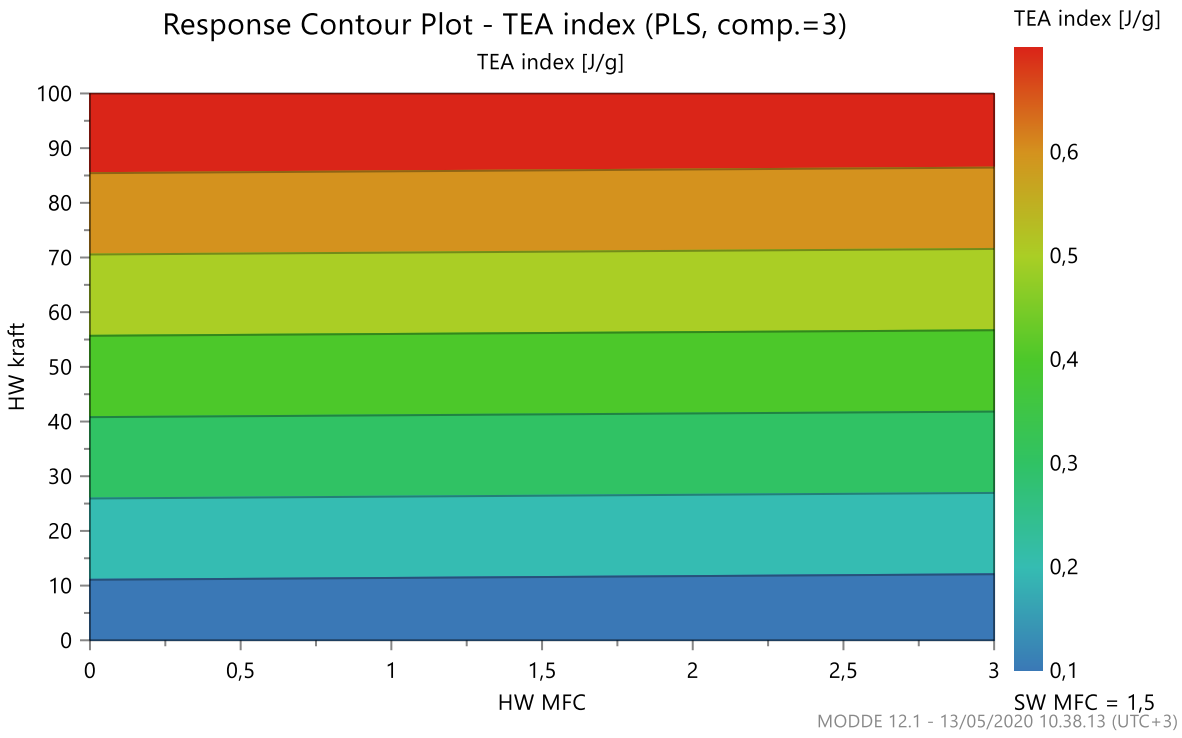

Figure 51 Response contour plot of TEA index showing kraft pulp as a function of HW MFC.

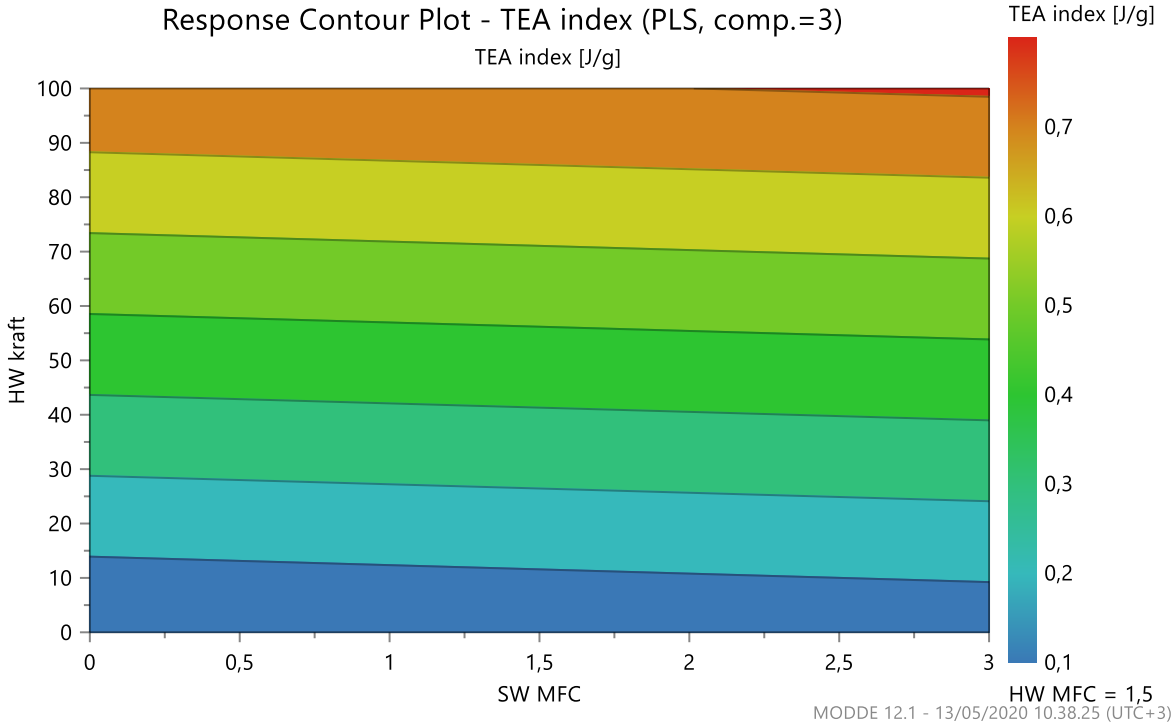

Figure 52 Response contour plot of TEA index showing kraft pulp as a function of SW MFC.

As seen from the contour plots TEA index increases slightly when SW MFC is added. No significant changes were seen when HW MFC was added, which was shown already from the coefficient plot. The effect of HW MFC is insignificant.

No significant impacts were shown in tensile stiffness, strain at break, modulus of elasticity, or break elongation. In Figure 53, are shown SCT indices.

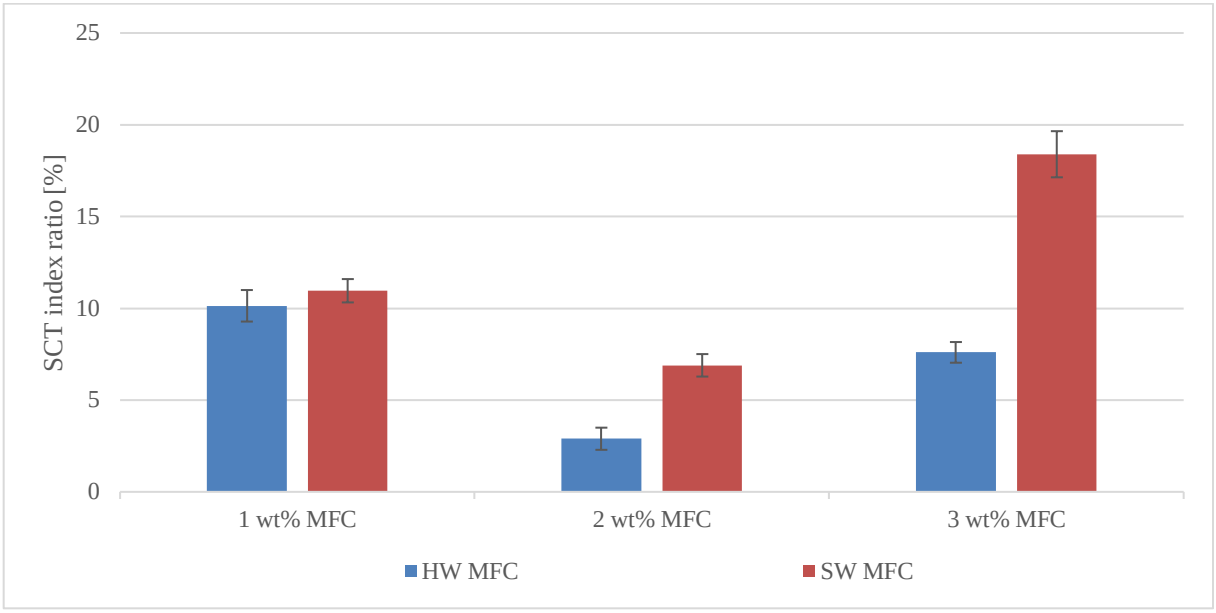

Figure 53 SCT indices of hard- and softwood MFC.

Both HW and SW MFC had an increasing impact on SCT. According to Figure 53, SW MFC has a slightly more increasing impact than HW MFC. In Figure 54, are shown the scaled and centered coefficients. The observed versus predicted plot is shown in Figure 55 when R2 is 0.83 and Q2 is only 0.26.

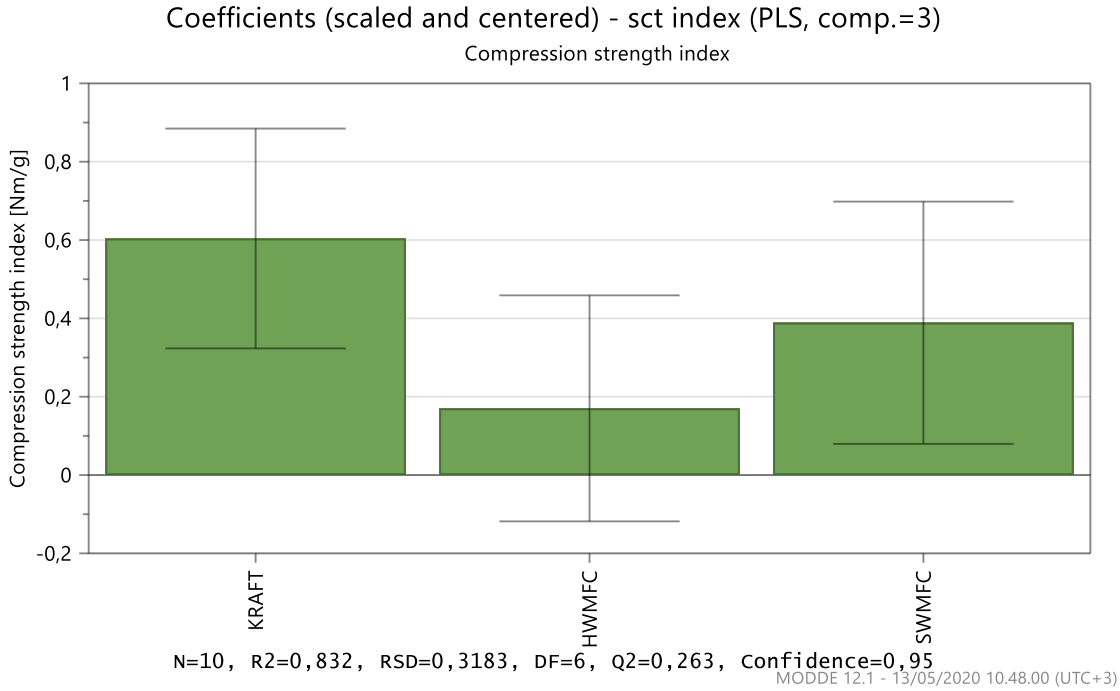

Figure 54 Scaled and centered coefficient plot of kraft pulp, HW MFC, and SW MFC for SCT index.

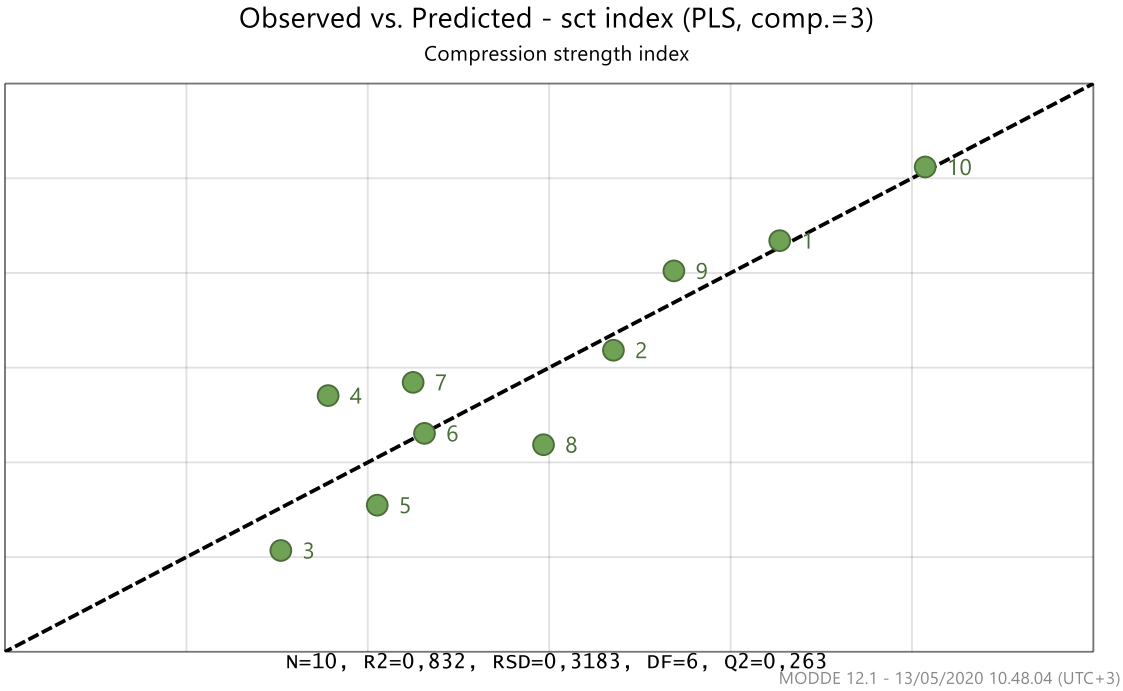

Figure 55 Observed vs. predicted plot of SCT indices for HW and SW MFC.

According to the observed versus predicted plot and the value of R2 the model can be considered good. However, the value of Q^2 is too low and the difference between these values is greater than 0.3. The points in observed versus predicted plot on the other hand are relatively close to the straight line. The reliability of the model is not clear. All the parameter values are smaller or the same size than the error bars to the effect of these parameters are not clear. Once again, the kraft pulp has the biggest impact on the SCT index. Figure 56 and Figure 57 shows the response contour plots.

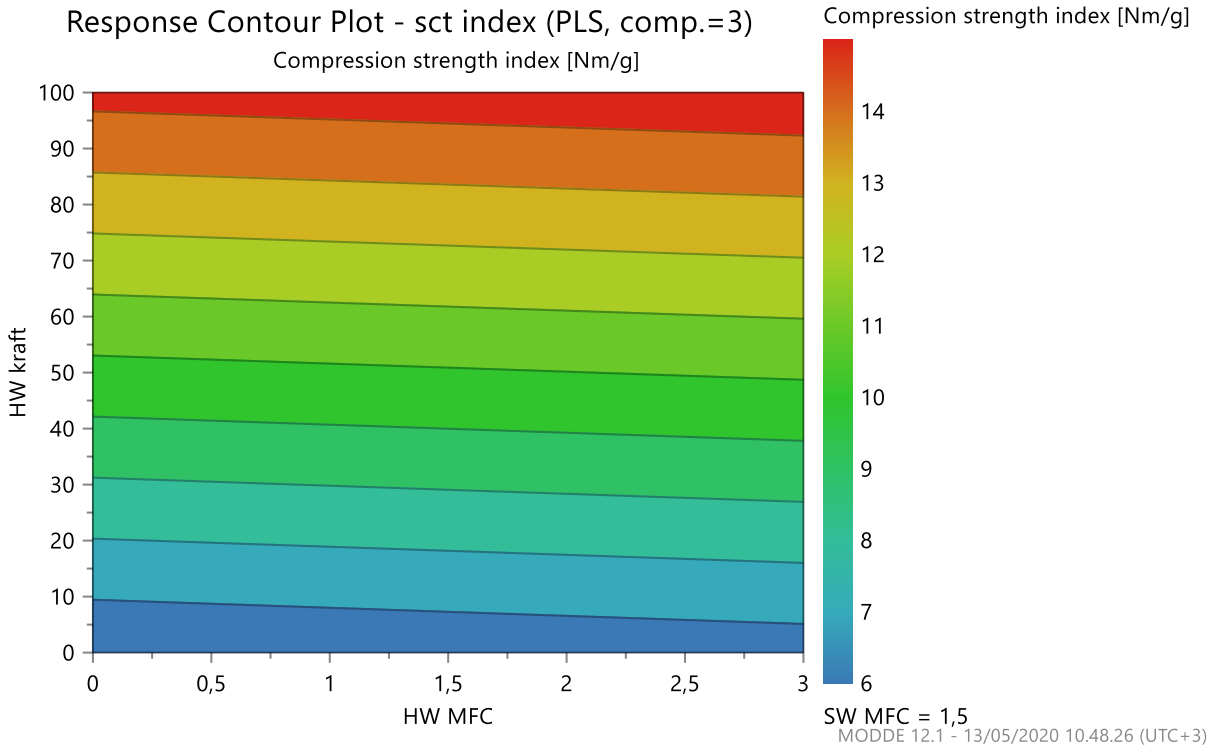

Figure 56 Response contour plot of SCT index showing kraft pulp as a function of HW MFC.

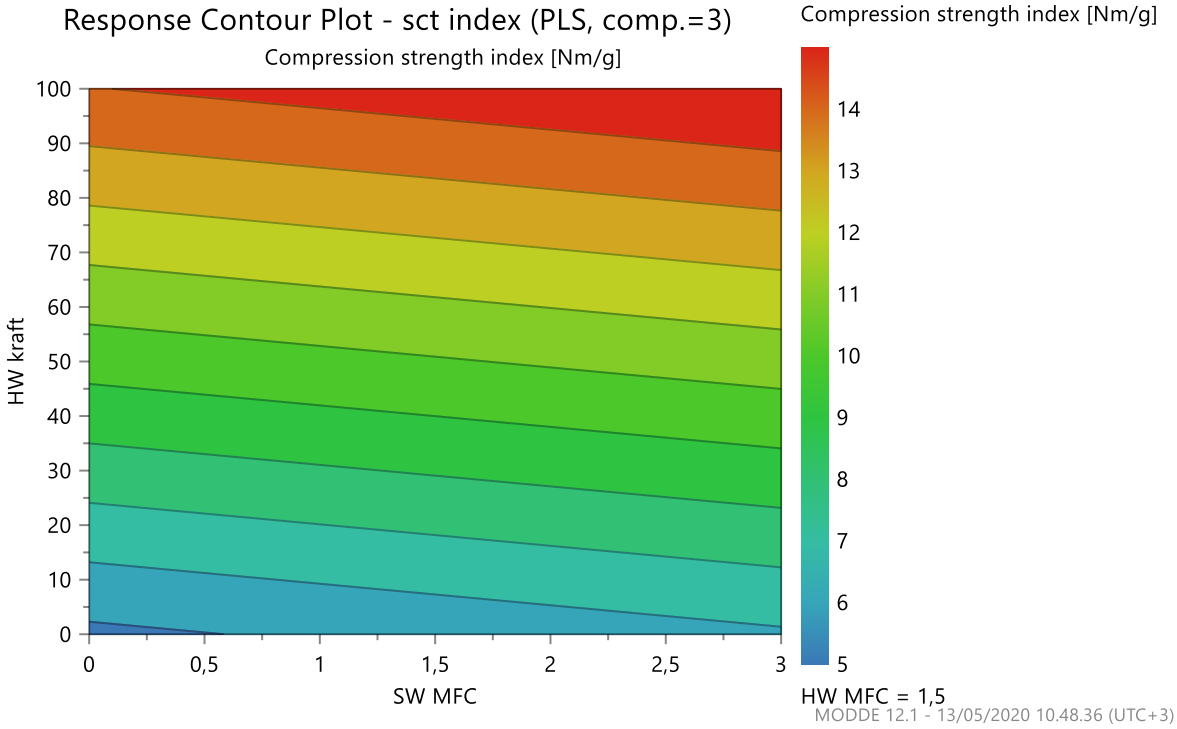

Figure 57 Response contour plot of SCT index showing kraft pulp as a function of SW MFC.

Both MFCs have an increasing impact on SCT. SW MFC has more clear impact than the HW MFC. However, since the Q^2 value is quite low the model for the SCT index is not that reliable than the other models.

It can be said that all the models except the SCT index were good or acceptable and gave reliable information about the effects. As seen from the results, MFC had a slightly increasing impact on all paper properties compared to the reference point where MFC was not used. Both MFCs had an increasing impact on internal bond strength. SW MFC showed an increasing impact on a tear and tensile strength. HW MFC had no impact on tear index or tensile properties. This can be due to the amount of fines B that was only 6% compared to the SW MFC where the amount was 38%. The amount of kraft pulp used had the clearest impact on all paper properties that were measured. Higher results in paper properties were gained in the work of Korelin (2020). Due to the FF1 fillings used in her work, the quality of the MFC was different, especially greater number of fines B was gained. Higher improvement in paper properties can be due to the number

of fines B. However, results cannot be compared, since different pulps were used in the works. Base pulp used in this work, consisted of bleached birch kraft pulp and CTMP. Korelin (2020) used CTMP and OCC separately for laboratory sheet making with 2.5 wt% of CS.

It was shown the MFCs improved some paper properties. However, the results were lower when MFC was used in sheets were CTMP/kraft pulp ratio was 60/40 than with sheets were no MFC was used and the CTMP/kraft pulp ratio was 45/55. According to the results, SW MFC improved some paper properties better than HW MFC due to the number of fines B. Results from internal bond strength showed that the ratio of CTMP/kraft pulp could be decreased from 45/55 to approximately to 50/50 by using 3 wt% of HW and SW MFC without compromising the results too much. According to tensile strength and TEA results, it was shown that with the addition of 3 wt% SW MFC the ratio could be decreased to 50/50. SCT results showed that with 3 wt% of HW MFC ratio could be decreased to 50/50 whereas with 1.5 wt% addition of SW MFC same results could be achieved.

9.2.2 Second laboratory sheet trial - Effect of cationic starch and storage time

In the first laboratory sheet trial, it was noticed that increased cationic starch dosage together with HW MFC had the best results. In the first laboratory trials, the starch dosage was increased from 0.5 to 0.8 wt%. Also, the CPAM and silica dosages were increased from 0.02 to 0.03 wt% and 0.05 to 0.075, respectively. It was shown that the starch addition had an increasing impact on internal bond strength, tear strength, tensile strength and TEA. The addition of CPAM and silica had no impact on any property. The results are shown in Appendix IV.

In the second laboratory trial, the effect of cationic starch was studied more to the sample point where 2 wt% HW MFC was used. Effect of cationic starch itself (0 wt% MFC) was not studied in this case. The dosage of CS in reference point was 0.5 wt%. MFC dosage was kept constant at 2 wt% and the CS dosage was increased to 0.8 and 1.0 wt%. Also, the effect of storage time of MFC and other substances has been studied since the second laboratory trial was done 34

days after the refining of HW MFC. In Figure 58, are shown internal bond indices for samples containing 2 wt% of HW MFC.

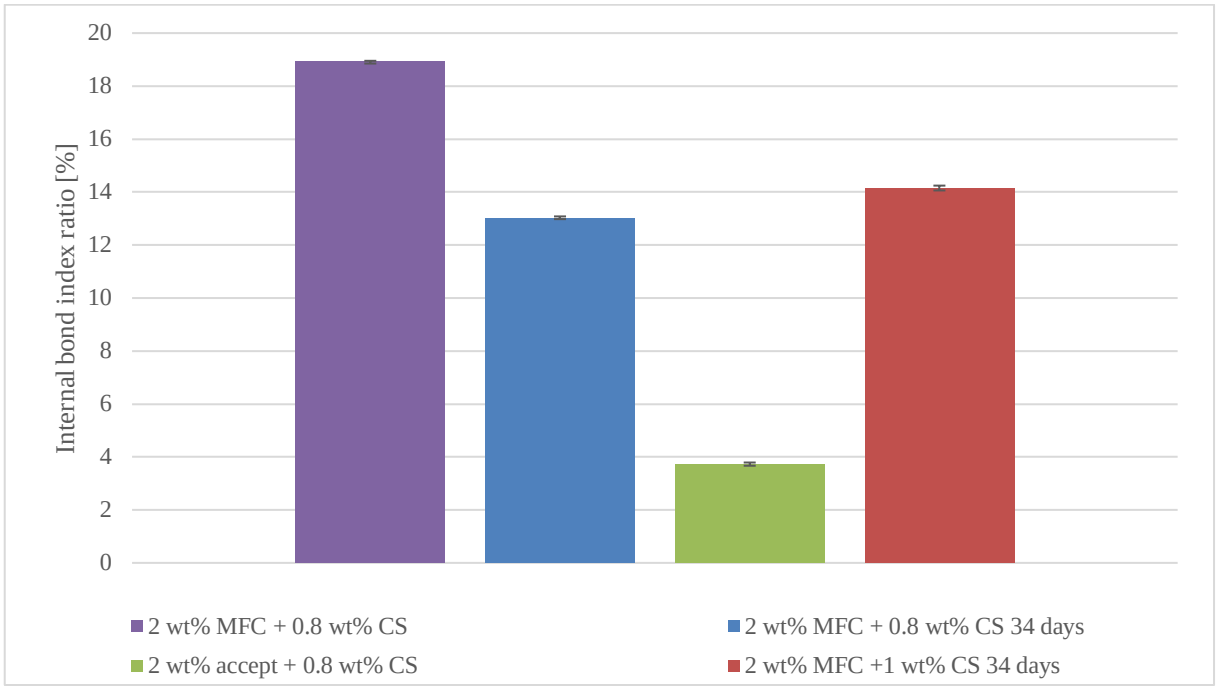

Figure 58 Internal bond index ratio for samples consisting of 2 wt% HW MFC and CS.

Cationic starch together with 2 wt % of HW MFC had an increasing effect on the internal bonding strength. Storage time of the MFC and other substances had a clear impact on internal bond strength also. The coefficient plot that shows the coefficients of the fitted model for which the factors were centered is shown in Figure 59. In Figure 60, is shown the observed versus predicted plot when R^2 is 0.82 and Q^2 is 0.56.

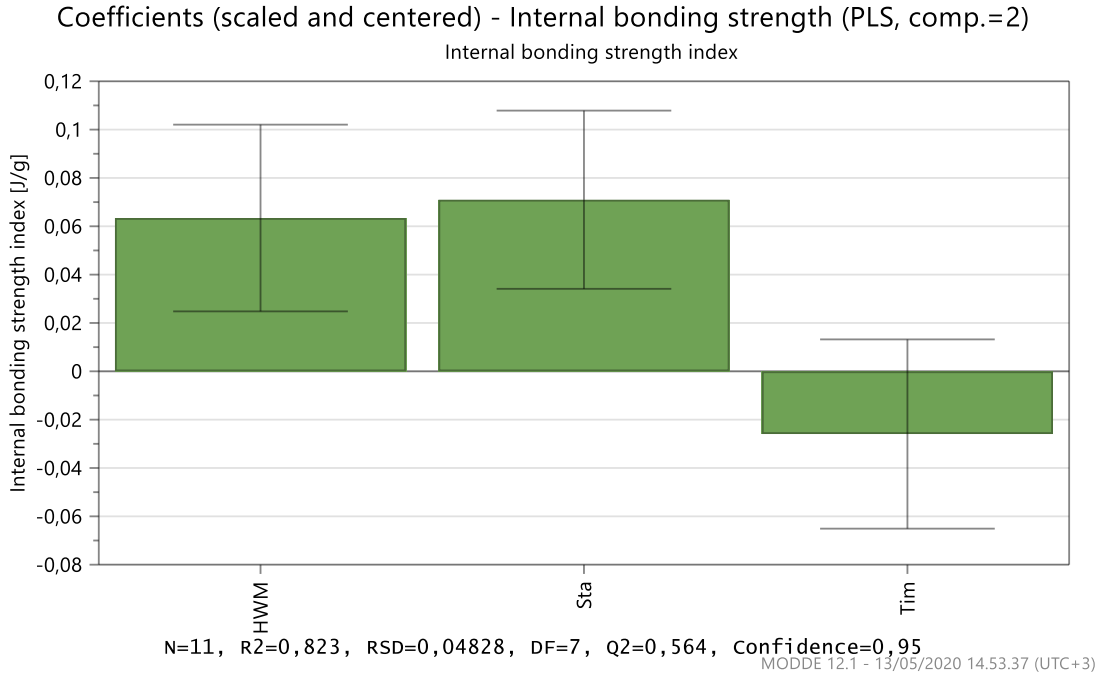

Figure 59 Scaled and centered coefficients for internal bond index. HWM= HW MFC, Sta= cationic starch and Tim=time.

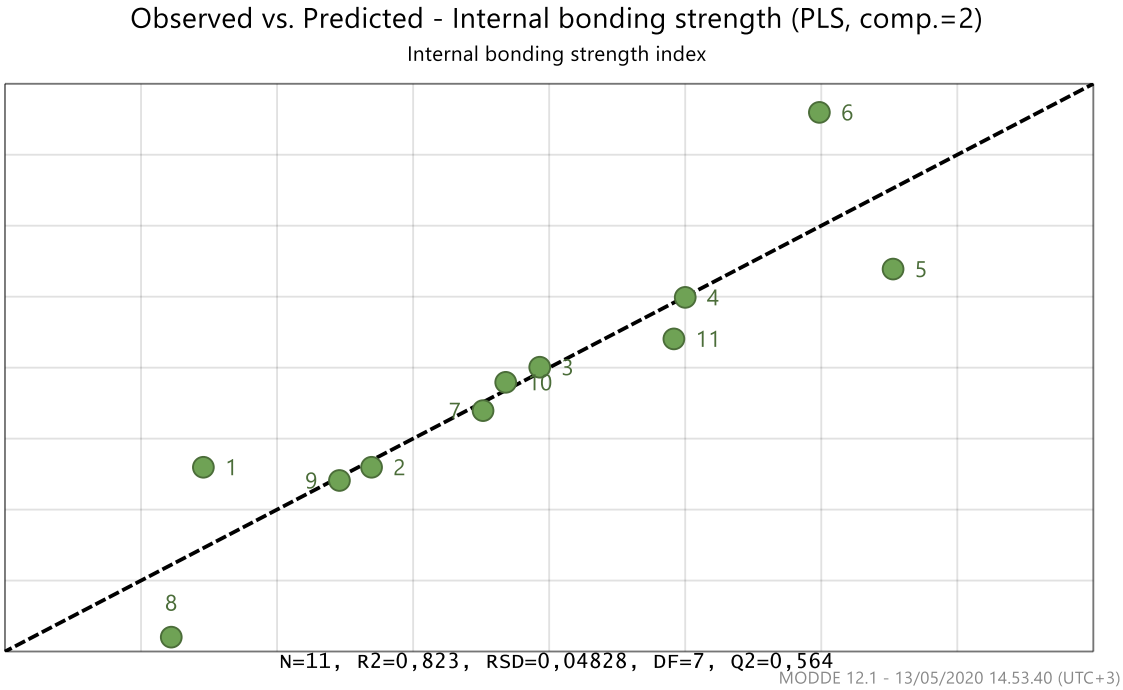

Figure 60 Observed vs. predicted plot of internal bond index for HW MFC, CS, and storage time.

According to the R^2 and Q^2 values and the points shown in the observed versus predicted plot it can be said that the model fit is acceptable. Even though the value of Q^2 could be better. Based on the coefficient plot the impact of the parameters are not significant because they all are close to y=0. However, the storage time has a negative impact on the internal bond index. Figure 61 and Figure 62 shows the response contour plots of the internal bond index.

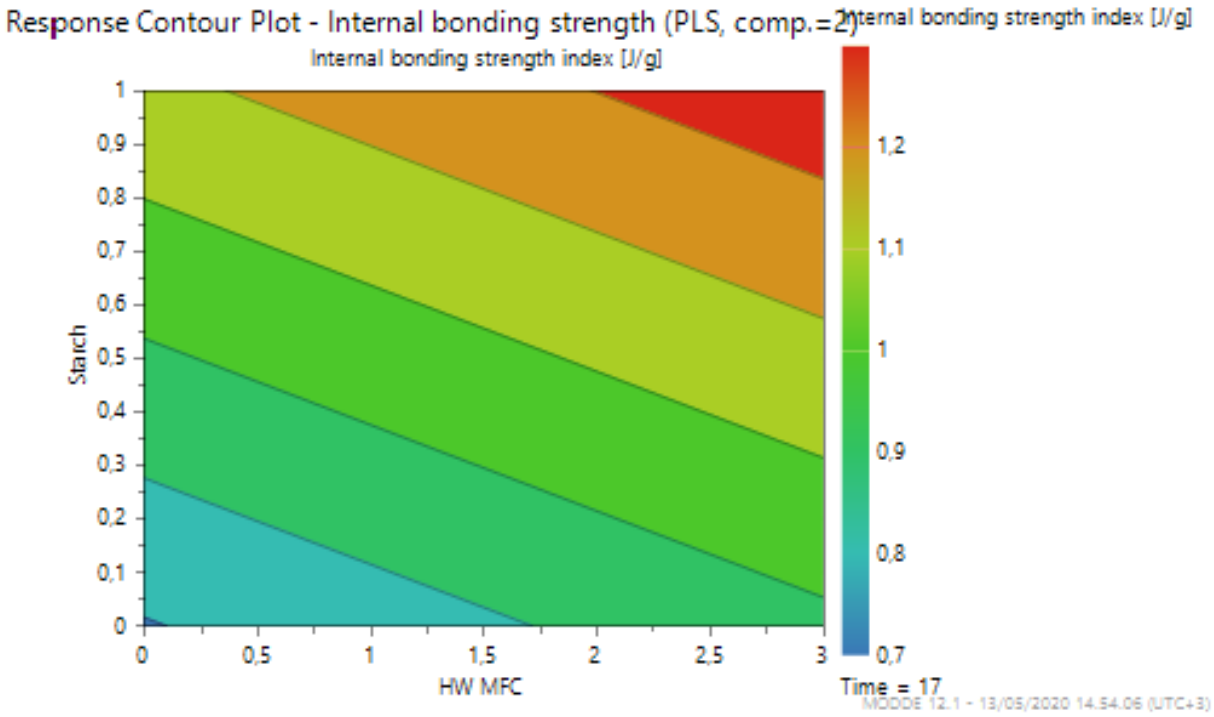

Figure 61 Response contour plot of internal bond index showing CS as a function of HW MFC.

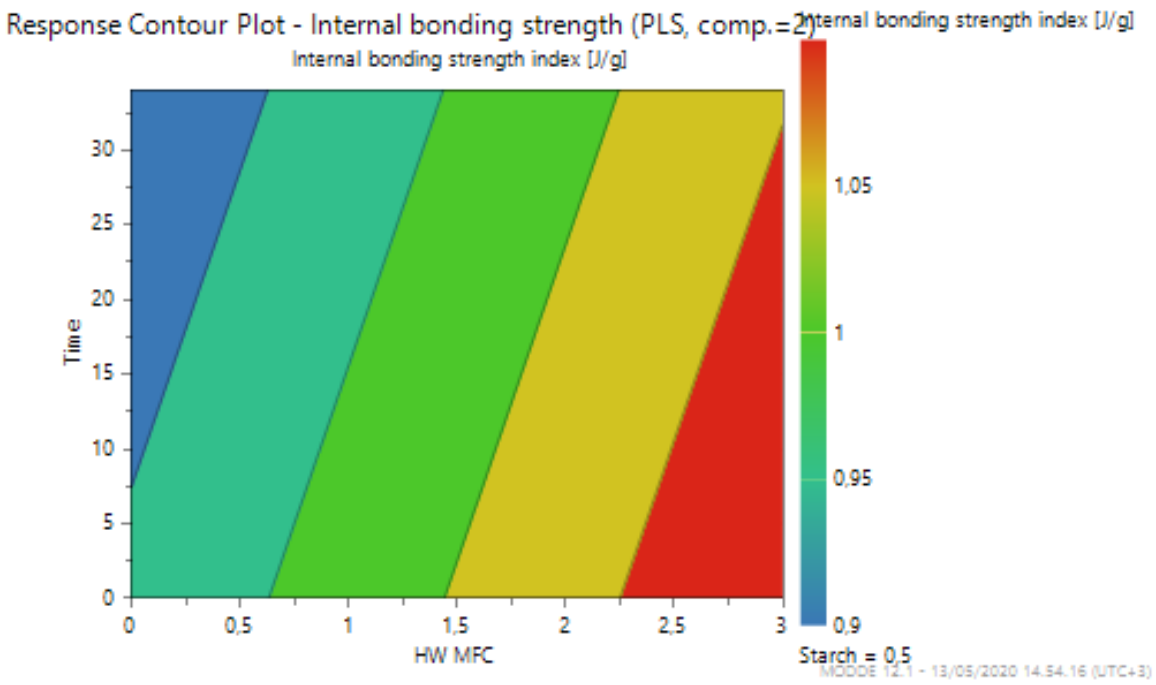

Figure 62 Response contour plot of internal bond index showing time as a function of HW MFC.

Correlation between the internal bond index and CS/storage time can be seen from the response contour plots. According to the results CS and MFC have an equal impact on internal bond strength. The storage time of MFC and other substances decreased the internal bond strength.

In Figure 63, are presented the tear index ratios for samples containing 2 wt% of HW MFC.

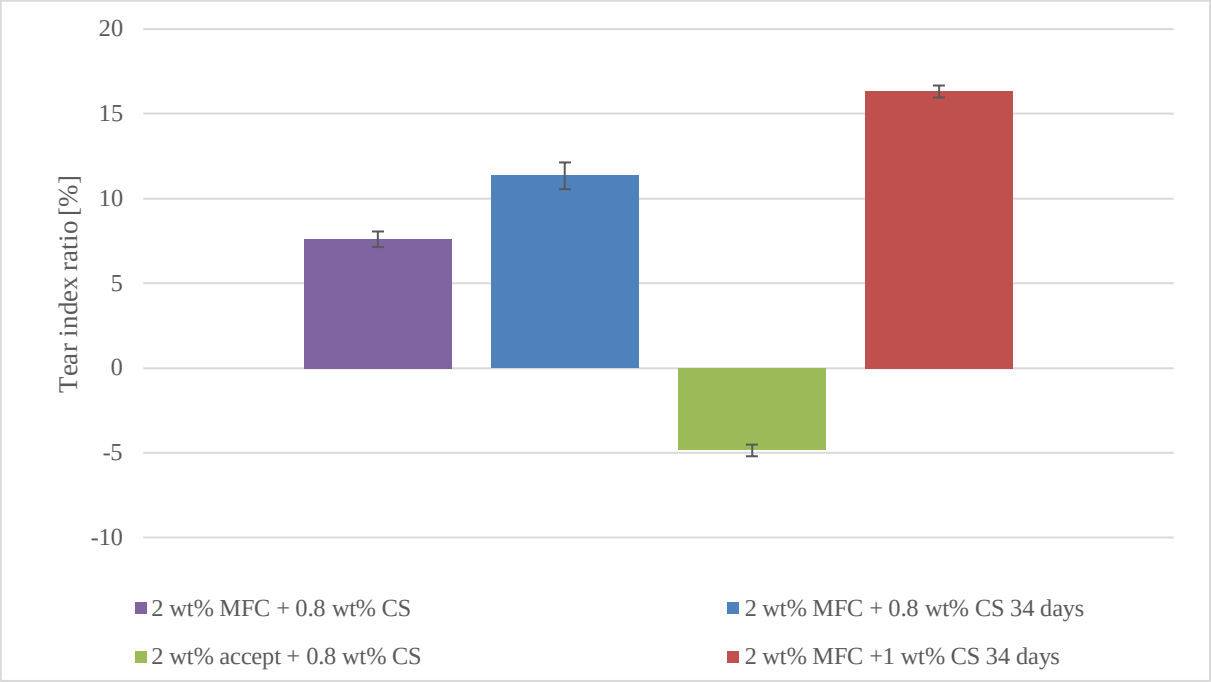

Figure 63 Tear index ratio for samples consisting of 2 wt% HW MFC and CS.

According to Figure 63 the more CS is added to the pulp the better the tear strength is. The effect of storage time is properly seen from the coefficient plot in Figure 64 that shows the coefficients of the fitted model for which the factors were centered. In Figure 65, is shown the observed versus predicted plot when R^2 is 0.81 and Q^2 is 0.52.

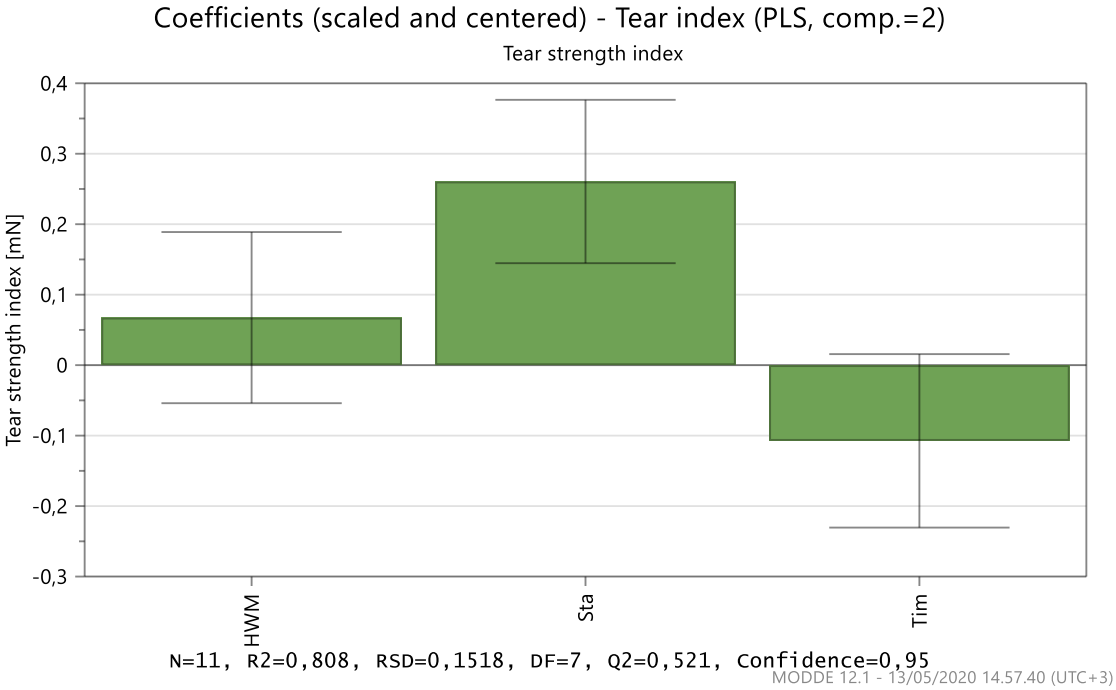

Figure 64 Scaled and centered coefficients for tear index. HWM= HW MFC, Sta= cationic starch and Tim=time.

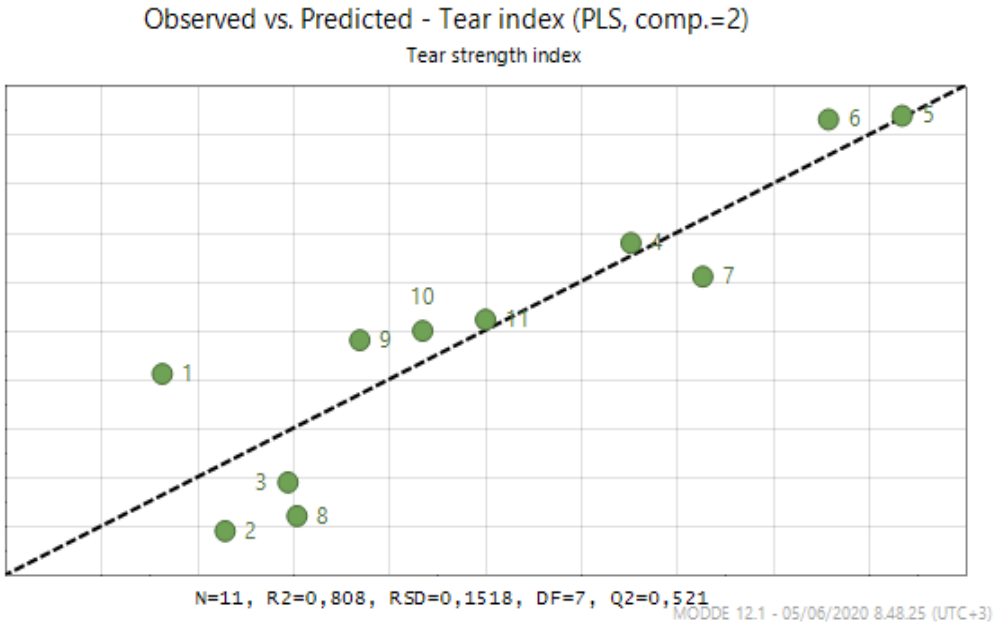

Figure 65 Observed vs. predicted plot of tear index HW MFC for HW MFC, CS, and storage time.

According to the R^2 and Q^2 values it can be said the model is average. Some points in observed versus predicted plot are farther from the straight line than others and the difference of the R^2 and Q^2 values is around 0.3. Based on the coefficient plot the impact of the CS is more significant than the storage time and MFC because they are closer to y=0 and the error bars are bigger than the parameter effect. Storage time has a negative impact on the internal bond index. Figure 66 and Figure 67 shows the response contour plots of the tear index.

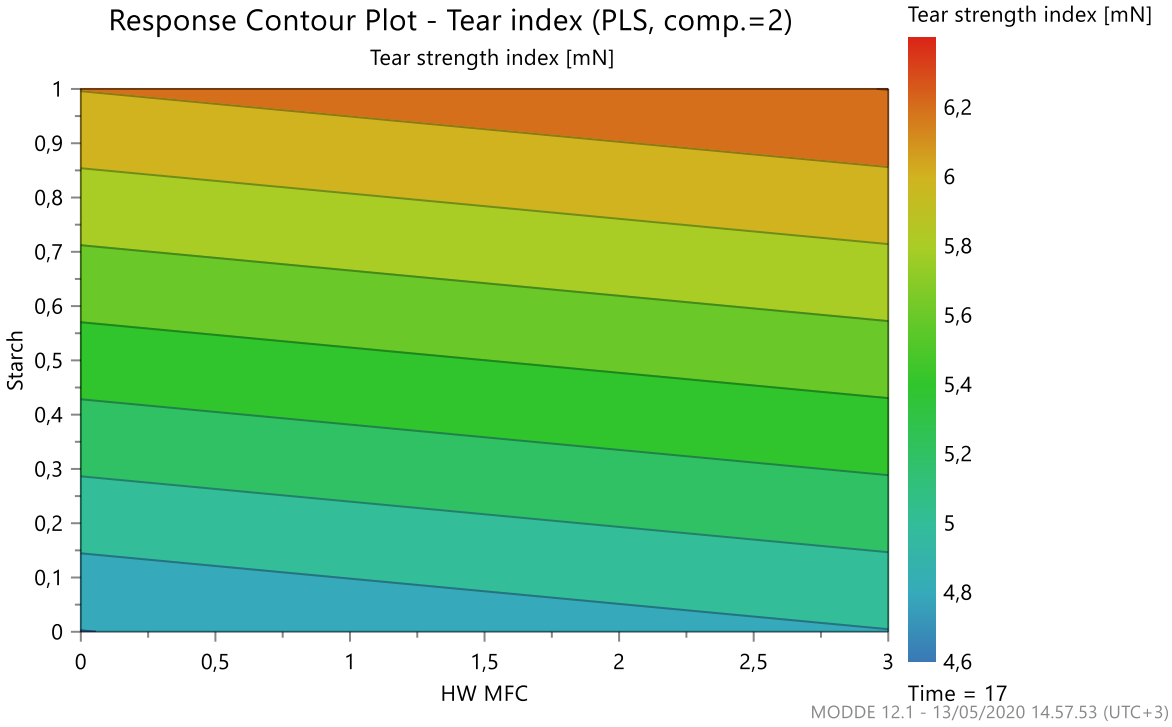

Figure 66 Response contour plot of tear index showing CS as a function of HW MFC.

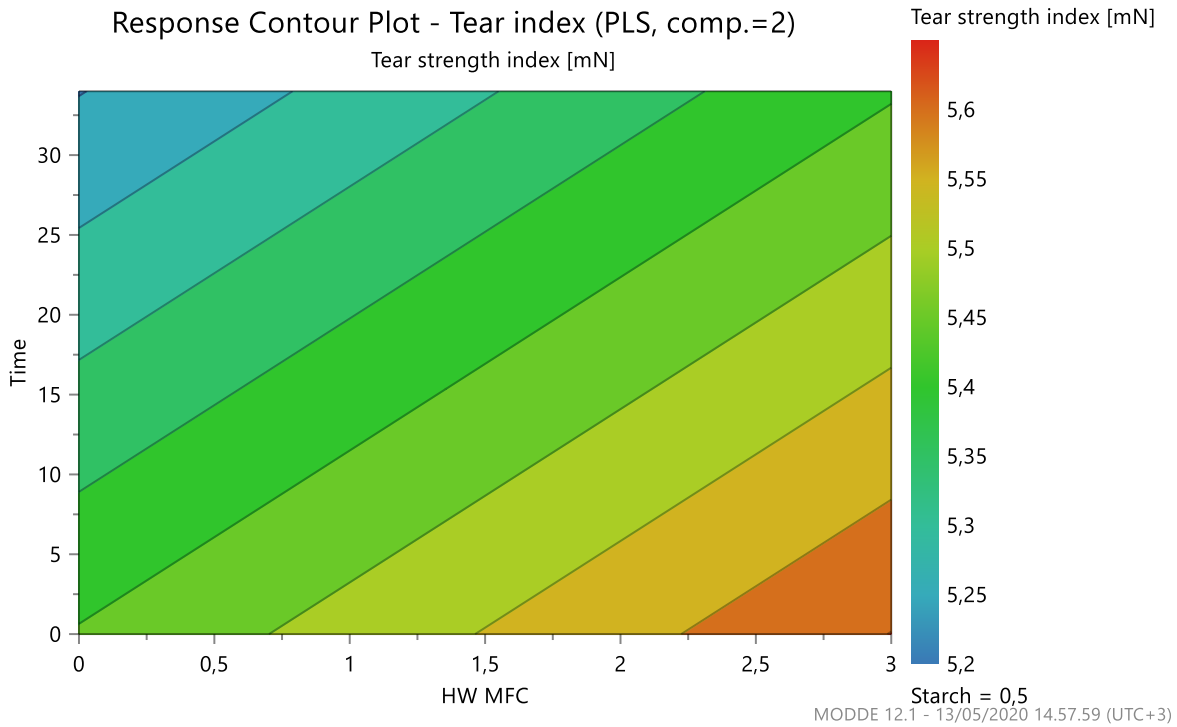

Figure 67 Response contour plot of tear index showing time as a function of HW MFC.

Correlation between tear index and CS/storage time can be seen from the response contours. A negative effect of storage time can be seen from the response contour and the coefficient plot. According to the results CS has a greater impact on the tear index than the HW MFC.

In Figure 68, are presented the tensile index ratios for samples containing 2 wt% of HW MFC.

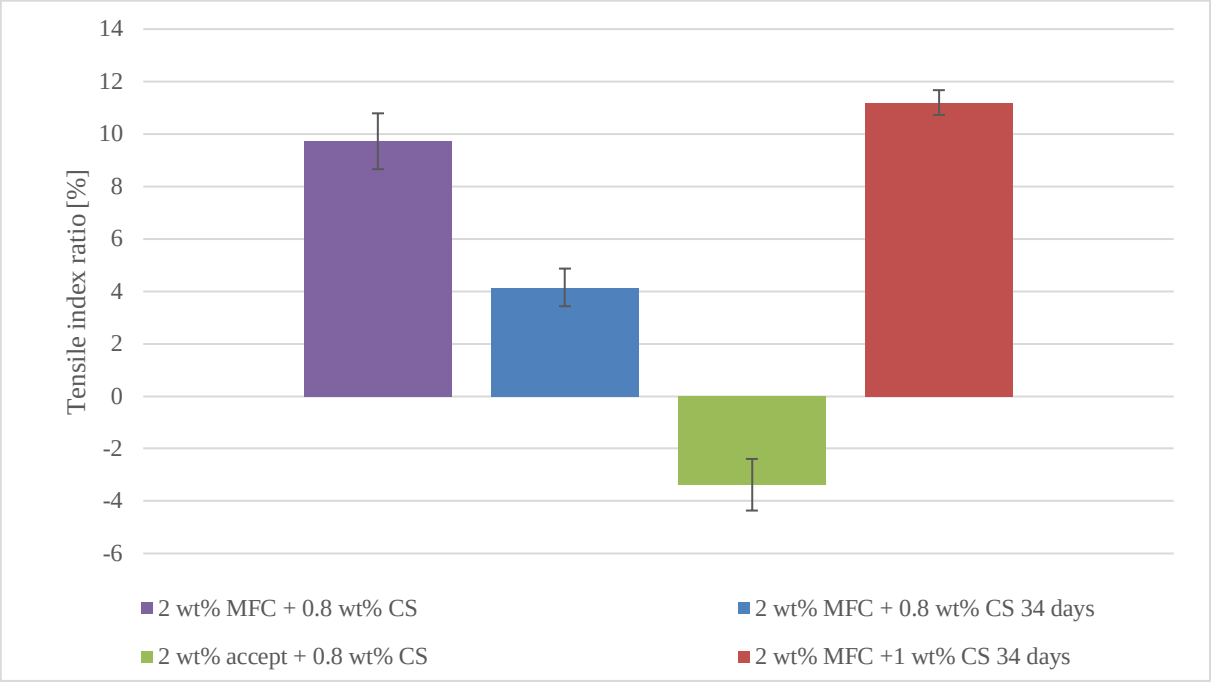

Figure 68 Tensile index ratio for samples consisting of 2 wt% HW MFC.

According to Figure 68, CS had an increasing impact on tensile strength. The effect of CS on the tensile index is presented more in the coefficient plot in Figure 69 that shows the coefficients of the fitted model for which the factors were centered. In Figure 70, is shown the observed versus predicted plot when R^2 is 0.85 and Q^2 is 0.64.

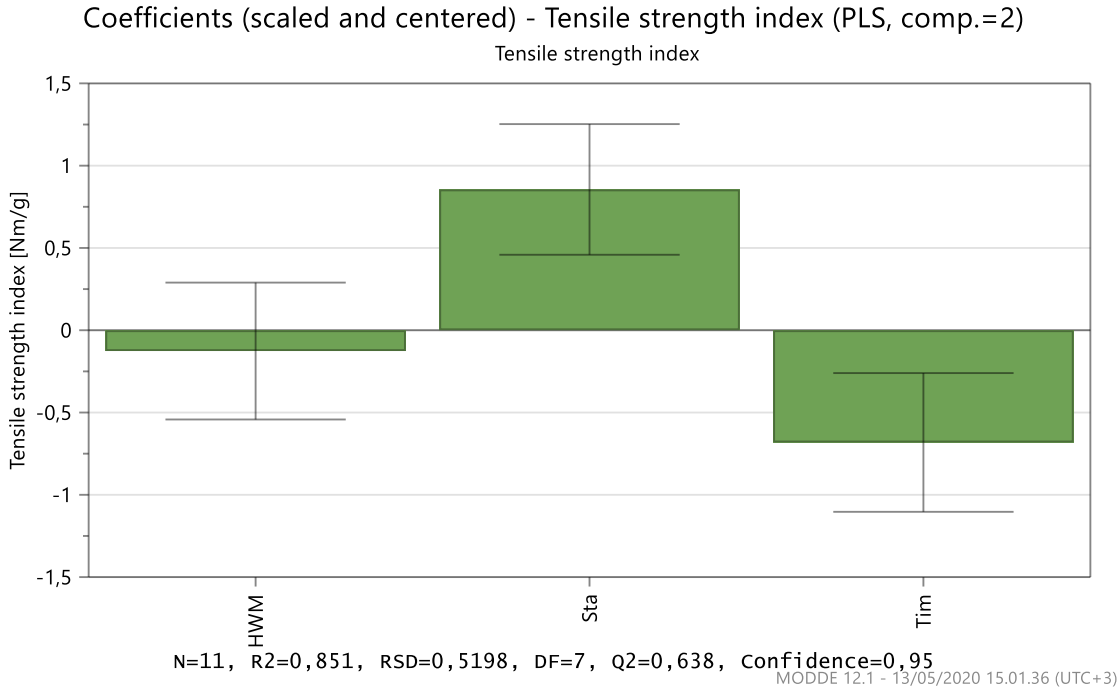

Figure 69 Scaled and centered coefficients for tensile index. HWM= HW MFC, Sta= cationic starch and Tim=time.

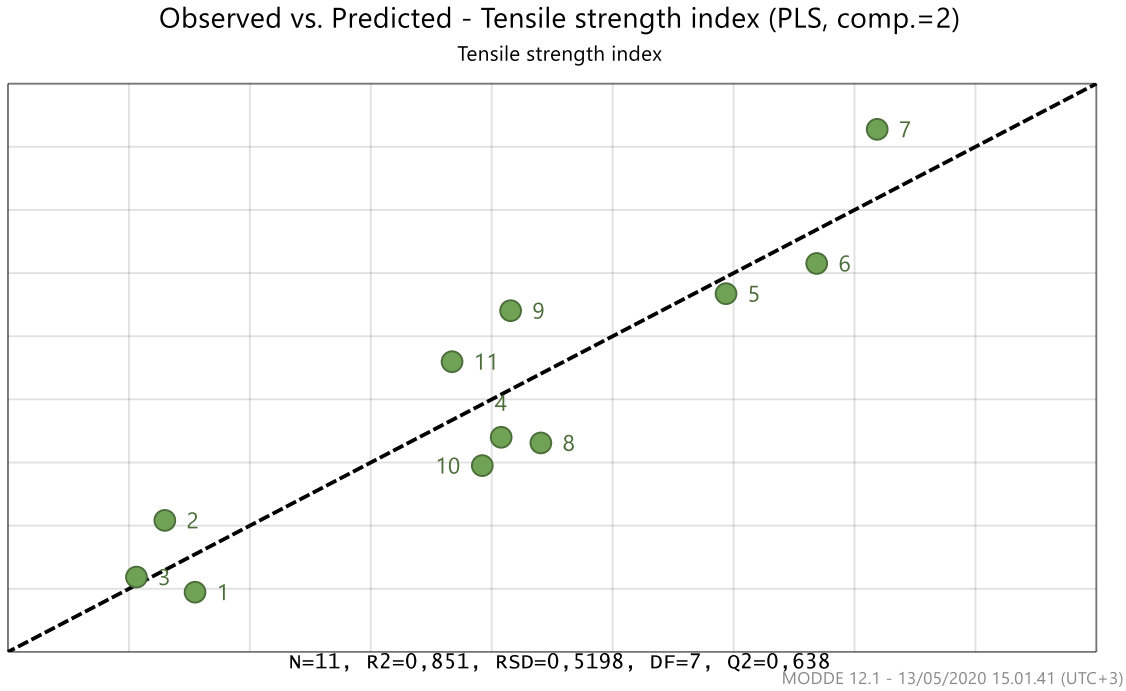

Figure 70 Observed vs. predicted plot of tensile index for HW MFC, CS, and storage time.

According to the R^2 and Q^2 values, it can be said the model is good. All the points in observed versus predicted plot are relatively close to the straight line. Based on the coefficient plot the impact of the CS is more significant than the storage time and MFC. Based on the results MFC has no impact on the tensile index because the parameter value is close to y=0 and the error bar is bigger than the effect. Storage time has a negative impact on the internal bond index. Figure 71 and Figure 72 shows the response contour plots of the tensile index.

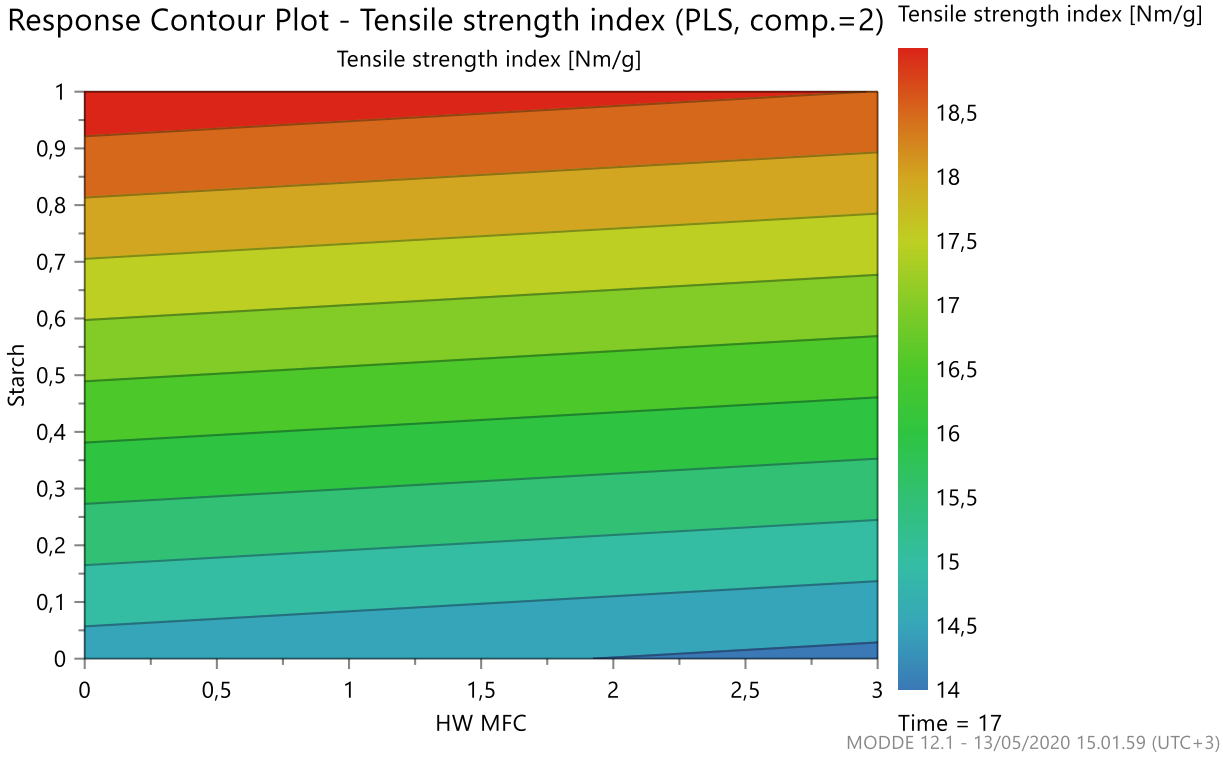

Figure 71 Response contour plot for tensile index showing CS as a function of HW MFC.

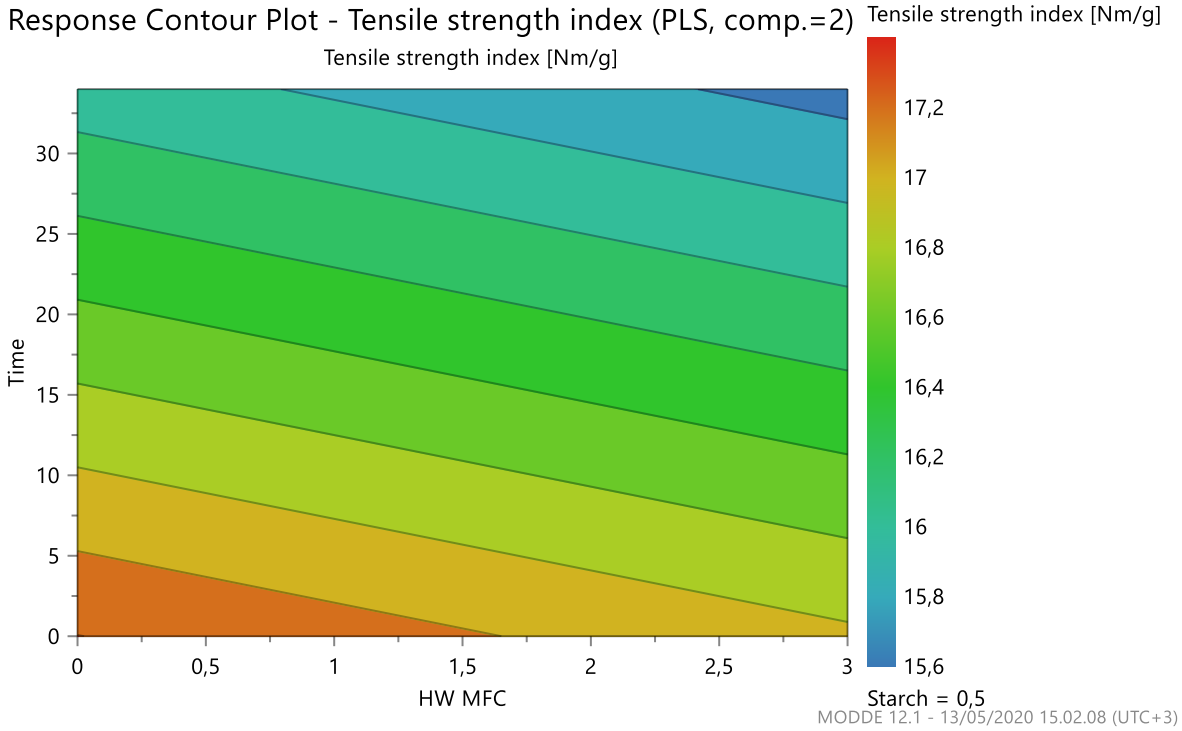

Figure 72 Response contour plot for tensile index showing time as a function of HW MFC.

From the coefficient plot, it can be seen that CS has greater impact on tensile strength than MFC. The effect of MFC is insignificant. Storage time has the same kind of negative impact on tensile strength than it does to internal bond and tear strength.

Storage time had a negative impact on every property. No significant changes were seen on any other properties like TEA index or tensile stiffness index with CS addition. Indices ratios can be seen in Appendix III. When comparing the results of screened MFC and the refined HW MFC it can be said that refined HW together with CS gave better results on paper properties. As seen from Figure 58, internal bond index increased 19% with refined MFC and 0.8 wt% of CS and only 4% with screened MFC together with 0.8 wt% of CS. According to Figure 63 and Figure 68, the screened MFC did not have an increasing impact either on tear or tensile index. This can be due to the quality of the accept compared to the quality of the refined MFC.

9.2.3 Third laboratory sheet trial - Effect of screening

The effect of screening was studied comparing accept, feed and refined HW MFC together. The base pulp consisted of 60 wt% of CTMP and 40 wt% of kraft pulp. 0.5 wt% of CS, 0.02 wt% of CPAM and 0.05 wt% of silica were added to the pulp mixture. In Figure 73, are shown the internal bond indices ratios of HW MFC, screened MFC and feed.

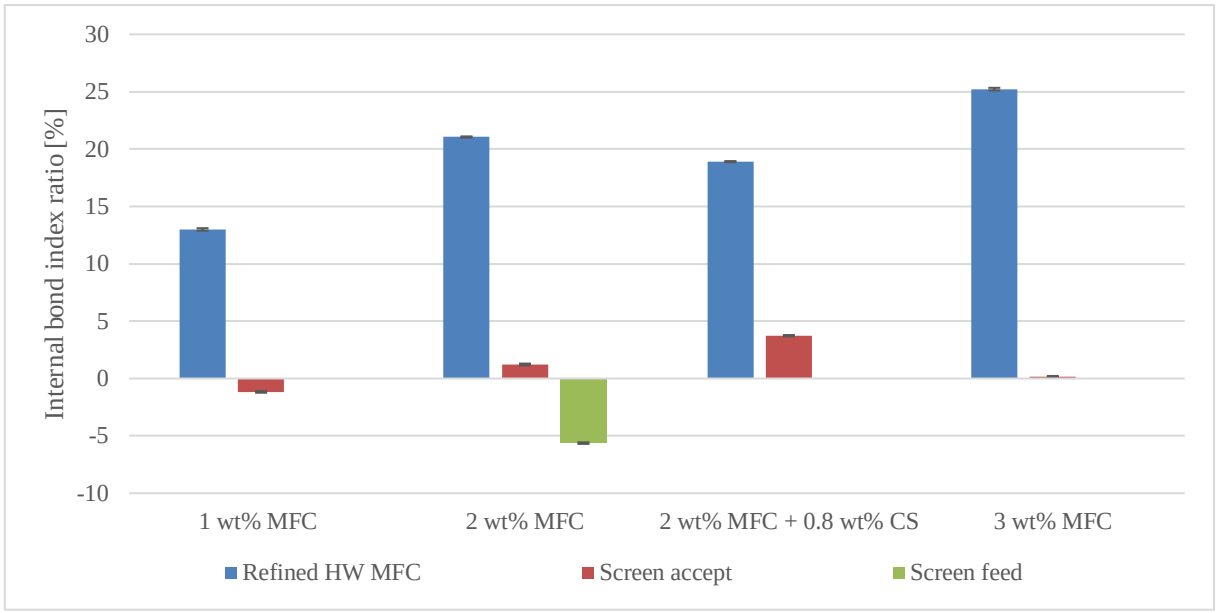

Figure 73 Internal bond index ratio for refined HW MFC, screened MFC accept and feed.

It was clearly shown that the refined HW MFC had a greater impact on the internal bond index than the screened MFC and feed. The effects of screening trial feed and accept (HW MFC) on internal bond index are presented in the coefficient plot in Figure 74. The coefficient plot shows the coefficients of the fitted model for which the factors were centered. In Figure 75, is shown the observed versus predicted plot when R^2 0.91 and Q^2 0.75.

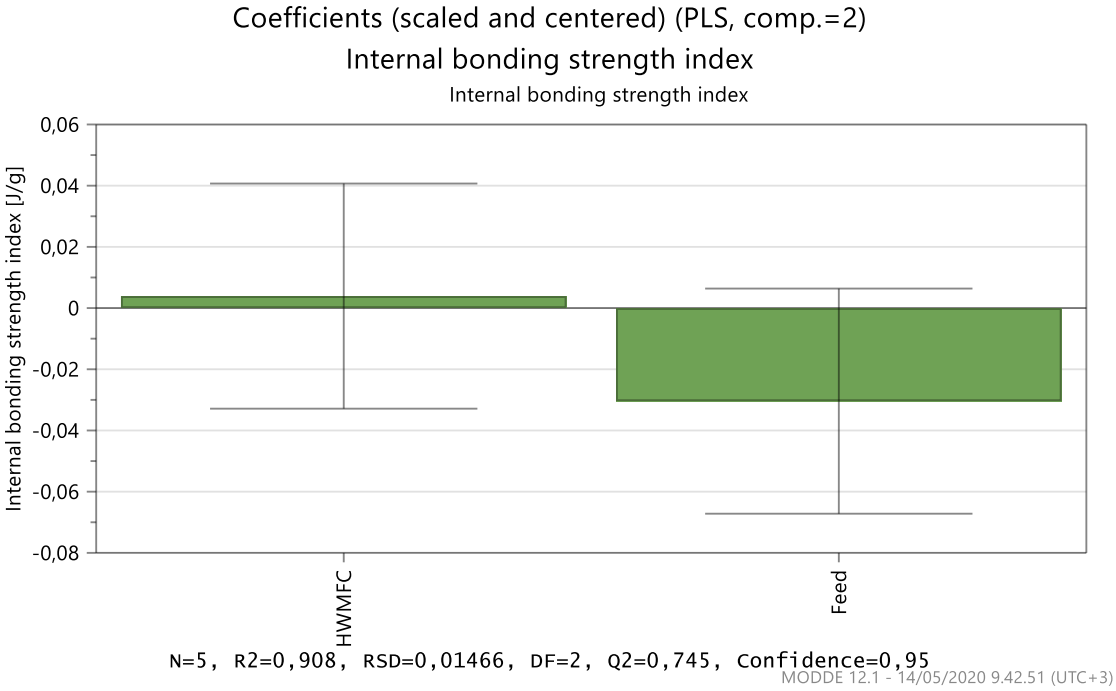

Figure 74 Scaled and centered coefficients for internal bond index, where HWMFC=screened MFC and FEED= feed in screening trials.

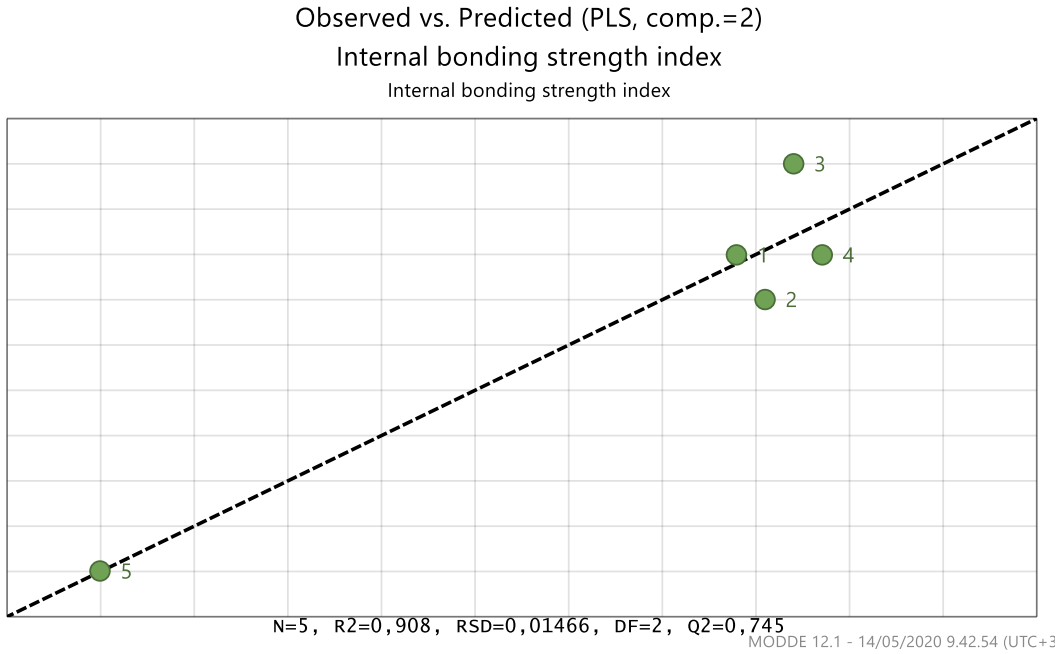

Figure 75 Observed vs. predicted plot for internal bond indices of screened MFC accept and feed.

According to R^2 and Q^2 value the model seems good. However, the Degrees of Freedom (DF) is 2 which gives false information about the model fit. Since both variables are close to y=0 the effect is insignificant. From Figure 74 can be seen that the screened MFC and feed have no impact on internal bond strength compared to the refined HW MFC. This can be due to the lower amount of fines B in accept and feed.

Not any kind of continuous trend was shown from the other properties. The results are shown in Appendix III. PLS regression done with MODDE Pro showed no correlation between any other variables.

9.5 Rheological properties of MFC

The effect of HW MFC concentration on rheology results was studied at three different concentrations: 1,2, and 3 wt%. Viscosity curves were measured at shear rates of 1-100 s^{-1} at 20 °C with all three concentrations. In Figure 76 and Figure 77 are shown viscosity and shear stress as a function of shear rate in different concentrations.

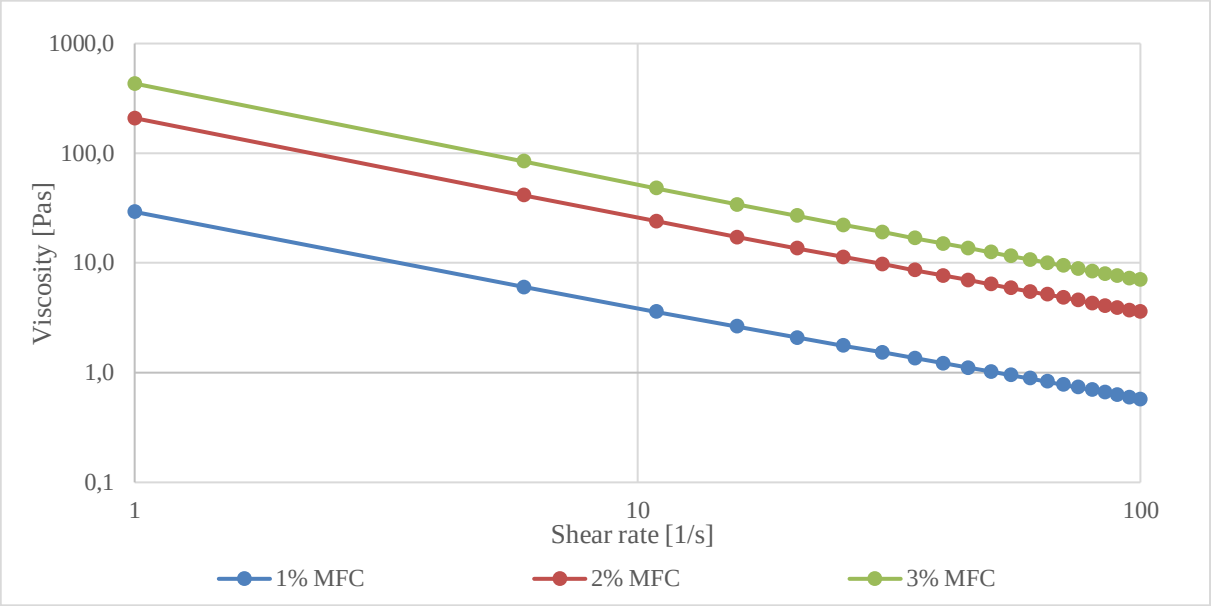

Figure 76 Viscosity curves for HW MFC in concentrations of 1 wt%, 2 wt% and 3 wt% at 20 °C

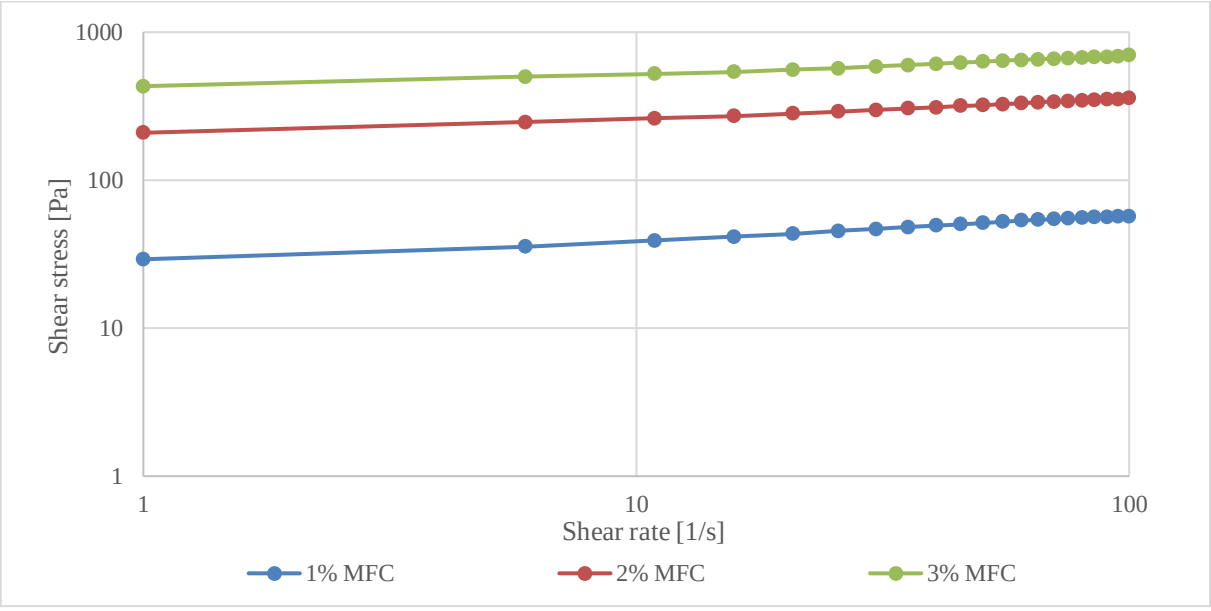

Figure 77 Flow behavior curves for HW MFC in concentrations of 1%, 2% and 3% at 20 °C

MFCs in all suspensions were highly viscous and dependent on the shear rate. Samples showed a shear-thinning behavior since the viscosity of each sample decreased when shear rate was increased. According to the results, MFC can be considered as a pseudoplastic material. The same kind of shear-thinning behavior was obtained from the literature for MFCs prepared mechanically. (Pääkkö et al., 2007) The viscosity of 1 wt% MFC decreased from 29 to 0.6 Pas when the shear rate was increased from 1 to 100 s^{-1}. The viscosity of 2 wt% MFC decreased from 209 to 3.6 Pas and with 3 wt% from 432 to 7.0 Pas. In their study Pääkkö et al. (2007) showed the same kind of shear-thinning behavior with different MFC concentrations. In their study it was shown that the viscosity of 1 wt% MFC decreased approximately from 5 to 0.05 Pas, with 2 wt% from 100 Pas to 0.5 Pas and with 3 wt% from 400 to 1 Pas with the shear rates 1 to 100 s^{-1}.

Also, the shear stresses increased slightly when the shear rate was increased. Shear stress with 1 wt% increased from 29 to 57 Pa, with 2 wt% from 209 to 358 Pas and with 3 wt% sample from 432 to 700 Pa when the shear rate was increased from 1 to 100 s^{-1}. In all MFC suspensions, a steady flow was shown, which can be obtained with a homogeneous structure of samples. No irregularities were shown in any of the samples.

Due to the highest concentration, 3 wt% MFC had the most viscous structure. When comparing the concentrations, the viscosity increased clearly when the concentration was increased from 1 to 2 wt%. The difference in viscosity between 2 and 3 wt% MFC was smaller.

The effect of temperature was studied with 2 wt% HW MFC at temperatures 10, 20, and 30 °C. In Figure 78 and Figure 79, is shown viscosity and shear stress as a function of shear rate.

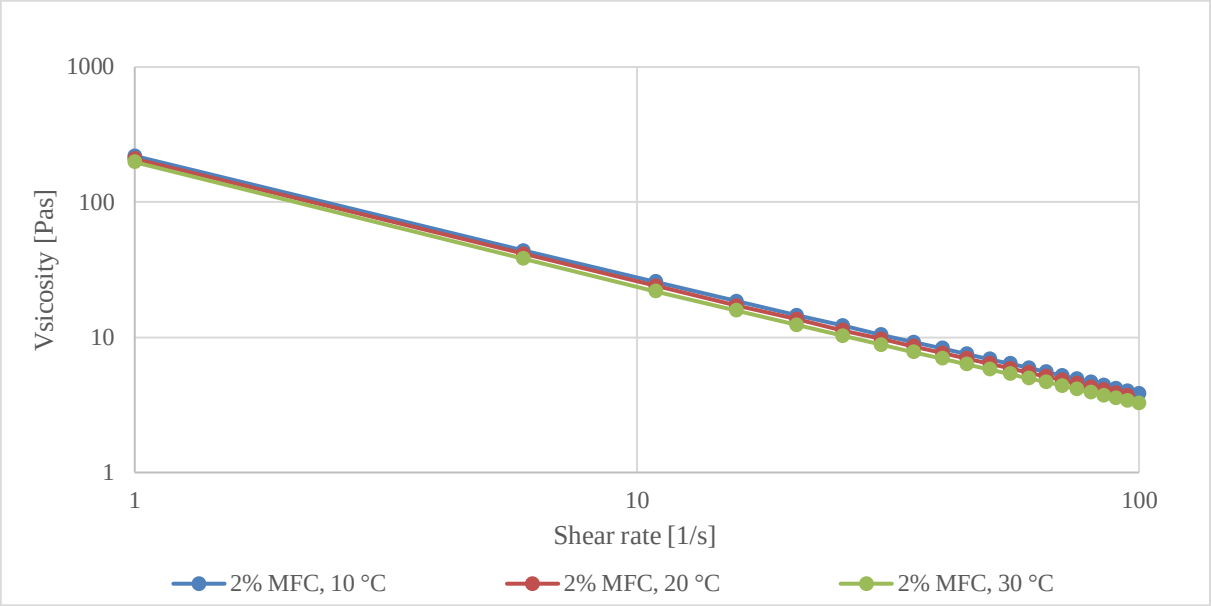

Figure 78 Viscosity curves for HW MFC in the consistency of 2 wt% at temperatures of 10 °C, 20 °C and 30 °C.

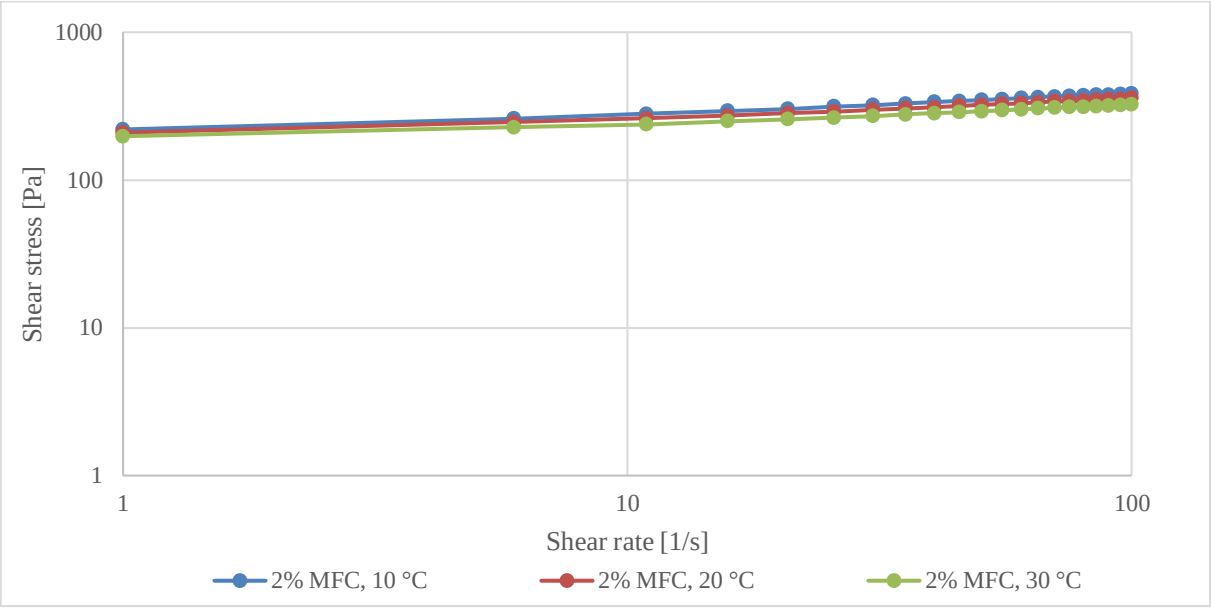

Figure 79 Flow behavior curves for HW MFC in the consistency of 2 wt% at temperatures of 10 °C, 20 °C and 30 °C

Viscosity decreased slightly when the temperature was increased. This can be due to the reduction of water and the deswelling of the fibers (Iotti et al., 2011). At shear rate of 1 s^{-1}

viscosities for 10, 20, and 30 °C were 220, 209, and 198 Pas, respectively. No great differences between each temperature were shown, therefore temperature does not affect the viscosity when MFC is transported or pumped. The linear viscoelastic region of the sample was determined with amplitude sweep. The results are presented in Figure 80.

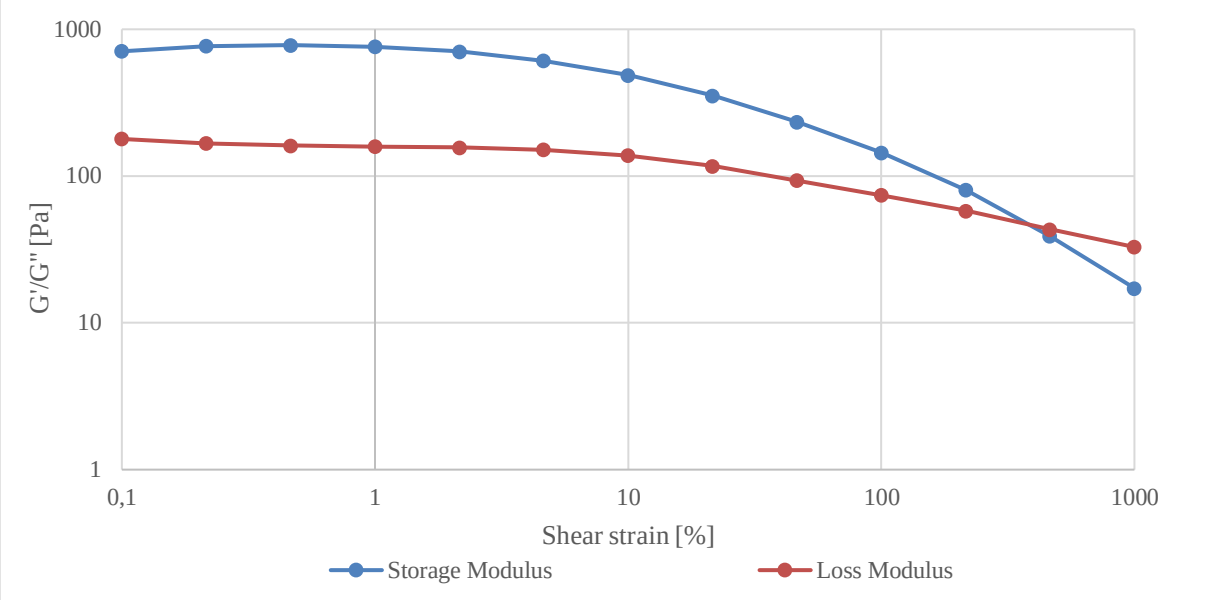

Figure 80 Storage (G') and loss (G") modulus as a function of shear strain for HW MFC at consistency of 2 wt% with angular frequency of 10 rad/s. Calculated flow-point (crossover) at τ = 255.6 Pa and G = 385,4% = 47.11 Pa.

As seen from the results gel-like consistency in low shear rates can be indicated since the elastic behavior is dominating the viscous behavior G'>G''. At the flow or cross-over point, where G'=G'', the sample starts to change from gel-like to fluid-like. (Mezger, 2011) Shear stress at the crossover point was 256 Pa and G'=G''=47 Pa. The crossover point tells the amount of stress needed to disturb and break down the structure. After this point, the material is flowing when the G' is smaller than the G'' the material. (Mezger, 2011) In Table XI are shown loss factor values in different shear strain values.

Table XI Loss factor for different shear strains.

Shear Strain, %	Loss Factor, tanδ	Viscoelastic behavior
0.1	0.25	Viscoelastic solid, gel
0.2	0.22	Viscoelastic solid, gel
0.5	0.21	Viscoelastic solid, gel
1.0	0.21	Viscoelastic solid, gel
2.2	0.22	Viscoelastic solid, gel
4.6	0.25	Viscoelastic solid, gel
10.0	0.28	Viscoelastic solid, gel
21.6	0.33	Viscoelastic solid, gel
46.4	0.40	Viscoelastic solid, gel
100.0	0.51	Viscoelastic solid, gel
216.0	0.72	Viscoelastic solid, gel
464.0	1.11	Viscoelastic liquid
1000.0	1.91	Viscoelastic liquid

According to the results, MFC is considered to have a viscoelastic liquid behavior when the loss factor is greater than 1. When loss factor is below 0 the materials are considered to have a viscoelastic soled/gel structure. The loss factor increased when the shear strain was increased. After the loss factor reaches the value of 1 (G'=G'') the material will flow. (Mezger, 2011) The calculated value of shear strain, G, must be over 47 Pa and the value of shear stress over 256 Pa before the 2 wt% MFC is starting to exhibit a viscoelastic liquid behavior and will flow. The shear rate for 2 wt% MFC can be calculated from Figure 77. The shear rate value is approximately 4.5 s^{-1} when shear stress is 256 Pa.

9.6 Full-scale trial planning

The shear rate in tubes can be calculated with the following Equation 13. (Haavisto et al., 2011) Shear rates are shown in Appendix V.

$$\dot{\gamma} = \frac{4Q}{\pi r^3} \quad (13)$$

Where,

Q = Volume flow rate, m^3/s

r = Radius of the tube, m

Apparent viscosity can be determined with Equation 14. (Mezger, 2011)

$$\eta = k\dot{\gamma}^{(n-1)} \quad (14)$$

The parameter n is the slope of the line from Figure 77. The consistency (thickness) factor k can be calculated with Equation 4. The parameter n and k values are presented in Appendix V. In Figure 81 and Figure 82 are shown the apparent viscosity as a function of flow rate in different pipe diameters with 1 wt% MFC suspension. Pipe diameters were set to be 100, 200, 300 and 400mm. The effect of temperature was not taken into consideration since the differences were very slight.

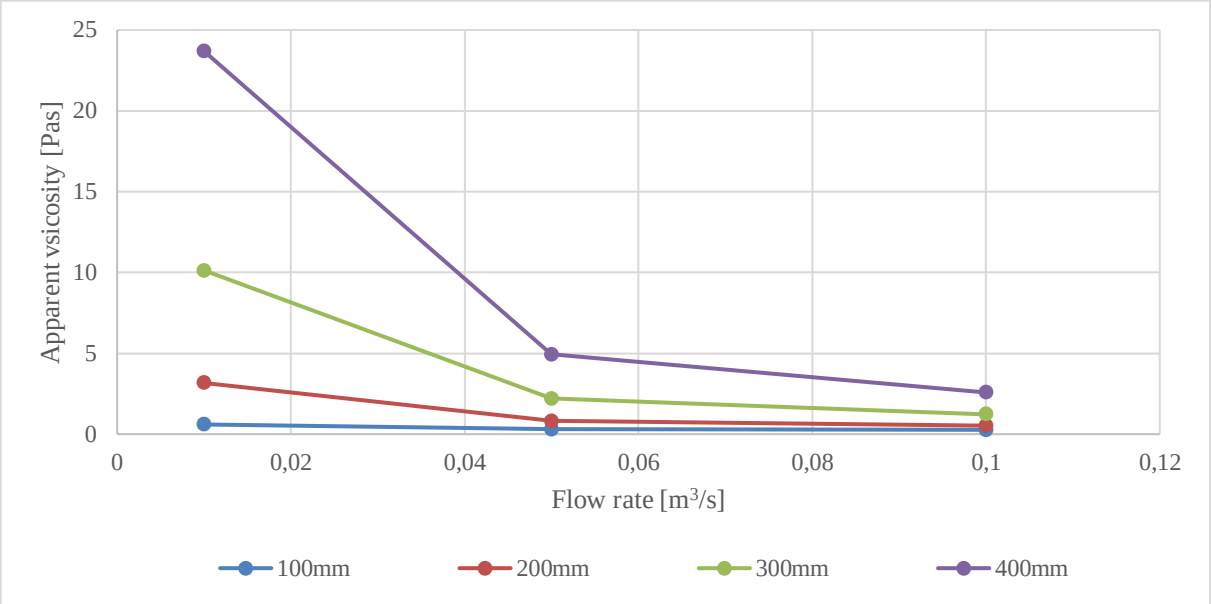

Figure 81 Apparent viscosity as a function of flow rate from 0.01 to 0.1 m^3/s for 1 wt% MFC at a temperature of 20 °C with pipe diameters 100, 200, 300, and 400 mm.

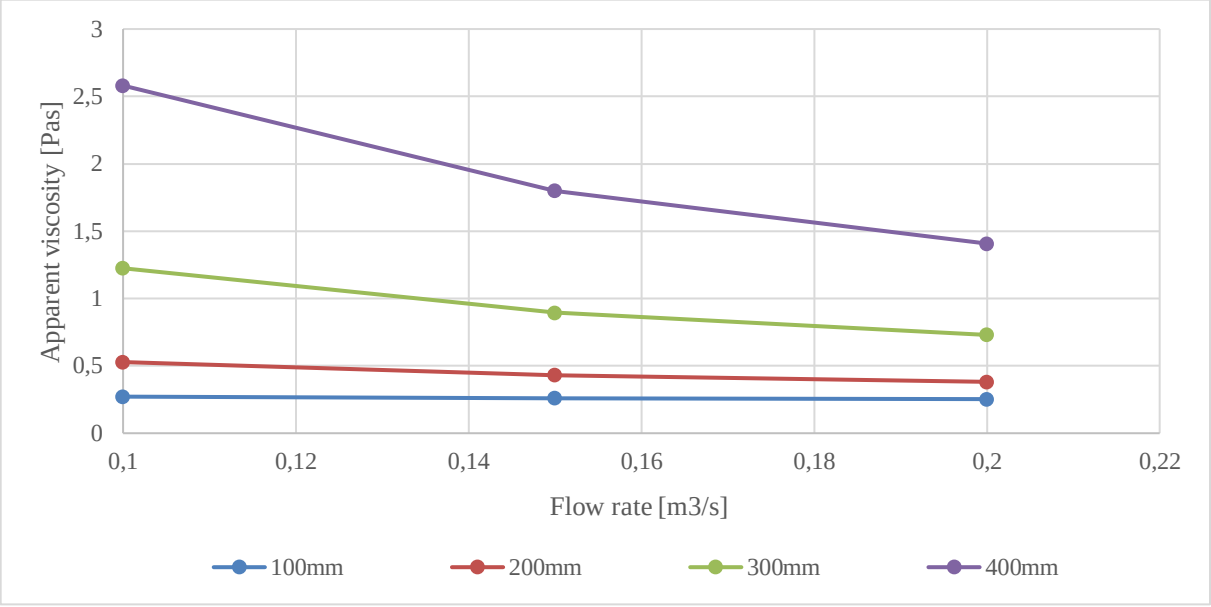

Figure 82 Apparent viscosity as a function of flow rate from 0.1 to 0.2 m3/s for 1 wt% MFC at a temperature of 20 °C with pipe diameters 100, 200, 300, and 400 mm.

The viscosity of 1 wt% MFC decreases in every pipe diameter when the flow rate is increased from 0.01 to 0.05 m^3/s. With pipe diameters 100 and 200 mm the viscosity stays constant after the flow rate is increased to 0.1 m^3/s. With pipe sizes 300 and 400 mm the viscosity decreases slightly. The same effects can be seen from the 2 and 3 wt% MFC suspensions shown in Figure 83 and Figure 84.

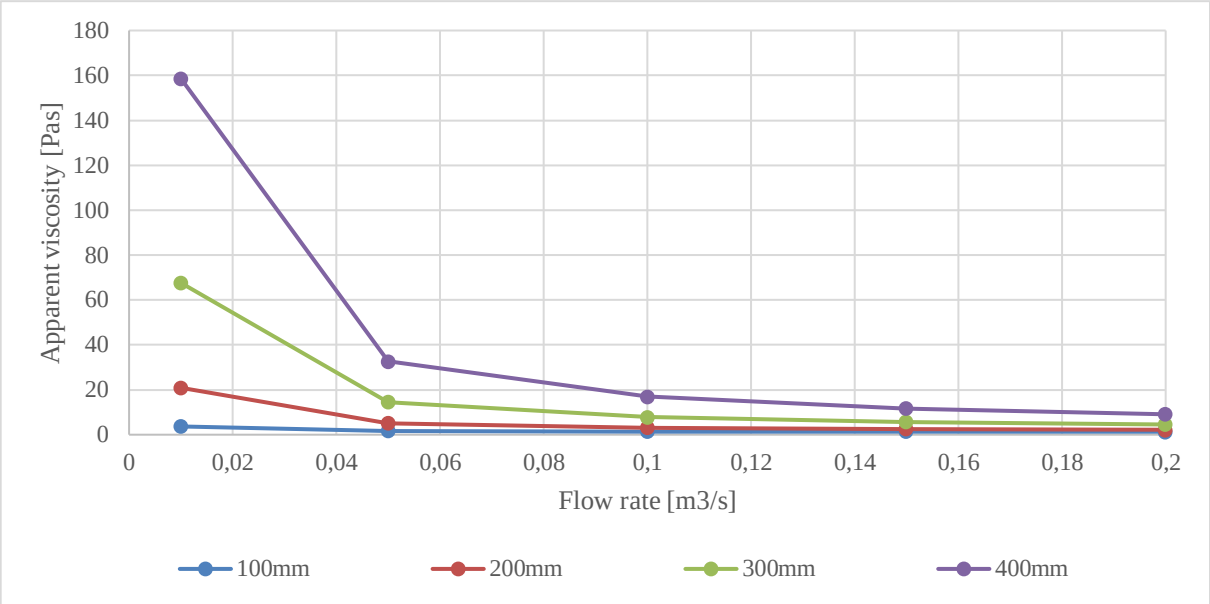

Figure 83 Apparent viscosity as a function of flow rate for 2 wt% MFC at a temperature of 20 °C with pipe diameters 100, 200, 300 and 400 mm.

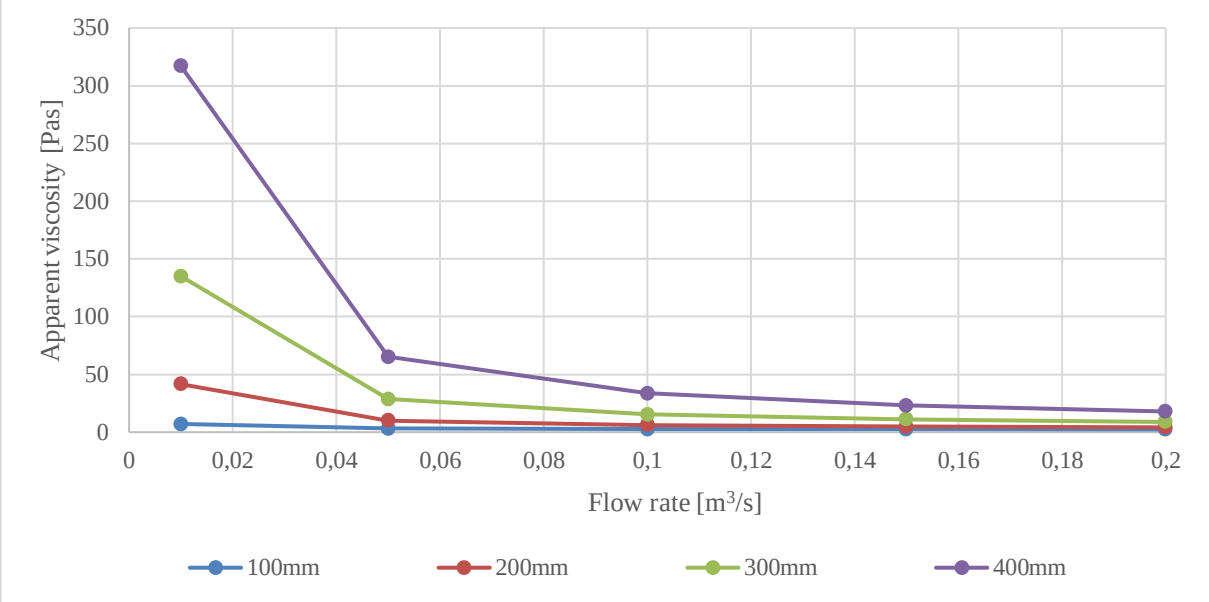

Figure 84 Apparent viscosity as a function of flow rate for 3 wt% MFC at a temperature of 20 °C with pipe diameters 100, 200, 300 and 400 mm.

The viscosity of each sample decreases when the flow rate is increased from 0.01 to 0.05 m^3/s. After this point the decreasing decelerates. With a bigger pipe diameter, the viscosity is greater. When comparing the concentrations, it can be seen, that with lower concentration the viscosity is lower. A great difference in viscosity can be seen between the 1 and 3 wt% MFC suspension. The biggest apparent viscosity with 3 wt% MFC (317 Pas) can be seen when pipe diameter 400mm was used and the flow rate was 0.1 m3/s. With the same parameters, the viscosity of 1 wt% MFC was only 24 Pas. In Table XII are shown dynamic viscosities of different materials for comparison.

Table XII Dynamic viscosities of different materials. 1) The Engineering Toolbox, 2020 2) Citerne et al., 2001 3) Edgeworth et al., 1984

Material	Dynamic viscosity [mPas]	Temperature [°C]
Benzene[1]	0.60	27
Water[1]	0.89	27
Glycerine[1]	950	27
Peanut butter[2]	10 000-1 000 000	-
Pitch[3]	$2.3*10^{11}$	20

The viscosities of MFC suspensions are similar to the viscosity of peanut butter. Since the apparent viscosity changes in different process conditions, statistic pipe mixers can be used if needed when handling viscous materials (>10 Pas). Also, storage containers should have mixing system to help the handling of the MFC.

Since the MFC needs to be transported to the mill site the concentration should be as high as possible, in this case around 3 wt%. Transportation and unloading the MFC to the storage container could be done by implementing the patent on Tamper et al. (2012) presented in chapter 6.3.1. In their publication Tamper et al. (2012) consider MFCs in which zero-shear viscosity is above 5000 Pas and especially above 10000 Pas hard to handle. The most difficult step of the transportation is to get the viscous MFC out of the truck container. In her work Kangas (2014) suggest that screw pumps could be used when handling MFC in high consistencies. As Tamper et al. (2012) suggested a progressive cavity pump could be used to discharge the MFC out of the container. This eccentric screw pump operates on a positive discharge placement principle. Kajanto et al. (2014) also suggested using the progressive cavity pump when the viscous material is mixed together with base pulp. Progressive cavity pumps and twin-screw pumps can be used to materials with high viscosity of 1 mPas to 3 000 000 mPas. For example, Wangen Pumpen hygienic progressive cavity pumps and twin-screw pumps can be used to viscosities up

to 1 000 000 mPas (FlowExperts, 2020; SPA, 2020) However, it has been shown that centrifugal MC pumps can be used when handling 4 wt% of refined MFC (Huhtanen, 2020)

MFC is transported to the mill site by truck. A usual container capacity of a truck container is around 44 m^3 (Tamper et al., 2012). It means that with one truck container 1320 kg of 3 wt% MFC as a dry substance can be transported at once. MFC needs to be unloaded to a bigger storage container and diluted to lower consistency before the trial if possible. This would help the handling and pumping. If MFC is dosed to the thick stock in lower consistency the mixing to the pulp is easier. According to the studies MFC at 1 wt% behaves like water when being mixed with kraft pulp. (FIBIC, 2013) If this is not possible MFC can be unloaded to a smaller storage container at 3 wt% concentration. MFC is pumped to the wet end system using a screw pump preferably a progressive cavity pump. In a trial, the MFC dosage should be as close to starch dosage as possible. In Figure 85, is shown the layout of the MFC dosage in the case mill.

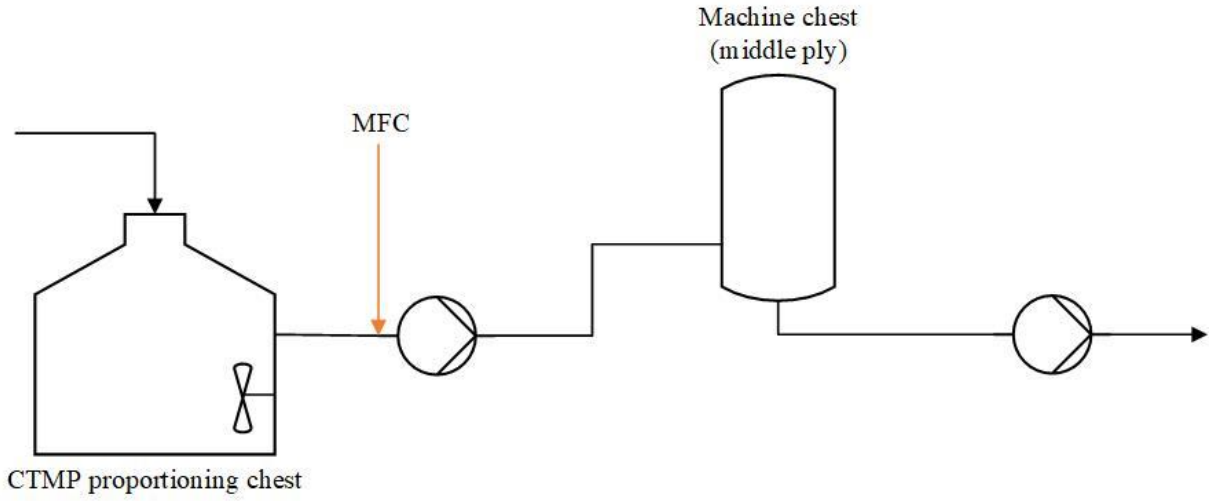

Figure 85 MFC dosing in the case mill.

MFC is dosed to the thick stock after the CTMP proportioning chest to the suction side of the pump. Starch is dosed closely after this before the machine chest. If possible MFC should be pumped using a progressive cavity pump.

In board machine trial MFC is applied to the middle ply of a multi-ply board product. The dosage of MFC in the middle ply should be around 1-2 wt%. Since the case mill uses POMix mixers the residence time is quite short approximately 1 min (Eiroma, 2008). At the beginning of the trial, it is preferable to start at a lower dosage (1 wt%) and after a certain time, the dosage can be ramped up to 2 wt%. The middle ply's production depends on the grade. For example, if the production is 25 t/h and the MFC dosage to the middle ply is 2 wt% this would mean that the MFC consumption as dry substance would be 500 kg/h. With one truck container (capacity 44 m3; 3wt% MFC) the trial would last approximately 2.5 hours.

The goal of the board machine trial is to replace some of the kraft pulp with CTMP using MFC. According to the results that were gained from the laboratory sheet trials it might be possible to reduce the CTMP/kraft pulp ratio 45/55 to 50/50 without compromising the paper properties too much. However, this was shown to be possible when 3 wt% of MFC was added to the pulp suspension. In a trial this could be done by first increasing the MFC dosage to the desired level and then increasing the CTMP dosage in small steps by keeping the quality homogeneous and constant. In the trial first-pass retention, dewatering on the wire section, dry content before and after the pressing should be monitored together with steam consumption and flows through disc filter. Laboratory sheets can be made from samples that are collected near the headbox and compared to the results that were gained from the laboratory sheet trials. All the necessary paper properties need to be tested from the end product after every reel. Reference material should be collected before and after the trial.

10 CONCLUSIONS

Better results in MFC quality were achieved with softwood as a raw material of MFC. However, energy consumption in softwood refining was much higher, 1540 kWh/t, than with hardwood refining, 820 kWh/t. The fibrillation proceeded quicker with softwood refining requiring less energy to a certain fibrillation level. However, approximately the same fiber length fractions were achieved using more energy in softwood refining. This is due to the longer fibers of softwood. Better quality of hardwood MFC could have been achieved using different fillings.

The difference between different fillings in MFC quality could be studied more in the future. Mainly due to the softwood refining costs it was decided that further studies focused more on hardwood MFC.

To lower the energy consumption of hardwood refining, screening trials were done by circulating the hardwood kraft pulp through the refiner 13 times. Energy consumption in this trial was 340 kWh/t. After this, the refined pulp was screened with slotted screen basket (#0,10 mm 90 (0,0)). However, the quality of the screened hardwood MFC was not as good as the refined hardwood MFC. For further studies, different process parameters and smaller slot widths and hole baskets should be tested. Also, the timing of the screening stage should be studied more. In this case, the screening was done from pulp that was in the middle of the refining process. Screening in early stages and at the end should also be studied more. Production of MFC would be more cost and energy-efficient if the screening could provide MFC that is the same or better in quality than with refining. For further studies the screening of softwood pulp could be done. Since the fibrillation proceeded faster and the quality was better the screening could lower the energy consumption. Screening could be done in the middle of the refining process. After the screening, the reject could be refined further to achieve the desired quality. Screening could be used together with refining to produce MFC on a paper/board mill site. Since the refining of MFC is a batch process it would be difficult to produce MFC continuously. Screening could be used to make the production more continuous. Accept could be used in the papermaking process and the reject could be fed back to the refiner.

The impact of different variables on paper properties was studied. It was shown that both soft- and hardwood MFCs improved some of the paper properties. The PLS regression models were shown to be good or acceptable in all properties except with the SCT which effects were not clear. Internal bond strength was increased clearly when 1-3 wt% of MFC was added. Any great differences between SW and HW MFC in internal bond strength were not shown. Tear strength was improved slightly when SW MFC was added. Tensile properties such as tensile strength and TEA were increased only with SW MFC. This can be due to the higher amount of fines B. Both MFCs had a slightly increasing impact on the SCT index. Because of the model fit of SCT index the effects were not clear. No significant changes were seen on tensile stiffness, strain at break, modulus of elasticity or break elongation. When comparing the results to the reference

point were the CTMP/kraft pulp ratio was 45/55 instead of 60/40 the results were lower. It can be said that based on these trials the CTMP dosage cannot be increased to 60 wt% when MFC is added. According to the results, it might be possible to reduce the CTMP/kraft pulp ratio from 45/55 to 50/50 with the addition of 3 wt % of MFC. More studies need to be done with different base pulp ratios. In a board machine trial, the CTMP dosage needs to be ramped up slowly to maintain the desired quality.

Effect of cationic starch addition from 0.5 to 0.8 and 1 wt% was studied with samples of 2 wt% of HW MFC. It was shown that the more CS was added the better the results were. CS had a greater impact on tensile strength than HW MFC. The effect of storage time was studied also. It was shown that the longer the MFC and other substances were stored the lower the results were. When screened and refined HW MFC were compared together it was shown that screened MFC accept had no significant impact on any of the measured paper properties. This can be due to the low fines B amount. It was also shown that neither tear nor tensile index did not improve with a greater amount of CS together with screened MFC than compared to the refined HW MFC. The internal bond index was increased slightly when 0.8 wt% of CS was added together with screened MFC. However, with refined HW MFC and 0.8 wt% of CS internal bond index increased by 19%. It was clearly shown that the feed in screening trials had no impact at all on the paper properties. This is due to the quality of the MFC. Compared to the refined HW MFC the same quality in fiber properties were not achieved yet. Fiber properties were slightly improved with screened MFC compared to the feed.

In rheological measurements, it was shown that all the MFC suspensions were highly viscous and dependent on the shear rate. Samples showed shear-thinning or pseudoplastic behavior. Due to the highest concentration, 3 wt% HW MFC had the most viscous structure. The temperature had no significant impact on viscosity. In 2 wt% MFC suspension, G'=G'' point was achieved with shear strain value of 47 Pa and shear stress value of 256 Pa. The shear rate value at this point was approximately 4.5 s^{-1}. This point tells how much stress is needed to break the structure and get the MFC to flow.

In board machine trial, it would be possible to transport the MFC in higher consistency of 3 wt% since the progressive cavity pump can be used to handle viscous MFC. These types of pumps

can be used to discharge highly viscous (1000-3000 Pas) materials. It has been shown that centrifugal MC pumps can also be used for handling 4 wt% of refined MFC. Method of Tamper et al. (2012) could be used when transporting and unloading the MFC. After transportation to mill site the MFC should be diluted to a lower concentration (~1 wt%) to guarantee the best possible mixing to the pulp. Due to the POMix mixers, that the case mill uses, and short residence times the dosage to the middle ply has to be ramped up from 1 to 2 wt%. At the beginning of the trial, the CTMP dosage should be kept as it is to make sure that the MFC increases the strength properties of the end product. After this, the CTMP dosage could be increased slowly to a targeted level keeping the quality constant. The addition of cationic starch could also be studied by increasing the dosage if wanted. All necessary paper properties should be done from every reel according to the case mill's instructions. Process conditions and parameters such as first-pass retention, dewatering on the wire section, dry content before and after the pressing should be monitored together with steam consumption and flows through disc filter.

REFERENCES

Adanur S. 1997. Paper machine clothing: Key to the Paper Making Process. Switzerland: Technomic Publishing.

Agoda-Tandjawa G., Durand S., Berot S., Blassel C., Gaillard C., Garnier C., Doublier J.-L. 2010. Rheological characterization of microfibrillated cellulose suspensions after freezing. Carbohydrate Polymers vol. 80 pp. 677-686

Alèn R. 2000. Structure and chemical composition of wood. In Stenius P. Forest Products Chemistry, Papermaking Science and Technology, Book 3, Jyväskylä: Fapet.

Ankerfors M., Lindström T., Song H. & Hoc M. 2009. Composition for coating of printing paper. Patent no. WO 2009/123560.

Ankerfors M., Duker E. & Lindström T. 2013. Topo-chemical modification of fibres by grafting of carboxymethyl cellulose in pilot scale. Nordic Pulp & Paper Research Journal vol. 28 pp. 6-14

Ankerfors M., Lindström T. & Söderberg D. 2014. The use of microfibrillated cellulose in fine paper manufacturing – Results from a pilot scale papermaking trial. Nordic Pulp & Paper Research Journal vol. 29 pp. 476-483

Ankerfors M. 2015. 5. Microfibrillated cellulose: Energy-efficient preparation techniques and applications in paper, Doctoral Thesis, KTH Royal Institute of Technology, Fibre and Polymer Technology.

Ankerfors M., Lindström T. & Nordmark G.G. 2016. Multilayer assembly onto pulp fibres using oppositely charged microfibrillated celluloses, starches, and wet strength resins − Effect on mechanical properties of CTMP-sheets. Nordic Pulp & Paper Research Journal vol. 31 pp. 135-141

Ankerfors M. 2020. Plural communication [interview] [15.1.2020]

Aulin C., Gällstedt M. & Lindström T. 2010a. Oxygen and oil barrier properties of microfibrillated cellulose films and coatings. Cellulose vol. 17 pp.559-57

Björkqvist T., Koskinen T., Nuopponen M., Vehniäinen, A. & Gustafsson H. 2011. A Method And An Apparatus For Producing Nanocellulose. WO2012089930(A1)

Blanco A., Concepcion Monte M., Campano C., Balea A., Merayo N. & Negro C. 2018. Chapter 5: Nanocellulose for Industrial Use: Cellulose Nanofibers (CNF), Cellulose Nanocrystals (CNC), and Bacterial Cellulose (BC) In Hussain C. M. Handbook of Nanomaterials for Industrial Applications. Elsevier.

Brodin F. W., Gregersen Ø. W. & Syverud K. Cellulose nanofibrils: Challenges and possibilities as a paper additive or coating material – A review. Nordic Pulp & Paper Research Journal vol. 29. pp. 156-166

Chaker A., Alila S., Mutjè P., Vilar M. R. & Boufi S. 2013. Key role of the hemicellulose content and the cell morphology on the nanofibrillation effectiveness of cellulose pulps. Cellulose vol. 20 pp. 2863-2875.

Citerne G. P., Carreau P. J. & Moan M. 2001. Rheological properties of peanut butter. Rheologica Acta vol. 40 pp. 86–96.

Desmaisons J., Boutonnet E., Ruedd M., Dufresne A. & Bras J. 2017. A new quality index for benchmarking of different cellulose nanofibrils. Carbohydrate polymers vol. 174 pp. 318-329

Edgeworth R., Dalton B.J., & Parnell T. 1984. The pitch drop experiment. European Journal of Physics vol 5 pp. 198–200.

Eiroma E. 2008. POMppu ja paperikoneen kompakti vesikierto. In Huuskonen et al, Yhteenveto innovaatioista sellu-, paperi- ja kartonkiteollisuudessa. [Online] [Accessed 28.5.2020] Available: https://www.puunjalostusinsinoorit.fi/biometsateollisuus/innovaatiot/4-paperin-ja-kartongin-valmistus/4.22-pomppu-ja-paperikoneen-kompakti-vesikierto/

Eriksen Ø, Syverud K. & Gregersen Ø. 2008. The use of microfibrillated cellulose produced from kraft pulp as strength enhancer in TMP paper. Nordic Pulp & Paper Research Journal vol. 23 pp.299-304

Eyholzer Ch., Bordeanu N., Lopez-Suevos F., Rentsch D., Zimmenmann T. & Oksman K. 2010. Preparation and characterization of water-redispersible nanofibrillated cellulose in powder form. Cellulose vol. 17 pp. 19-30

Fall A. B., Burman A. & Wågberg L. 2014. Cellulosic nanofibrils from eucalyptus, acacia and pine fibers. Nordic Pulp & Paper Research Journal vol. 29 pp.176-184.

Fellers C., Sören Ö., Mäkelä P. 2012. Evaluation of the Scott bond test method, Nordic Pulp and Paper Research Journal vol. 27 pp. 231-236

FIBIC Finnis Bieconomy Cluster. 2013. Efficient Networking Towards Novel Products and Processes. EFFNET Programme Report 2010–2013.

FloeExperts. 2020. Epäkeskoruuvipumput – Wangen. [Online] [Accessed 15.6.2020] Available: https://flowexperts.fi/hygieeniset-epakeskoruuvipumput/

Gharekhani S., Sadeghinezhad E., Kazi S.N., Yarmand H., Badarudin A., Safaei M.R., & Zubir M.N.M. 2014. Basic effects of pulp refining on fiber properties – A review, Carbohydrate Polymers vol. 115 pp. 785-803.

González I., Vilaseca F., Alcalá M., Pèlach M. A., Boufi S. & Mutjé P. Effect of the combination of biobeating and NFC on the physico-mechanical properties of paper. Cellulose vol. 20 pp. 1425-1435

González I., Boufi S., Pèlach M. A., Alcalá M., Vilaseca F. & Mutjé P. 2012. Nanofibrillated cellulose as paper additive in eucalyptus pulps. BioResources vol. 7 pp. 5167-5180

Haavisto S., Liukkonen J. Jäsberg A., Koponen A., Lille M. & Salmela J. 2010. Laboratory-Scale Pipe Rheometry: A Study of a Microfibrillated Cellulose Suspension. In Proceedings of the 7th International Symposium on Ultrasonic Doppler Methods for Mechanics and Fluid Engineering: Chalmers University of Technology, Gothenburg, Sweden, April 7-8, 2010 (pp. 103-106) Available: https://www.isud-conference.org/ISUD-07/ISUD_7_proceedings.pdf

Heiskanen I., Axrup L. & Laitinen R. 2011. Process for the production of a paper or board product and a paper or board produced according to the process. Patent no. WO/2011/056135.

Heiskanen I., Kastinen H., Axrup L., Pöllänen S., Korjonen J., Suhonen P., Tiainen T & Väkeväinen M. 2017a. Method and apparatus for producing microfibrillated cellulose fiber. Patent no. WO/2017/033125.

Heiskanen I., Lampainen S. & Kankkunen J. 2017b. Board with improved compression strength. Patent no. WO/2017/163176.

Herrick F.W. 1983. Process for preparing microfibrillated cellulose. US Patent no. 4481077A.

Hofmann P. & Jones M.A. 1989. Structure and Degradation Process for Waterlogged Archaeological Wood. Archeological wood. Advances in Chemistry vol. 225 pp. 35-65.

Hollertz R., Durán V.L., Larsson P.A. and Wågberg L. 2017. Chemically modified cellulose micro-and nanofibrils as paper-strength additives. Cellulose vol 24 pp. 3883-3899.

Huhtanen J-P. 2019. Intelligent refining to contribute minimized operating costs, optimal quality and increased stability – solutions and results. PaperCon 2019, Indianapolis.

Huhtanen J-P. 2020. Plural communication [interview] [25.16.2020]

Huhtanen J-P. & Partanen M. 2013. Mill Experience With Metso's New Low Consistency Refining Concept OptiFiner Pro. PaperCon 2013, Atlanta.

Hult E.-L., Larsson P.T. & Iversen T. 2000. Cellulose fibril aggregation - an inherent property of kraft pulps. Polymer vol. 42 pp. 3309-3314

Häggblom-Ahnger U. & Komulainen P. 2006. Kemiallinen metsäteollisuus II - Paperin ja kartongin valmistus. 5. ed. Gummerus Kirjapaino: Jyväskylä.

Investing. 2020a. Bleached Softwood Kraft Pulp Futures. [Online] [Accessed 9.6.2020] Available:https://www.investing.com/commodities/shfe-bleached-softwood-kraft-pulp-futures-streaming-chart

Investing. 2020b. Corn Starch Futures. [Online] [Accessed 9.6.2020] Available: https://www.investing.com/commodities/corn-starch-futures-streaming-chart

Iotti M., Gregersen Ø., Moe S., Lene, M. 2011. Rheological studies of microfibrillar cellulose water dispersions. Journal of Polymers and the Environment vol. 19 pp. 137-145

ISO/TS 20477:2017. Nanotechnologies - Standard terms and their definition for cellulose nanomaterial.

ISO 534:2011. Paper and board — Determination of thickness, density and specific volume.

Jahangir E. S. & Olson J. A. 2020. Low consistency refined ligno-cellulose microfibre: an MFC alternative for high bulk, tear and tensile mechanical pulp papers. Cellulose.

Kajanto, I. 2008. Structural mechanics of paper and board. In Niskanen K., Paper Physics, Papermaking Science and Technology, Book 16, Second edition. Helsinki: Finnish Paper Engineers' Association/Paperi ja Puu

Kajanto I. & Kosonen M. 2012. The potential use of micro- and nanofibrillated cellulose as a reinforcing element in paper. Journal of Science & Technology for Forest Products and Processes vol. 2 pp. 42-48

Kajanto I., Tienvier T. & Tamper J. Method for making nanofibrillar cellulose and for making a paper product. Patent no. WO/2014/184442A1

Kangas H. 2014. Opas selluloosa- nanomateriaaleihin. Espoo: Valtion teknillinen tutkimuskeskus (VTT). Tiedotteita 199.

Karppinen A. 2014. Rheology and flocculation of polymer-modified microfibrillated cellulose suspensions. Doctoral dissertation. Helsinki: Aalto University.

Kekäläinen K., Liimatainen H., Illikainen M., Maloney T.C. & Niinimäki J. 2014. The role of hornification in the disintegration behavior of TEMPO-oxidized bleached hardwood fibres in a high-shear homogenizer. Cellulose vol. 21 pp. 1163-1174

Kinnunen K. & Hjelt T. 2013. Fibrous web of paper or board and method of making the same. Patent no. WO/2013/160553.

Kinnunen-Raudaskoski K., Hjelt T., Kenttä E. & Forsström U. 2014. Thin coating for paper by foam coating. Tappi Journal vol. 13 pp. 9-19.

Kiviranta A., 2000. Paperboard grades In Paulapuro, H. Paper and Board Grades, Papermaking Science and Technology, Book 18, Jyväskylä: Fapet.

Klemm D., Kramer F., Moritz S., Lindström T., Ankerfors M., Gray D. & Dorris A. 2011. Nanocelluloses: A New Family of Nature-Based Materials. Angewandte chemie-international edition vol. 50 pp. 5438-5466.

KnowPap. Learning Environment for Papermaking and Automation 21.0. AEL & Prowledge Oy., [Accessed 15.1.2020].

Kohonen J, Reinikainen S-P., Aaljoki K. & Höskuldsson A. 2009. Non-linear PLS approach in score surface. Chemometrics and Intelligent Laboratory Systems vol. 97 pp.159–163.

Korelin A. 2020. Optimizing refining amount for microfibrillated cellulose in paperboard applications. Master's thesis. Aalto University, Fiber and polymer engineering.

Koskenhely K. 2007. Refining of chemical pulp fibers. In Paulapuro H. Papermaking Part 1, Stcok Preparation and Wet End. Papermaking Science and Technology, Book 8, Second edition. Helsinki: Finnish Paper Engineers' Association/Paperi ja Puu

Krogerus B. 2007. Papermaking additives. In Alèn R. Papermaking chemistry, Papermaking Science and Technology, Book 4, Jyväskylä: Finnish Paper Engineers' Association/Paperi ja Puu.

Lampainen S., Peng F., Laakso A., & Määttänen A-P. 2020. A ply of a linerboard and a light weight linerboard for corrugated board. Patent no. WO/2020/003129

Lavoine N., Desloges I., Dufresne A. & Bras J. 2012. Microfibrillated cellulose – Its barrier properties and applications in cellulosic materials: A review. Carbohydrate Polymers vol. 90 pp. 735–764.

Lehmonen J., Pere J., Hytönen E. & Kangas H. 2016. Effect of cellulose microfibril (CMF) addition on strength properties of middle ply of board. Cellulose vol. 24 pp. 1041-1055.

Levlin J-E. 1999. In . In Levlin J-E. Pulp and Paper Testing, Papermaking Science and Technology, Book 17, Jyväskylä: Fapet.

Li D. & Xia Y. 2004. Electrospinning of Nanofibers: Reinventing the Wheel? Advanced Materials vol. 19 pp. 1151-1170.

Lindström T., Aulin C., Nadrei A. & Ankerfros M. 2014. Microfibrillated cellulose. Encyclopedia of Polymer Science and Technology.

Masuko. 2020. Ultra-fine friction grinder "Supermasscolloider". [Online] [Accessed 16.3.2020] Available: http://www.masuko.com/English/product/Masscolloder.html

Mezger, T. G. 2011. The Rheology Handbook. 3rd revised edition. Hannover, Vincentz Network. 432p.

Moberg T. & Rigdahl M. 2012. On the Viscoelastic Properties of Microfibrillated Cellulose (MFC) Suspensions. Annual transactions of the Nordic Rheology Society vol. 20 pp. 123-130.

Nechyporchuk O., Belgacem M. N. & Bras J. 2016. Production of cellulose nanofibrils: A review of recent advances. Industrial Crops and Products vol. 93 pp. 2-25.

Olivieari A. C. 2018. Introduction to Multivariate Calibration: A Practical Approach. Switzerland, Springer.

Osong S. H., Norgren S. & Engstrand P. 2016. Processing of wood-based microfibrillated cellulose and nanofibrillated cellulose, and applications relating to papermaking: a review. Cellulose vol. 23 pp. 93-123

Osong S. H., Norgren S., Petterson G & Engstrand P. 2017. The use of cationic starch and microfibrillated cellulose to improve strength properties of CTMP-based paperboard.

Paunonen S. 2013. Strength and barrier enhancements of composites and packaging boards by nanocelluloses – A literature review. Nordic Pulp & Paper Research Journal vol. 28 pp.165-181

Pereira Damásio R. A. & Coelho dos Santos Muguet Soares M. 2019a. Paper and process for manufacturing paper using microfibrillated cellulose between the layers thereof. Patent no. WO/2019/227186

Pereira Damásio R. A. & Coelho dos Santos Muguet Soares M. 2019b. Paper and process for manufacturing paper using microfibrillated cellulose in the cellulose pulp. Patent no. WO/2019/227187

Pèrez J., Muñoz-Dorado J., de la Rubia T. & Martínez J. 2002. Biodegradation and biological treatments of cellulose, hemicellulose and lignin: an overview. Int Microbiol vol. 5 pp. 53–63.

Plackett D., Anturi, H., Hedenqvist M., Ankerfors M., Gällstedt M., Lindström T., Sirò I. 2010. Physical properties and morphology of films prepared from microfibrillated cellulose and microfibrillated cellulose in combination with amylopectin. Journal of Applied Polymer Science vol. 117 pp. 3601-3609.

Pääkkö M., Ankerfors M., Kosonen H., Nykänen A., Ahola, S., Österberg M., Ruokolainen J., Laine J., Larsson P.T. & Ikkala O. 2007. Enzymatic hydrolysis combined with mechanical shearing and high-pressure homogenization for nanoscale cellulose fibrils and strong gels. Biomacromolecules, vol. 8 pp. 1934-1941.

Rantanen J. & Maloney T. C. 2013. Press dewatering and nip rewetting of paper containing nano- and microfibril cellulose. Nordic Pulp & Paper Research Journal vol. 28 pp. 582-587

Retulainen E., Moss P., Nieminen K. 1993. Effect of fines on the properties of fibre networks. In: Baker C.F. Products of papermaking, vol. 2, Transactions of the 10th fundamental research symposium September 1993. Oxford, Pira International.

Retulainen, E. and Nieminen, K. (1996): Fibre properties as control variables in papermaking. 2. Strengthening interfibre bonds and reducing grammage, Paperi ja Puu, vol. 78 pp. 305-312.

Ritala R. 2009. Managing paper machine operation. In Leiviskä K. Process and Maintenance Management, Papermaking Science and Technology, Book 14, Jyväskylä: Finnish Paper Engineers' Association/Paperi ja Puu.

Roper III J. 2009. In Paltakari J. Pigment Coationg and Surface Sizing of Paper, Papermaking Science and Technology, Book 11, Jyväskylä: Finnish Paper Engineers' Association/Paperi ja Puu.

Ryy J-Y. & Lee H.L. 2007. Improvement of plybond strength of two-ply sheets by spraying of starch blends. Tappi Journal vol. 6 pp. 3-8.

Saarikoski E., Saarinen T., Salmela J. & Seppälä J. 2012. Flocculated flow of microfibrillated cellulose water suspensions: an imaging approach for characterisationof rheological behaviour. Cellulose vol. 19 pp.647-659.

Sartorius Stedim Data Analytics. 2017. User Guide to MODDE. [Online] [Accessed 1.6.2020] Available: https://blog.umetrics.com/hubfs/Download%20Files/MODDE%2012.0.1%20User%20Guide.pdf

Shcmid C.F. & Klingenberg D. J. 2000. Mechanical Flocculation in Flowing Fiber Suspensions. Physical review letters vol. 84 pp. 290-293

Siró I. & Plackett D., 2009. Microfibrillated cellulose and new nanocomposite materials: a review. Cellulose vol. 17 pp. 459-494.

Sirviö J. 2008 Fibers and bonds. In Niskanen K., Paper Physics, Papermaking Science and Technology, Book 16, Second edition. Helsinki: Finnish Paper Engineers' Association/Paperi ja Puu

Sjöström E. 1993. Wood Chemistry. Fundamentals and Applications. Second edition. San Diego: Academic press.

Smook G. A. & Kocurek M.J. 2002. Handbook for pulp & paper technologists. 3rd edition. Vancouver : Angus Wilde Publication

Solala I., Volperts A., Andersone A., Dizhbite T., Mironova-Ulmane N., Vehniäinen A., Pere J. & Vuorinen T. 2011. Mechanoradical formation and its effects on birch kraft pulp during the

preparation of nanofibrillated cellulose with Masuko refining. Holzforschung vol. 66 pp. 477–483.

SPA. Star pump alliance. 2020. Progressing cavity pumps. . [Online] [Accessed 15.6.2020] Available: https://www.starpumpalliance.com/progressing-cavity-pumps/

Spence K.L., Venditti R. A., Habibi Y., Rojas O. J. & Pawlak J.J. 2010. The effect of chemical composition on microfibrillar cellulose films from wood pulps: Mechanical processing and physical properties. Bioresource Technology vol. 101 pp. 5961-5968

Spence K.L., Venditti R. A., Rojas O. J., Habibi Y. & Pawlak J.J. 2011. A comparative study of energy consumption and physical properties of microfibrillated cellulose produced by different processing methods. Cellulose vol. 18 pp. 1097-1111

Steffe, J.F. 1996. Rheological methods in food process engineering. Second edition. Freeman Press. Michigan. 418p.

Stelte W. & Sanadi A. R. 2009. Preparation and Characterization of Cellulose Nanofibers from Two Commercial Hardwood and Softwood Pulps. Industrial & Engineering Chemistry Research vol. 48 pp. 11211-11219

Sulzer. 2020. Medium-consistency products. [Online] [Accessed 25.6.2020] Available: https://www.sulzer.com/en/products/medium-consistency-products

Suzuki M. & Hattori Y. 2003. Method and Apparatus for Manufacturing Microfibrillated Cellulose Fiber. US7381294(B2)

Syverud K. & Stenius P. Strength and barrier properties of MFC films. 2009. Cellulose vol. 16 pp.75-85

Taipale T., Österberg M., Nykänen A., Ruokalainen J. & Laine J. 2010. Effect of microfibrillated cellulose and fines on the drainage of kraft pulp suspension and paper strength. Cellulose vol. 17 pp. 1005-1020

Tamper J., Kajanto I., Alajääski M., Tienvieri T. & Nuopponen M. 2012. Method and apparatus for transportin viscous material. FI126300 B.

TAPPI Standard WI-3021: Standard Term and Their Definition for Cellulose Nanomaterial. Draft. [Online] [Accessed 8.1.2020] Available: https://www.tappi.org/content/hide/draft3.pdf

The Engineering Toolbox. 2020. Dynamic Viscosity of common Liquids. [Online] [Accessed 15.6.2020] Available: https://www.engineeringtoolbox.com/absolute-viscosity-liquids-d_1259.html

Tomberg J. 2009. Special measurements in pulp and paper process. In Leiviskä K. Process and Maintenance Management, Papermaking Science and Technology, Book 14, Jyväskylä: Finnish Paper Engineers' Association/Paperi ja Puu

Turbak A. F., Snyder F. W., & Sandber K.R. 1981. Microfibrillated cellulose. US Patent no. 4374702A.

Umetrics. 2020. MODDE Pro. [Online] [Accessed 2.6.2020] Available: https://umetrics.com/product/modde-pro

Valmet. 2020a. Refining: OptiFiner Pro. [Online] [Accessed 14.1.2020] Available: https://www.valmet.com/board-and-paper/stock-preparation/refining/refining/radial-flow-refiners/

Valmet. 2020b. Valmet Paper Lab - automated board and paper testing laboratory. [Online] [Accessed 17.2.2020] Available: https://www.valmet.com/automation/analyzers-measurements/analyzers/paper-lab/#392e41f9

Valmet. 2020c. Valmet Wet End Applicator. [Online] [Accessed 25.6.2020] Available: https://valmetsites.secure.force.com/solutionfinderweb/FilePreview?id=0694H00000CJSNTQA5&_ga=2.47243559.1841782037.1593077364-904933448.1591097558

Valmet. 2020d. Valmet Pulp Expert. [Online] [Accessed 25.6.2020] Available: https://www.valmet.com/automation/analyzers-measurements/analyzers /pulp-expert/

Valmet. 2020e. Valmet Fiber Furnish Analyzer - Valmet MAP Q. [Online] [Accessed 25.6.2020]Available:https://www.valmet.com/automation/analyzers-measurements/analyzers/pulp-analyzer/?page=1

Vartiainen J., Pöhler T., Sirola K., Pylkkänen L., Alenius H., Hokkinen J., Tapper U., Lahtinen P., Kapanen A., Putkisto K., Hiekkataipale P., Eronen P., Ruokolainen J. & Laukkanen A. 2011. Health and environmental safety aspects of friction grinding and spray drying of microfibrillated cellulose. Cellulose vol.18 pp. 775-786

Vikman M., Vartiainen J., Tsitko I. & Korhonen P. 2014. Biodegradability and Compostability of Nanofibrillar Cellulose-Based Products. Journal of Polymers and the Environment vol.23 pp. 206-215

Wolfgang K. H & Léopold S. Applied Multivariate Statistical Analysis. Springer-Verlag, Berlin Heidelberg. 516 p.

Ålander E., Östlund I., Lindgren K., Johansson M. & Gimåker M. 2017. Towards a More-Cost-Efficient Paper and Board Making using Microfibrillated Cellulose. NWBC 2017, Stockholm, March 28-30

Österberg M., Vartiainen J., Lucenius J., Hippi U., Seppälä J., Serimaa R. & Laine J., A Fast Method to Produce Strong NFC Films as a Platform for Barrier and Functional Materials. ACS Applied Materials & Interfaces vol.5 pp. 4640−4647

APPENDICES

Table XIII Refining results of HW MFC from the feed, homogenization round and passes 1 to 13.

Passes through refiner	Feed	Homogenization	1st	4th	7th	10th	13th
SRE cumulative, kWh/t	0	3	33	187	326	449	551
Consistency, %	3.91	4.21	4.22	4.23	4.24	4.14	3.85
SR, °	17	17	27	71	88	92	94
Lc(l) ISO, mm	0.94	0.95	0.95	0.84	0.72	0.60	0.51
Lc(l) Tappi, mm	0.90	0.91	0.91	0.76	0.61	0.48	0.40
Fr(l) 0.00-0.20 mm, %	22.1	22.9	23.5	35.5	46.0	53.8	59.9
Fr(l) 0.20-0.60 mm, %	11.2	10.9	11.1	16.3	21.4	25.4	27.5
Fr(l) 0.60-1.20 mm, %	52.9	51.5	50.2	39.6	28.6	19.3	12.1
Fr(l) 1.20-2.00 mm, %	13.2	14.1	14.6	8.4	3.9	1.4	0.6
Fr(l) 2.00-3.20 mm, %	0.5	0.6	0.6	0.2	0.1	0.0	0.0
Fr(l) 3.20-7.60 mm, %	0.1	0.1	0.0	0.0	0.0	0.0	0.0
Fines A, %	13.9	14.4	14.6	23.5	32.5	40.6	47.2
Fines B, %	0.1	0.0	0.2	1.0	2.2	3.1	3.7
Fines F(n), %	82.5	83.4	84.2	89.1	91.2	92.2	93.0
Fibrillation, %	0.21	0.2	0.32	0.68	1.09	1.31	1.58

Table XIV Refining results of HW MFC from passes 16 to 26.

Passes through refiner	**16th**	**19th**	**22nd**	**25th**	**26th**
SRE cumulative, kWh/t	638	699	754	805	822
Consistency, %	3.96	4.14	4.10	3.97	4.05
SR, °	95	94	93	93	94
Lc(l) ISO, mm	0.46	0.43	0.40	0.38	0.37
Lc(l) Tappi, mm	0.35	0.32	0.30	0.28	0.28
Fr(l) 0.00-0.20 mm, %	63.4	65.3	66.9	68.8	69.4
Fr(l) 0.20-0.60 mm, %	28.1	28.4	28.5	27.8	27.7
Fr(l) 0.60-1.20 mm, %	8.2	6.1	4.5	3.3	3.0
Fr(l) 1.20-2.00 mm, %	0.3	0.1	0.1	0.0	0.0
Fr(l) 2.00-3.20 mm, %	0.0	0.0	0.0	0.0	0.0
Fr(l) 3.20-7.60 mm, %	0.0	0.0	0.0	0.0	0.0
Fines A, %	51.6	54.2	56.6	59.2	60.1
Fines B, %	4.1	4.5	4.9	4.9	5.6
Fines F(n), %	93.4	93.6	93.8	94.1	94.2
Fibrillation, %	1.67	1.85	1.9	2.01	2.03

Table XV Refining results of SW MFC from the feed, homogenization round and passes 1 to 13.

Passes through refiner	Feed	Homogenization	1st	4th	7th	10th	13th
SRE cumulative, kWh/t	0	10	56	216	396	567	714
Consistency, %	3.87	4.17	4.23	4.09	4.00	3.96	3.90
SR, °	13	14	18	50	82	90	93
Lc(l) ISO, mm	1.77	1.74	1.74	1.57	1.28	1.07	0.90
Lc(l) Tappi, mm	1.65	1.63	1.63	1.45	1.15	0.96	0.79
Fr(l) 0.00-0.20 mm, %	16.5	16.6	16.0	19.6	25.3	26.4	28.8
Fr(l) 0.20-0.60 mm, %	9.2	9.1	9.3	13.4	20.6	26.1	30.6
Fr(l) 0.60-1.20 mm, %	23.6	24.7	24.0	23.8	23.4	24.8	24.7
Fr(l) 1.20-2.00 mm, %	18.9	18.1	19.7	17.6	14.7	12.2	9.7
Fr(l) 2.00-3.20 mm, %	22.4	22.8	21.7	19.1	12.3	8.5	5.4
Fr(l) 3.20-7.60 mm, %	9.4	8.7	9.3	6.5	3.6	2.1	0.8
Fines A, %	11.4	11.6	11.5	16.6	24.1	27.3	31.1
Fines B, %	0.9	0.8	1.6	7.0	16.1	24.2	27.9
Fines F(n), %	77.0	77.2	76.8	79.4	81.0	79.8	79.9
Fibrillation, %	0.2	0.21	0.31	0.98	2.03	2.84	3.3

Table XVI Refining results of SW MFC from passes 16 to 42.

Passes through refiner	**16th**	**19th**	**22nd**	**25th**	**28th**	**31st**	**34th**	**37th**	**40th**	**42nd**
SRE cumulative, kWh/t	842	966	1089	1191	1269	1337	1396	1446	1503	1538
Consistency, %	4.13	3.61	3.67	3.88	3.78	3.65	3.80	3.67	3.94	3.64
SR, °	94	95	95	95	95	95	95	95	95	95
Lc(l) ISO, mm	0.81	0.71	0.61	0.54	0.50	0.48	0.46	0.44	0.42	0.42
Lc(l) Tappi, mm	0.71	0.62	0.53	0.46	0.42	0.41	0.39	0.37	0.35	0.35
Fr(l) 0.00-0.20 mm, %	30.1	30.4	34.1	37.1	39.0	40.0	41.5	43.1	45.6	45.7
Fr(l) 0.20-0.60 mm, %	33.3	36.4	39.7	42.3	44.6	45.2	46.1	46.5	46.1	46.6
Fr(l) 0.60-1.20 mm, %	24.1	24.4	21.6	18.3	15.2	14.0	12.0	10.2	8.2	7.6
Fr(l) 1.20-2.00 mm, %	8.6	6.9	3.9	2.2	1.1	0.8	0.5	0.2	0.2	0.1
Fr(l) 2.00-3.20 mm, %	3.4	1.8	0.6	0.2	0.1	0.1	0.0	0.0	0.0	0.0
Fr(l) 3.20-7.60 mm, %	0.4	0.1	0.1	0.0	0.0	0.0	0.0	0.0	0.0	0.0
Fines A, %	33.4	34.8	39.4	42.7	45.2	46.5	48.3	50.0	52.0	52.8
Fines B, %	31.2	34.7	38.2	39.8	42.1	43.8	45.7	46.1	45.5	47.9
Fines F(n), %	79.9	79.0	80.4	81.3	81.7	82.1	82.6	83.2	84.1	84.1
Fibrillation, %	3.82	4.24	4.63	4.96	5.1	5.24	5.35	5.52	5.76	5.87

Table XVII Refining results of screening trials from feed and passes 1 to 13.

Passes through refiner	Feed	1st pass	4th pass	7th pass	10th pass	13th pass
SRE cumulative, kWh/t	0	32	139	229	294	340
Consistency, %	3.96	4.47	4.40	4.23	4.34	4.22
SR, °	16	22	68	86	91	93
Lc(l) ISO, mm	0.94	0.95	0.87	0.77	0.69	0.63
Lc(l) Tappi, mm	0.90	0.91	0.80	0.67	0.57	0.52
Fr(l) 0.00-0.20 mm, %	21.30	23.30	33.40	43.30	50.20	53.60
Fr(l) 0.20-0.60 mm, %	11.30	10.70	14.10	18.10	21.00	22.60
Fr(l) 0.60-1.20 mm, %	53.20	51.00	42.90	33.70	26.10	22.20
Fr(l) 1.20-2.00 mm, %	13.40	14.40	9.30	4.70	2.70	1.60
Fr(l) 2.00-3.20 mm, %	0.70	0.60	0.30	0.10	0.00	0.00
Fr(l) 3.20-7.60 mm, %	0.10	0.10	0.00	0.00	0.00	0.00
Fines A, %	13.47	14.64	21.81	29.74	36.00	39.36
Fines B, %	0.04	0.11	0.74	1.87	2.63	3.21
Fines F(n), %	81.95	84.22	89.20	91.49	92.49	92.83
Fibrillation, %	0.19	0.25	0.64	0.94	1.23	1.34

Table XVIII Results from screening trials.

Sample name	Screen feed	Screen accept
Consistency, %	1.57	0.89
SR, °	93	95
Lc(l) ISO, mm	0.67	0.63
Lc(l) Tappi, mm	0.57	0.50
Fr(l) 0.00-0.20 mm, %	48.40	59.10
Fr(l) 0.20-0.60 mm, %	22.90	20.60
Fr(l) 0.60-1.20 mm, %	26.00	18.70
Fr(l) 1.20-2.00 mm, %	2.70	1.60
Fr(l) 2.00-3.20 mm, %	0.10	0.00
Fr(l) 3.20-7.60 mm, %	0.00	0.00
Fines A, %	34.76	44.57
Fines B, %	2.59	2.74
Fines F(n), %	91.67	94.11
Fibrillation, %	1.21	1.28

Table XIX Composition of sheets in the first laboratory sheet trial shown in wt%.

Sample number	Kraft pulp	CTMP	HW MFC	SW MFC	CS	CPAM	Silica
1	55	45	0	0	0.5	0.02	0.05
2	50	50	0	0	0.5	0.02	0.05
3	40	60	0	0	0.5	0.02	0.05
4	40	60	1	0	0.5	0.02	0.05
5	40	60	2	0	0.5	0.02	0.05
6	40	60	3	0	0.5	0.02	0.05
7	40	60	0	1	0.5	0.02	0.05
8	40	60	0	2	0.5	0.02	0.05
9	40	60	0	3	0.5	0.02	0.05
10	55	45	3	0	0.5	0.02	0.05
11	40	60	2	0	0.8	0.02	0.05
12	40	60	0	0	0.8	0.02	0.05
13	40	60	2	0	0.5	0.03	0.075

Table XX Composition of sheets in the second laboratory sheet trial shown in wt%.

Sample number	Kraft pulp	CTMP	HW MFC	CS	CPAM	Silica
15	40	60	1	0.5	0.02	0.05
16	40	60	2	0.5	0.02	0.05
17	40	60	3	0.5	0.02	0.05
18	40	60	2	0.8	0.02	0.05
19	40	60	2	1.0	0.02	0.05

Table XXI Composition of sheets in the third laboratory sheet trial shown in wt%.

Sample number	Kraft pulp	CTMP	HW MFC accept	HW MFC feed	CS	CPAM	Silica
20	40	60	0	0	0.5	0.02	0.05
21	40	60	1	0	0.5	0.02	0.05
22	40	60	2	0	0.5	0.02	0.05
23	40	60	3	0	0.5	0.02	0.05
24	40	60	2	0	0.8	0.02	0.05
25	40	60	0	2	0.5	0.02	0.05

Table XXII Results shown as an index ratio for 1, 2, and 3 wt% HW MFC.

Sample	Internal bond index	Tear index	Tensile index	Strain at break	TEA index	Tensile stiffness	Modulus of elasticity	Break elongation	SCT index
1 wt% MFC	13.0	7.0	6.2	-2.5	3.4	-2.2	-2.3	2.0	10.1
2 wt% MFC	21.1	7.4	-1.2	2.2	1.4	-10.5	-7.9	-0.4	2.9
3 wt% MFC	25.2	7.7	3.8	-1.8	-2.2	-6.8	-0.7	1.2	7.6
2 wt% MFC + 0.8 CS	18.9	7.6	9.7	-4.2	3.6	10.4	14.7	9.7	18.9

Table XXIII Results shown as an index ratio for 1, 2, and 3 wt% SW MFC.

Sample	Internal bond index	Tear index	Tensile index	Strain at break	TEA index	Tensile stiffness	Modulus of elasticity	Break elongation	SCT index
1 wt%	24.8	4.8	6.0	0.4	5.1	-5.8	-2.7	1.9	11.0
2 wt%	20.4	7.1	5.8	3.7	10.0	-3.9	1.7	1.9	6.9
3 wt%	24.5	8.5	8.4	2.6	11.1	-4.6	-2.3	2.7	18.4

Table XXIV Results shown as an index ratio for 0.5, 0.8, and 1 wt% CS with different storage time.

Sample	Internal bond index	Tear index	Tensile index	Strain at break	TEA index	Tensile stiffness	Modulus of elasticity	Break elongation
2 wt% MFC + 0.8 wt% CS	18.9	7.6	9.7	-4.2	3.6	10.4	14.7	9.7
2 wt% MFC + 0.8 wt% CS 34 days	13.0	11.3	4.1	-1.5	1.6	2.4	1.7	4.1
2 wt% MFC +1 wt% CS 34 days	14.2	16.3	11.2	10.9	23.8	4.2	3.9	11.2
2 wt% accept + 0.8 wt% CS	3.7	-4.9	-3.4	-5.5	-9.7	-8.5	-11.7	-3.4

Table XXV Results shown as an index ratio for screened HW MFC accept and feed.

Sample	Internal bond index	Tear index	Tensile index	Strain at break	TEA index	Tensile stiffness	Modulus of elasticity	Break elongation
1 wt% HW MFC accept	-1.2	8.8	5.8	-1.5	4.6	4.8	6.4	5.8
2 wt% HW MFC accept	1.2	10.2	5.2	6.1	12.4	2.9	5.2	5.2
3 wt% HW MFC accept	0.2	1.2	-0.7	-6.7	-7.8	-1.7	-2.8	-0.7
2 wt% HW MFC feed	-5.6	3.6	-0.1	-2.7	-2.9	-3.3	-5.6	-0.1
2 wt% HW MFC accept + 0.8 wt% CS	3.7	-4.9	-3.4	-5.5	-9.7	-8.5	-11.7	-3.4

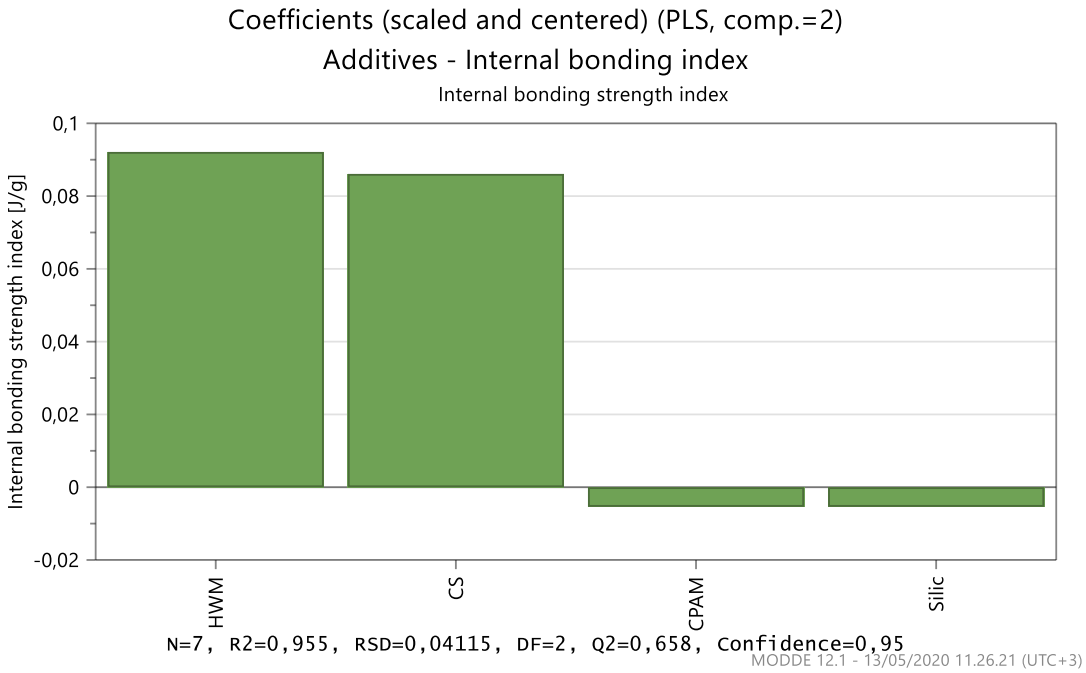

Figure 86 Coefficients plot of internal bond index in the first laboratory sheet trial. R2 is 0.96 and Q2 is 0.66.

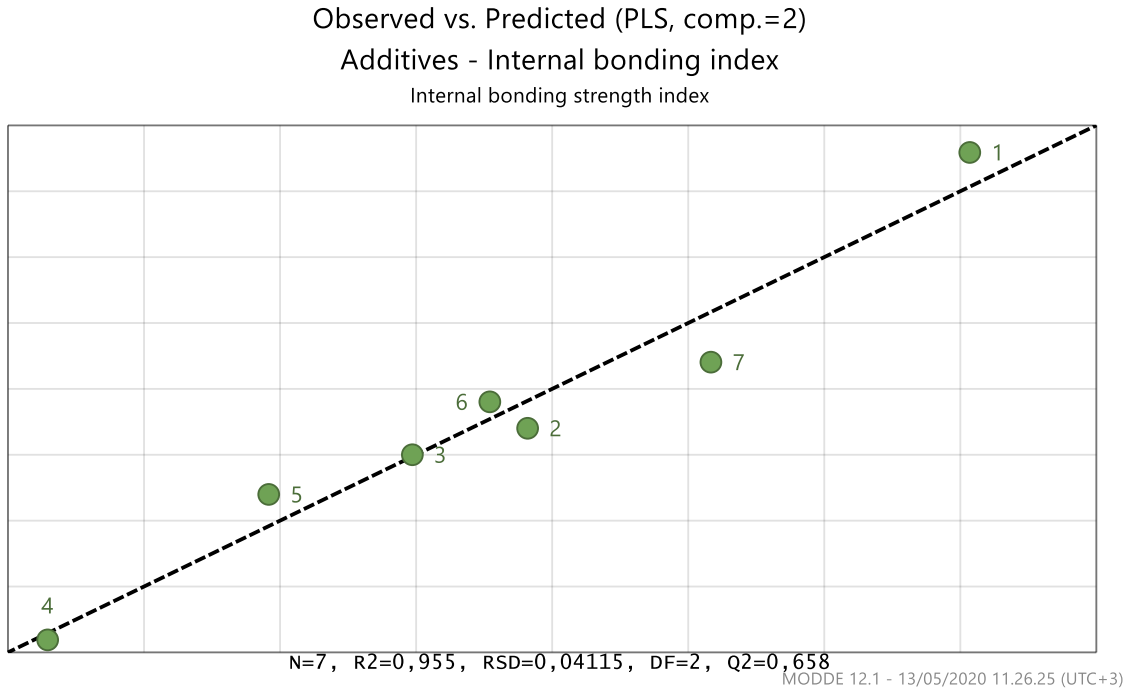

Figure 87 Observed vs. predicted plot of internal bond index in the first laboratory sheet trial.

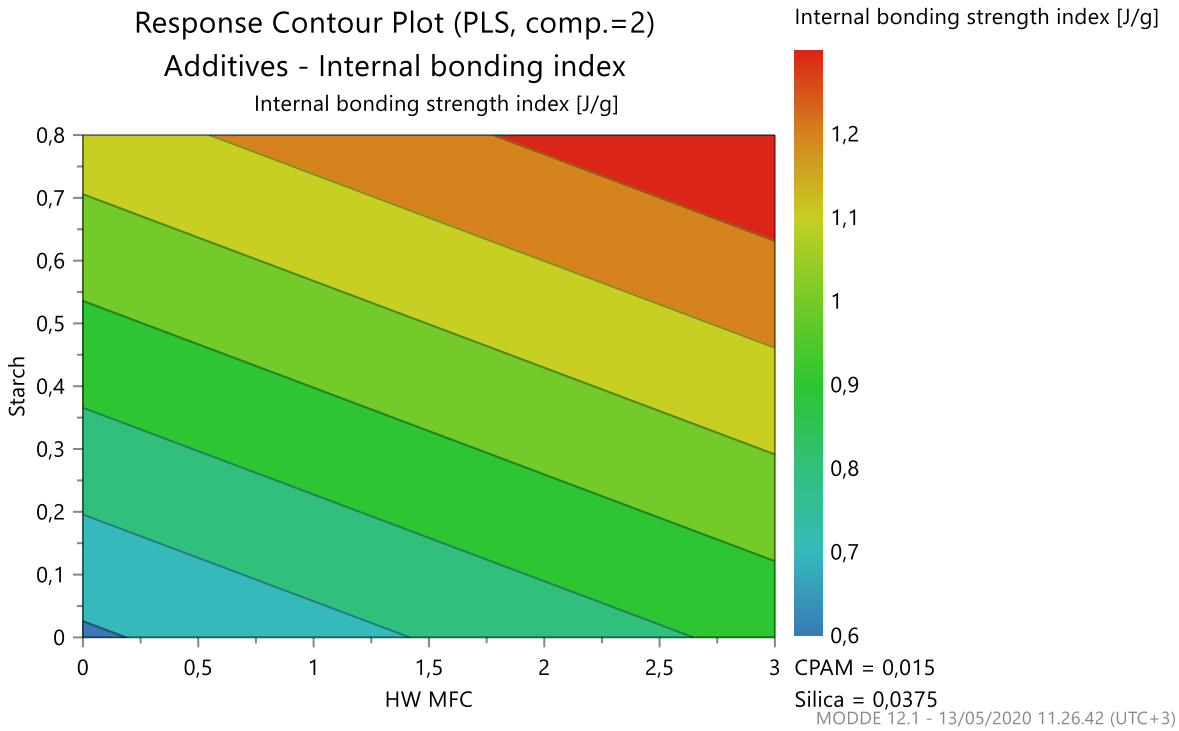

Figure 88 Response contour of internal bond index. CS as a function of HW MF

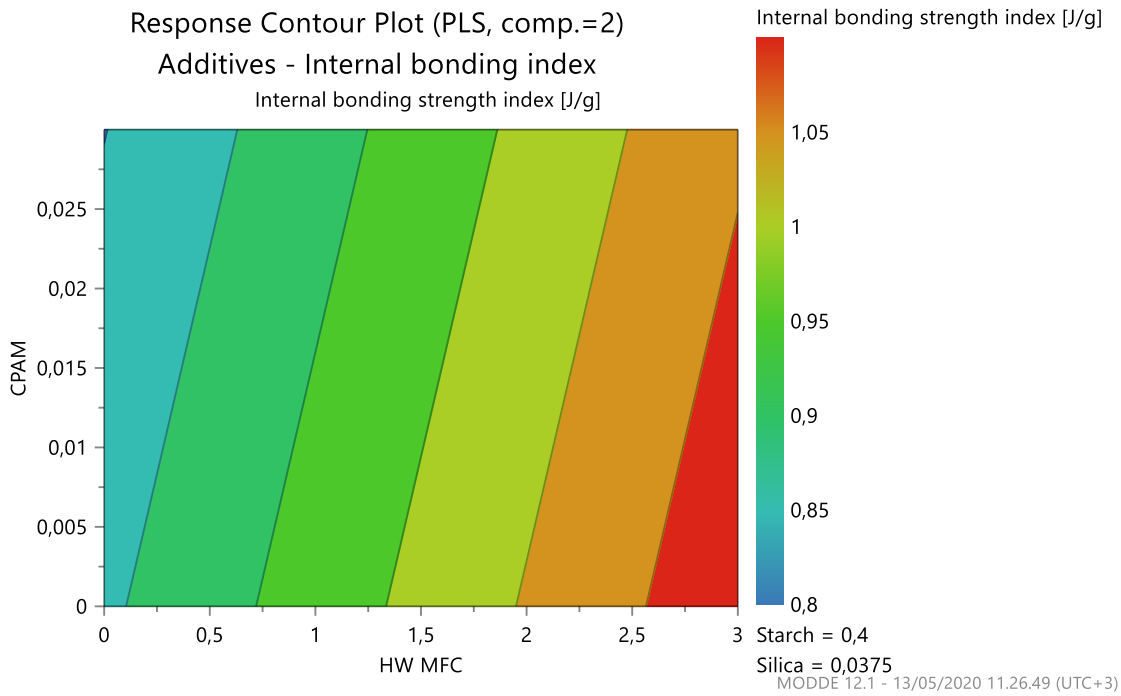

Figure 89 Response contour of internal bond index. CPAM as a function of HW MFC.

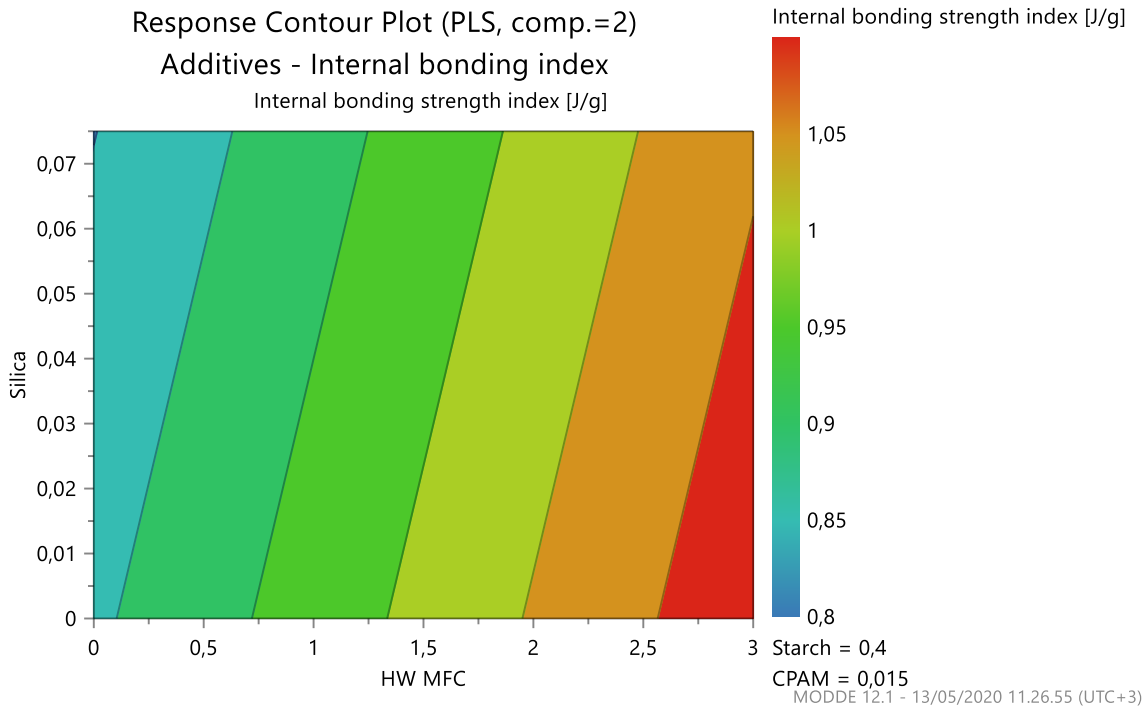

Figure 90 Response contour of internal bond index. Silica as a function of HW MFC.

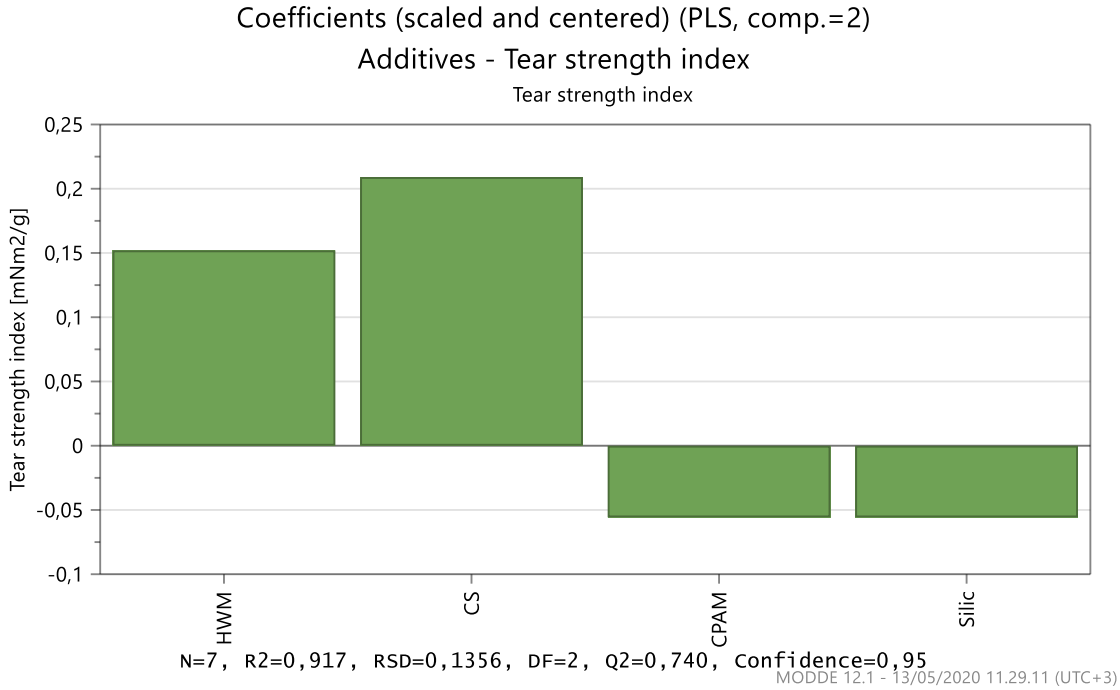

Figure 91 Coefficients plot of tear index in the first laboratory sheet trial. R2 is 0.92 and Q2 is 0.74.

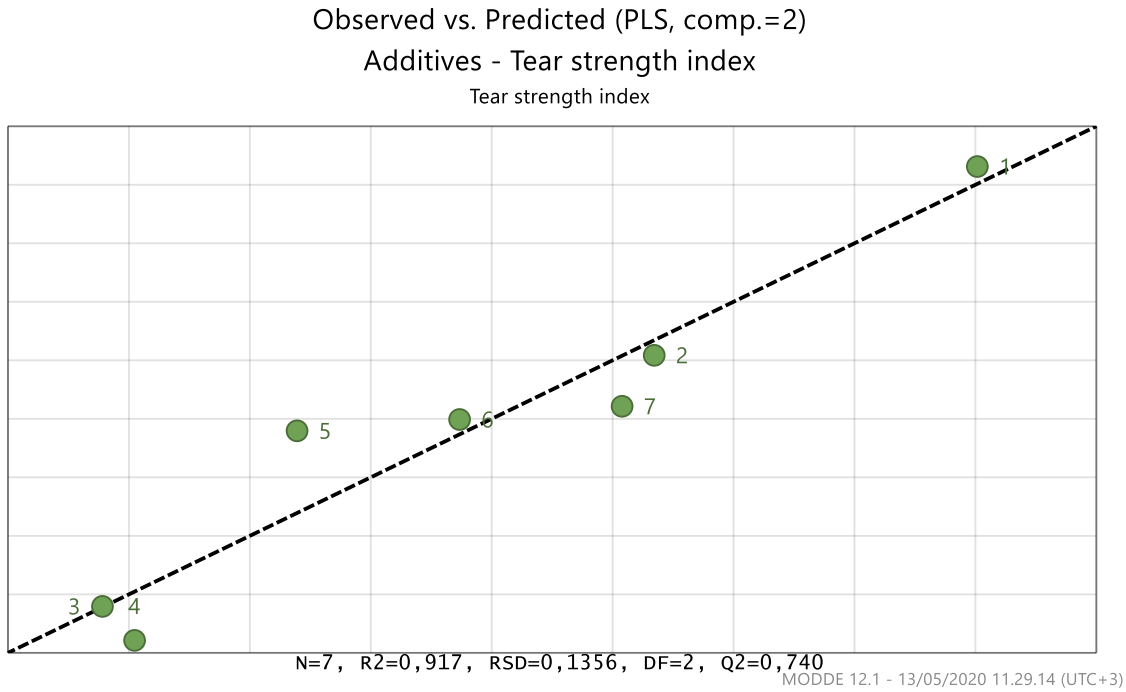

Figure 92 Observed vs. predicted plot of tear index in the first laboratory sheet trial.

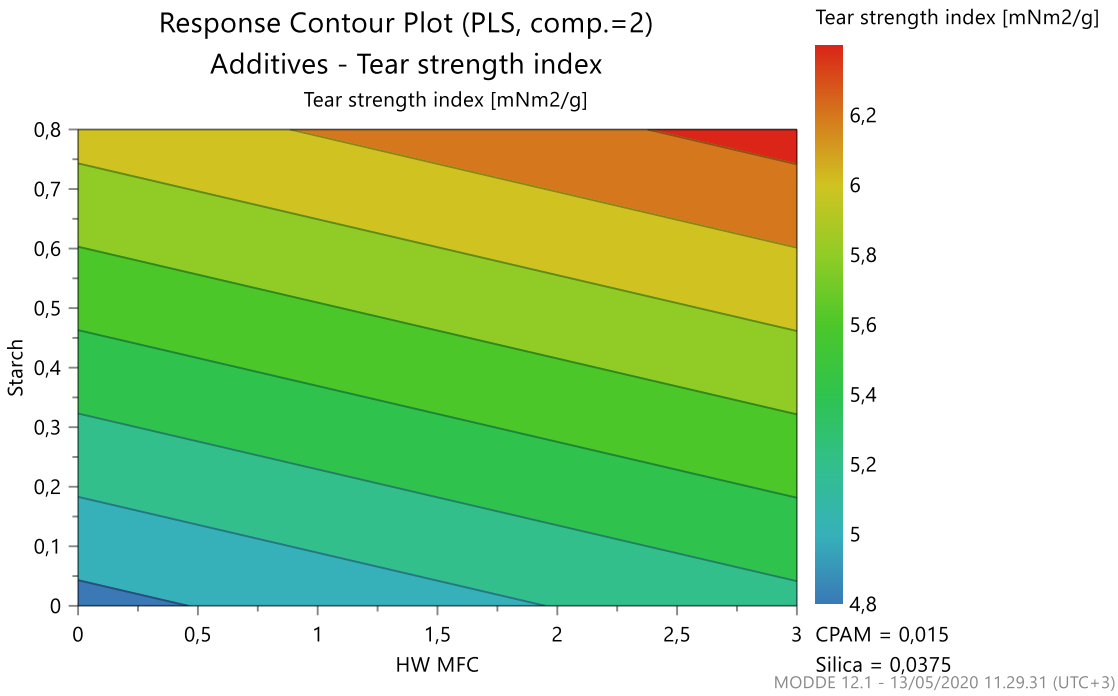

Figure 93 Response contour of tear index. CS as a function of HW MFC.

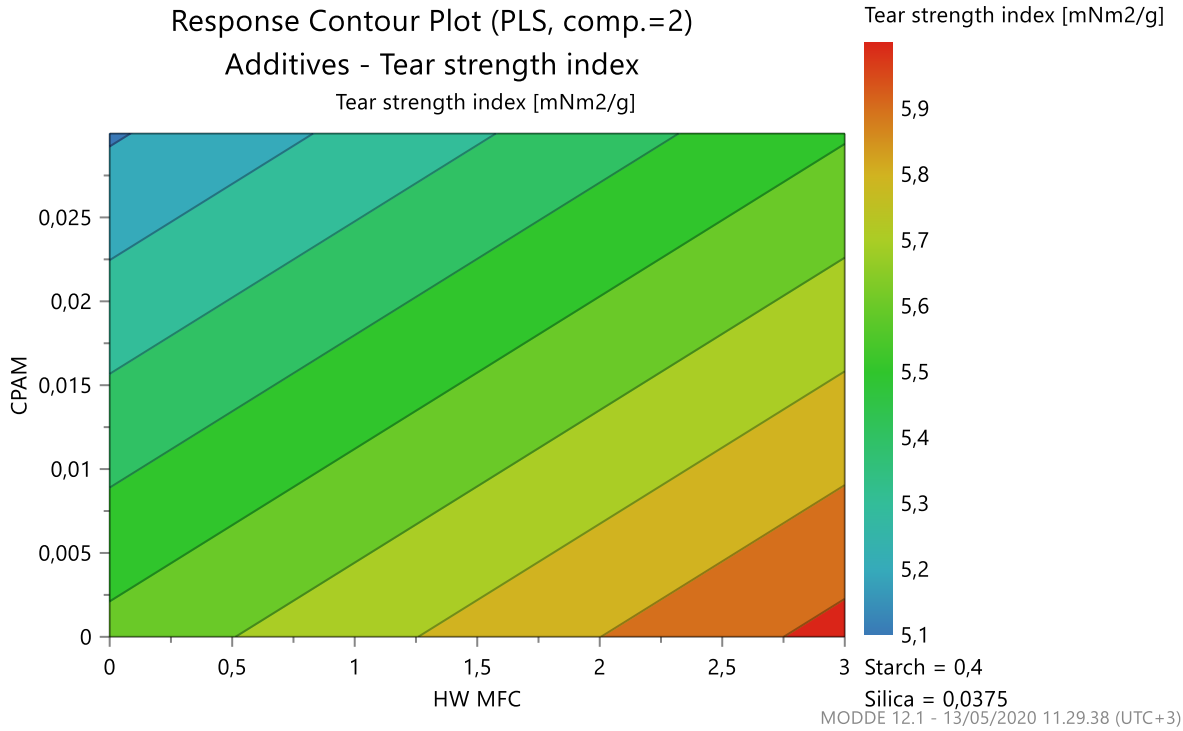

Figure 94 Response contour of tear index. CPAM as a function of HW MFC.

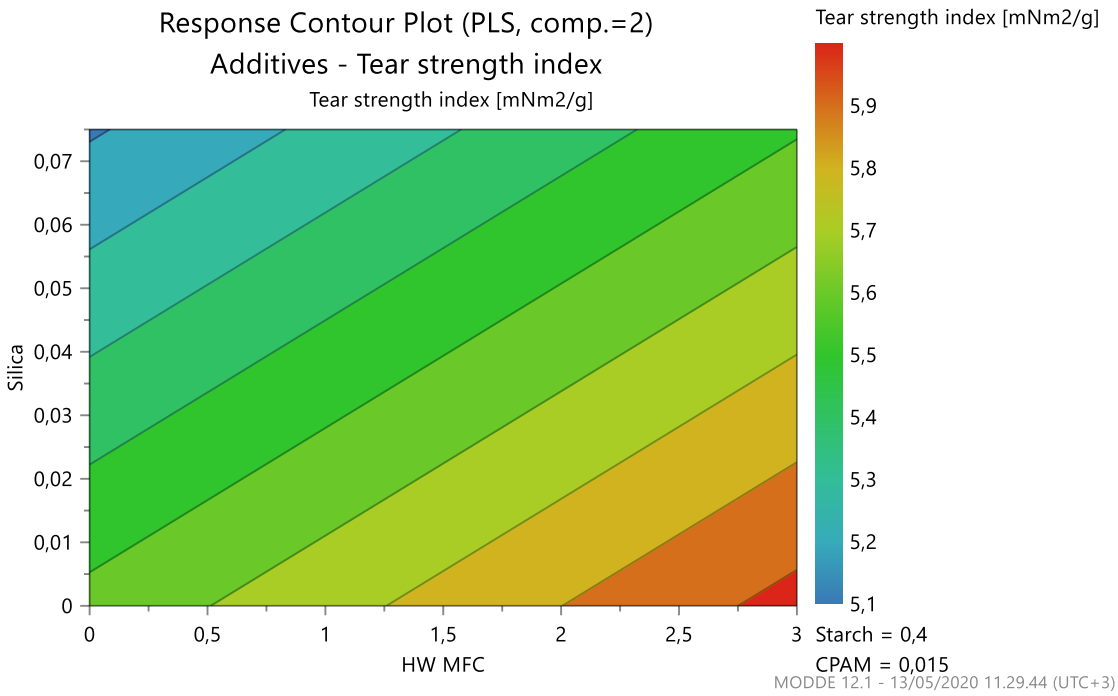

Figure 95 Response contour of tear index. Silica as a function of HW MFC

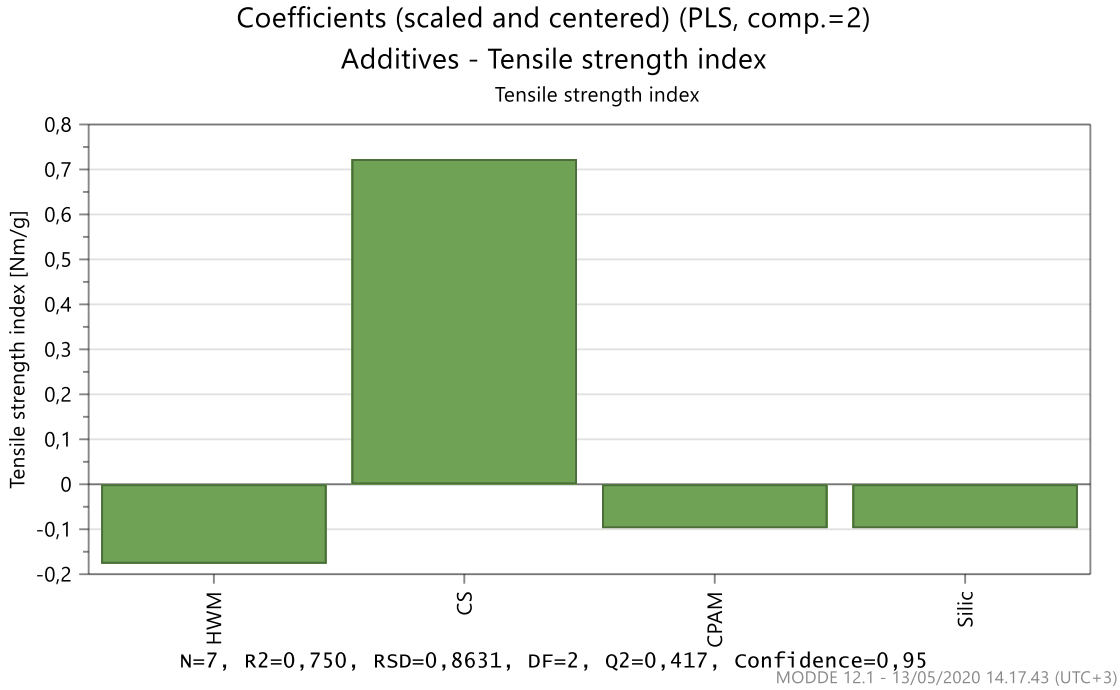

Figure 96 Coefficients plot of tensile index in the first laboratory sheet trial. R2 is 0.75 and Q2 is 0.42.

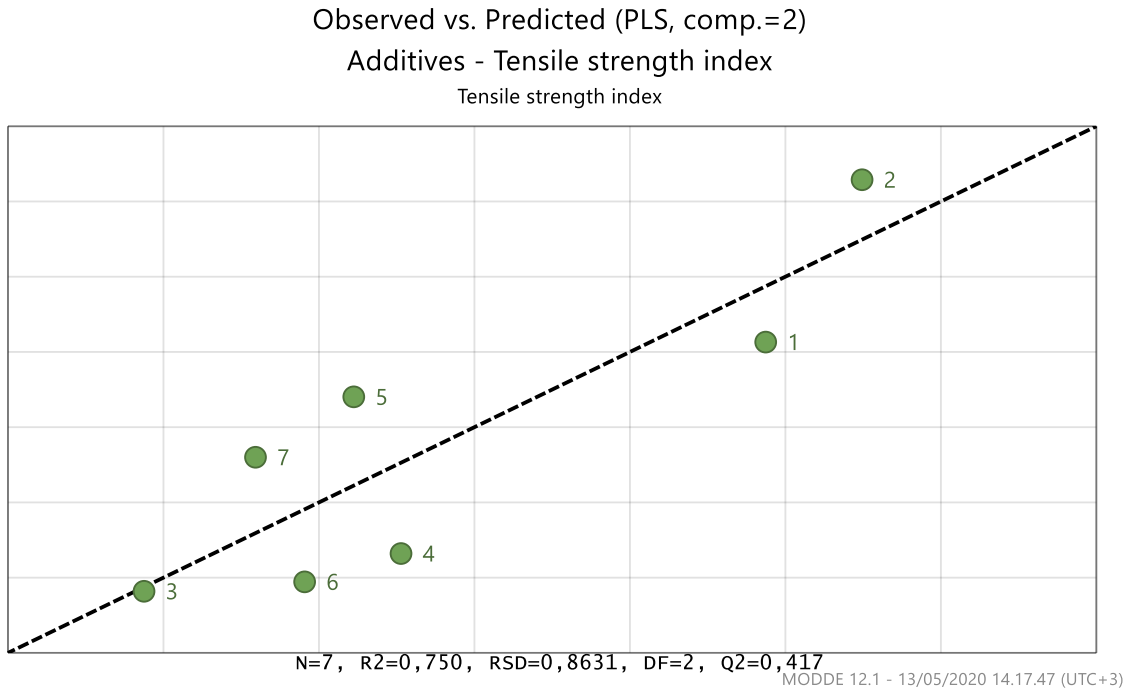

Figure 97 Observed vs. predicted plot of tensile index in the first laboratory sheet trial

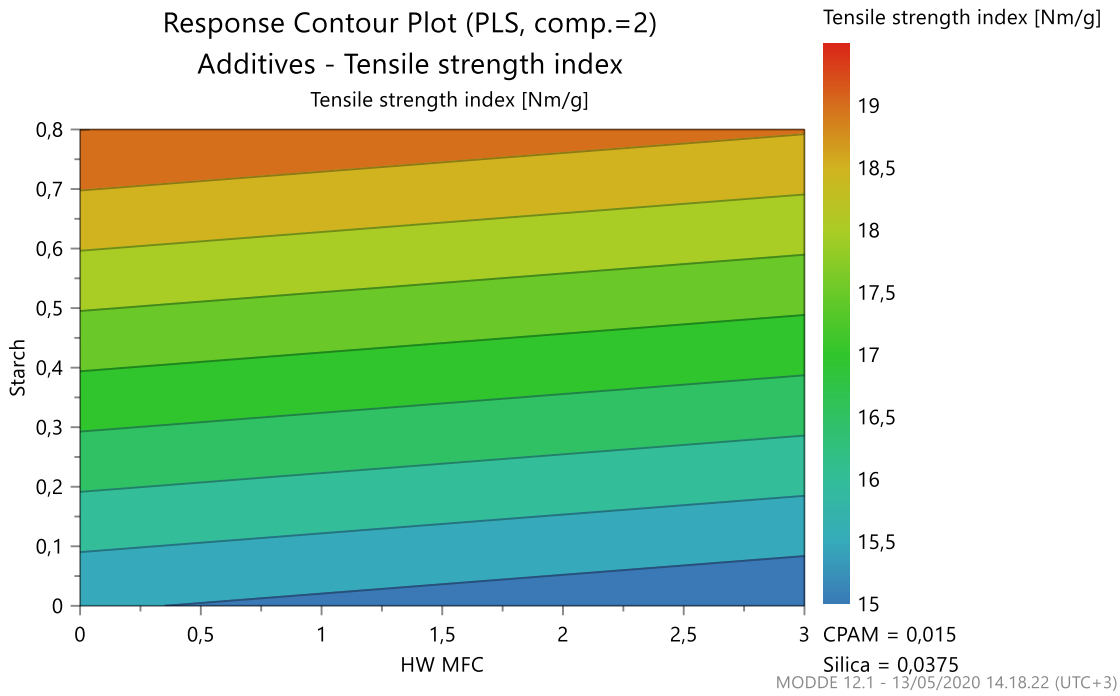

Figure 98 Response contour of tensile index. CS as a function of HW MFC.

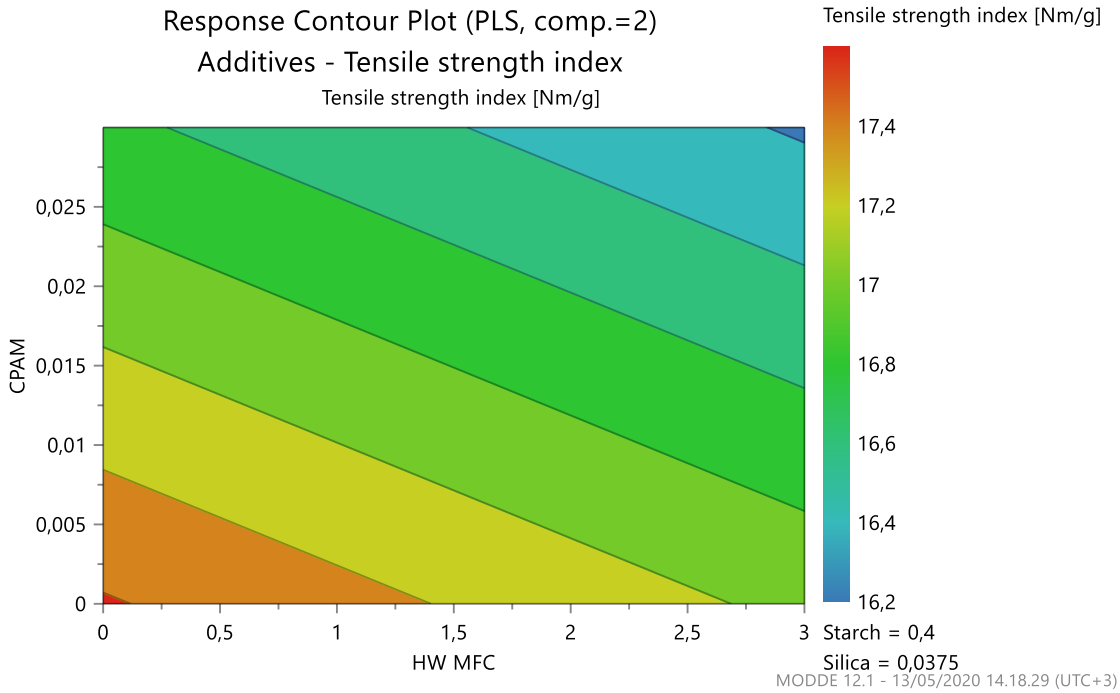

Figure 99 Response contour of tensile index. CPAM as a function of HW MFC.

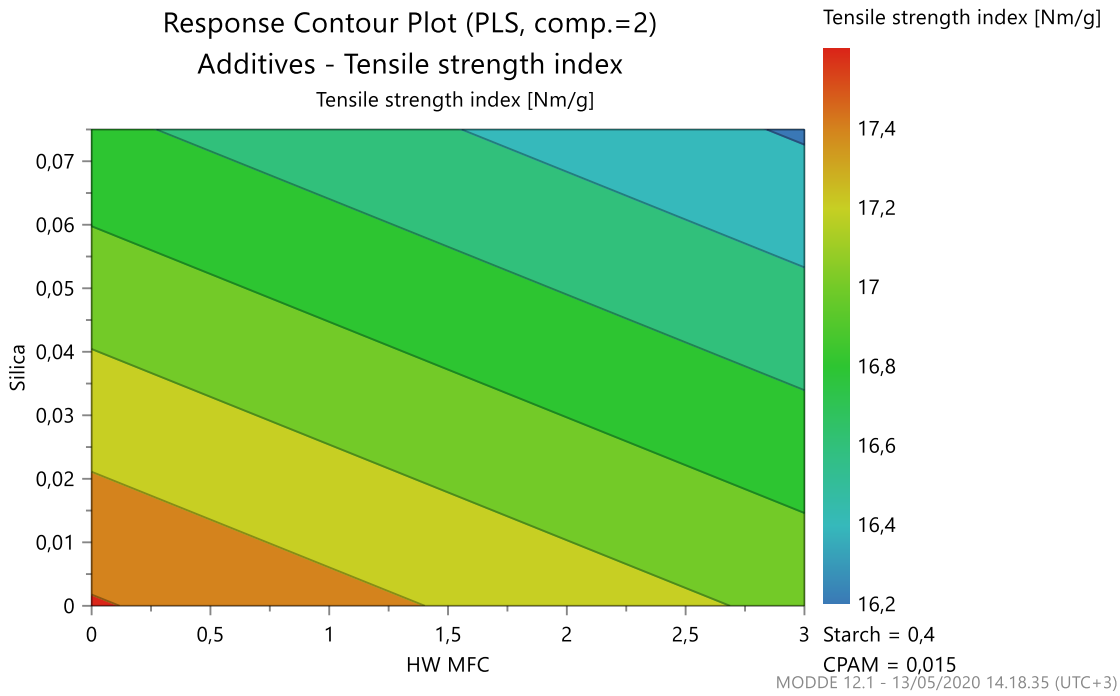

Figure 100 Response contour of tensile index. Silica as a function of HW MFC

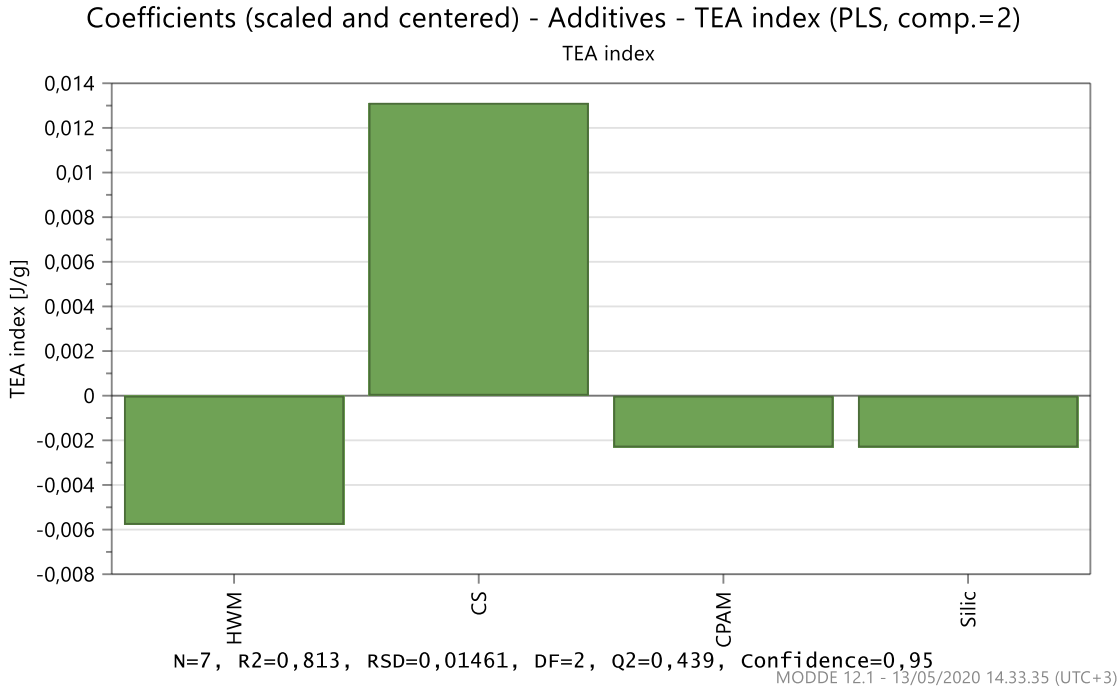

Figure 101 Coefficients plot of TEA index in the first laboratory sheet trial. R2 is 0.81 and Q2 is 0.44.

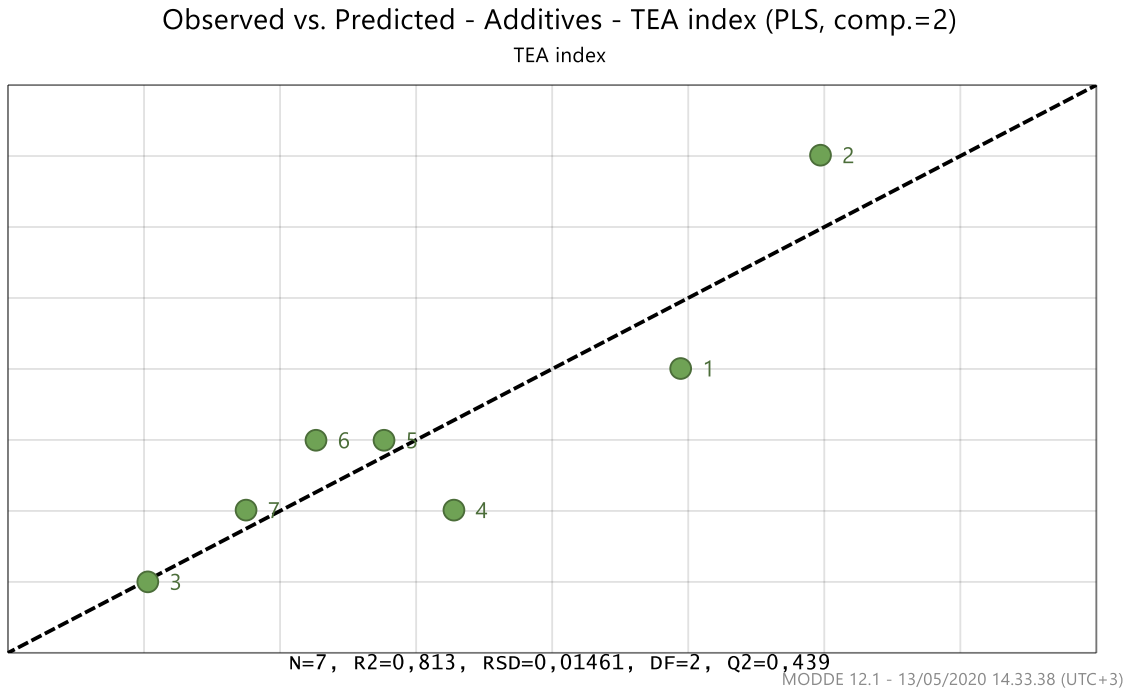

Figure 102 Observed vs. predicted plot of TEA index in first laboratory sheet trial.

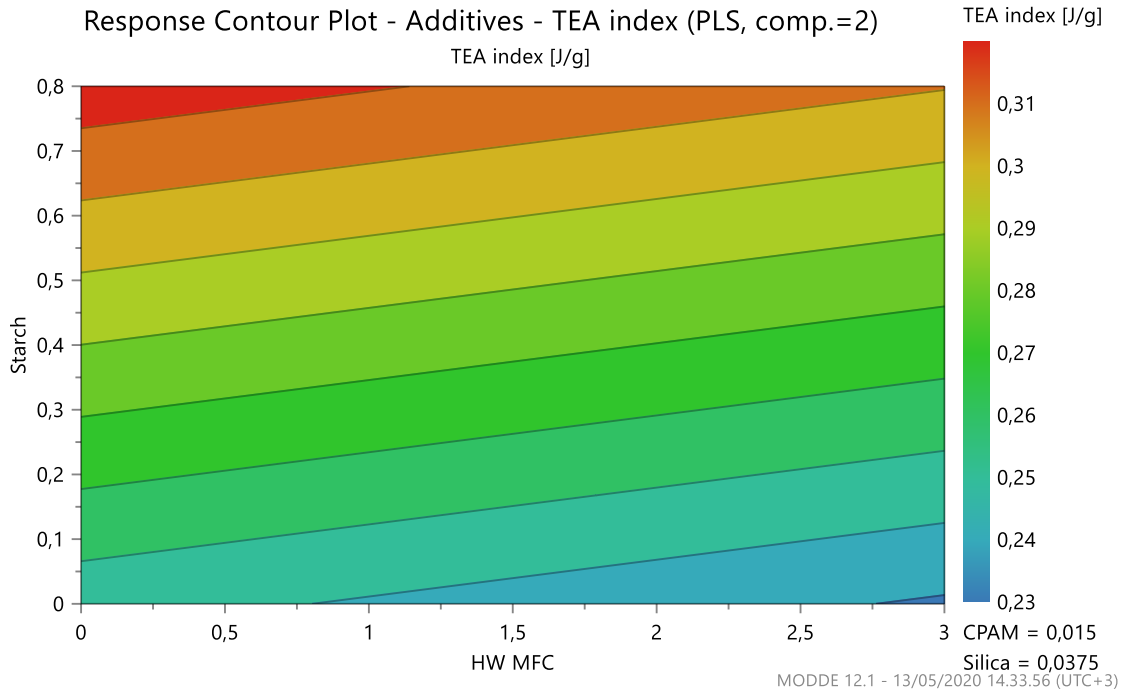

Figure 103 Response contour of TEA index. CS as a function of HW MFC.

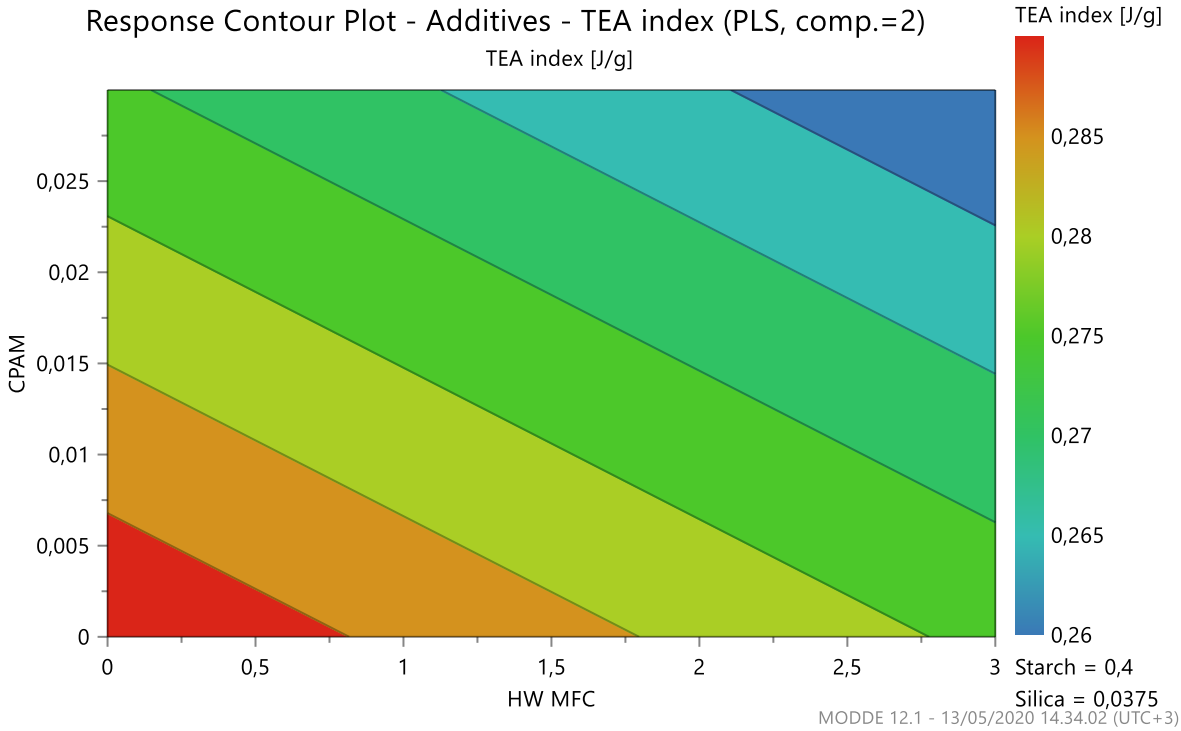

Figure 104 Response contour of TEA index. CPAM as a function of HW MFC.

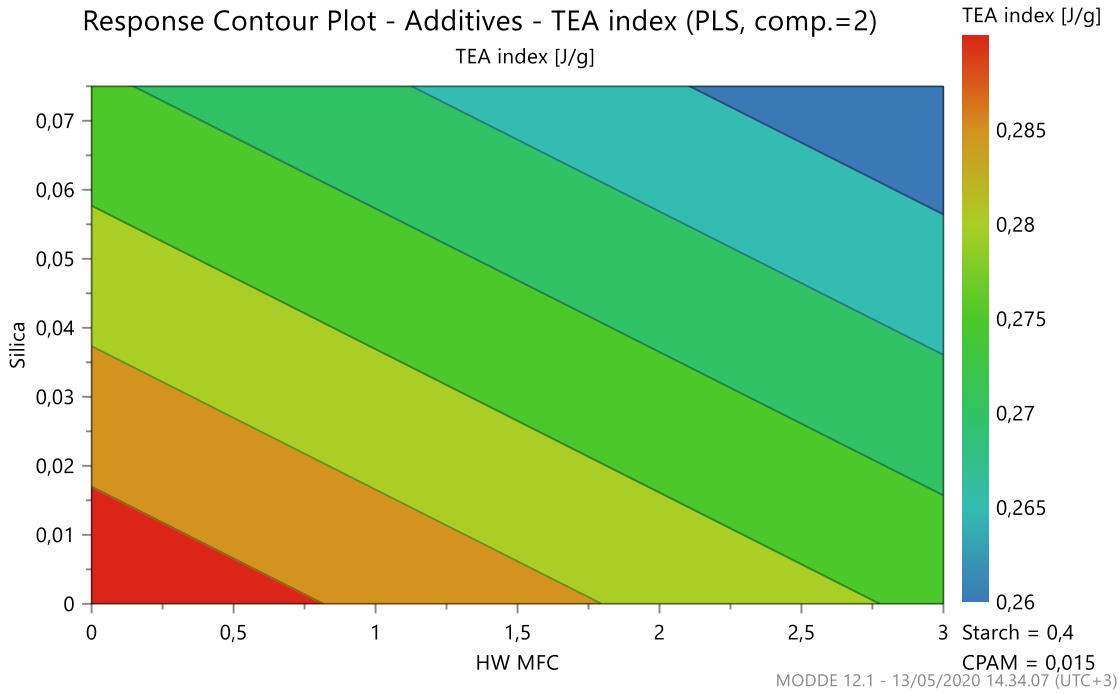

Figure 105 Response contour of TEA index. Silica as a function of HW MFC.

Table XXVI Viscosity measurements from 1 wt% MFC at 20°C.

Point No.	Shear Rate	Shear Stress	Viscosity
	[1/s]	[Pa]	[mPa·s]
1	100	57	572
2	95	57	598
3	90.1	57	628
4	85.1	56	660
5	80.2	56	695
6	75.2	55	733
7	70.3	55	776
8	65.3	54	827
9	60.4	53	884
10	55.4	53	948
11	50.5	51	1019
12	45.5	50	1109
13	40.6	49	1216
14	35.6	48	1355
15	30.7	47	1524
16	25.7	45	1760
17	20.8	43	2085
18	15.8	42	2623
19	10.9	39	3586
20	5.95	36	5994
21	1	29	29208

Table XXVII Viscosity measurements from 2 wt% MFC at 20°C.

Point No.	Shear Rate	Shear Stress	Viscosity
	[1/s]	[Pa]	[mPa·s]
1	100	358	3 577
2	95	353	3 718
3	90.1	351	3 896
4	85.1	348	4 084
5	80.2	345	4 298
6	75.2	343	4 555
7	70.3	340	4 835
8	65.3	336	5 139
9	60.4	331	5 483
10	55.4	327	5 895
11	50.5	322	6 373
12	45.5	318	6 973
13	40.6	311	7 650
14	35.6	306	8 578
15	30.7	299	9 735
16	25.7	290	11 273
17	20.8	283	13 597
18	15.8	272	17 154
19	10.9	262	24 045
20	5.95	246	41 380
21	1	209	209 020

Table XXVIII Viscosity measurements from 3 wt% MFC at 20°C.

Point No.	Shear Rate	Shear Stress	Viscosity
	[1/s]	[Pa]	[mPa·s]
1	100	700	7000
2	95	688	7243
3	90.1	683	7581
4	85.1	680	7983
5	80.2	672	8377
6	75.2	666	8854
7	70.3	662	9416
8	65.3	654	10014
9	60.4	648	10734
10	55.4	641	11556
11	50.5	632	12526
12	45.5	622	13665
13	40.6	610	15020
14	35.6	600	16824
15	30.7	587	19105
16	25.7	570	22119
17	20.8	558	26832
18	15.8	540	34062
19	10.9	522	47901
20	5.95	502	84285
21	1	432	431627

Table XXIX Viscosity measurements from 2 wt% MFC at 10°C.

Point No.	Shear Rate	Shear Stress	Viscosity
	[1/s]	[Pa]	[mPa·s]
1	100	384	3842
2	95	380	3996
3	90.1	378	4197
4	85.1	376	4418
5	80.2	374	4667
6	75.2	370	4923
7	70.3	366	5211
8	65.3	363	5549
9	60.4	359	5937
10	55.4	353	6374
11	50.5	348	6893
12	45.5	342	7515
13	40.6	337	8303
14	35.6	328	9211
15	30.7	321	10445
16	25.7	314	12187
17	20.8	303	14555
18	15.8	293	18483
19	10.9	281	25735
20	5.95	260	43687
21	1	220	219717

Table XXX Viscosity measurements from 2 wt% MFC at 30°C.

Point No.	Shear Rate	Shear Stress	Viscosity
	[1/s]	[Pa]	[mPa·s]
1	100	326	3261
2	95	323	3398
3	90.1	320	3552
4	85.1	317	3719
5	80.2	313	3903
6	75.2	312	4146
7	70.3	307	4375
8	65.3	305	4675
9	60.4	301	4981
10	55.4	297	5351
11	50.5	292	5787
12	45.5	287	6309
13	40.6	283	6969
14	35.6	277	7776
15	30.7	271	8817
16	25.7	264	10268
17	20.8	258	12380
18	15.8	250	15796
19	10.9	238	21845
20	5.95	228	38239
21	1	198	197763

Table XXXI Shear rates in different tube sizes and flow rates.

	Tube diameter. m			
	0.1	0.2	0.3	0.4
Flow rate. m^3/s	**Shear rate. s^{-1}**			
0.01	102	13	4	2
0.05	509	64	19	8
0.1	1019	127	38	16
0.15	1528	191	57	24
0.2	2037	255	75	32

Table XXXII Parameter n in different concentrations of MFC.

Sample	**1 wt% MFC**	**2 wt% MFC**	**3 wt% MFC**
Parameter n. -	0.235	1.214	2.191

Table XXXIII Consistency factors for 1 wt% MFC with different pipe diameters and flow rates.

Flow rate. m^3/s	**Pipe diameter. m**			
	0.1	0.2	0.3	0.4
	Consistency (thickness) factor. k			
0.01	20.7	22.2	28.0	33.8
0.05	36.3	19.7	21.0	24.1
0.1	54.4	21.5	19.7	21.4
0.15	70.8	23.9	19.6	20.4
0.2	86.2	26.4	19.9	19.9

Table XXXIV Consistency factors for 2 wt% MFC with different pipe diameters and flow rates.

Flow rate. m^3/s	**Pipe diameter. m**			
	0.1	0.2	0.3	0.4
	Consistency (thickness) factor. k			
0.01	1.4	12.1	50.9	143.6
0.05	0.4	2.1	7.7	21.0
0.1	0.3	1.1	3.6	9.4
0.15	0.3	0.8	2.4	5.9
0.2	0.3	0.7	1.8	4.3

Table XXXV Consistency factors for 3 wt% MFC with different pipe diameters and flow rates.

Flow rate. m^3/s	**Pipe diameter. m**			
	0.1	0.2	0.3	0.4
	Consistency (thickness) factor. k			
0.01	0.029	2.01	27.7	182.3
0.05	0.002	0.07	0.87	5.5
0.1	0.0007	0.02	0.21	1.25
0.15	0.0004	0.009	0.09	0.53
0.2	0.0003	0.006	0.05	0.29